Performance Evaluation and Multiobjective Optimization of Passive Vehicle Suspension Systems

by

Iyad Talal Al-Zahrnah

A Thesis Presented to the

FACULTY OF THE COLLEGE OF GRADUATE STUDIES

KING FAHD UNIVERSITY OF PETROLEUM & MINERALS

DHAHRAN, SAUDI ARABIA

In Partial Fulfillment of the
Requirements for the Degree of

MASTER OF SCIENCE

In

MECHANICAL ENGINEERING

January, 1993

INFORMATION TO USERS

This manuscript has been reproduced from the microfilm master. UMI films the text directly from the original or copy submitted. Thus, some thesis and dissertation copies are in typewriter face, while others may be from any type of computer printer.

The quality of this reproduction is dependent upon the quality of the copy submitted. Broken or indistinct print, colored or poor quality illustrations and photographs, print bleedthrough, substandard margins, and improper alignment can adversely affect reproduction.

In the unlikely event that the author did not send UMI a complete manuscript and there are missing pages, these will be noted. Also, if unauthorized copyright material had to be removed, a note will indicate the deletion.

Oversize materials (e.g., maps, drawings, charts) are reproduced by sectioning the original, beginning at the upper left-hand corner and continuing from left to right in equal sections with small overlaps. Each original is also photographed in one exposure and is included in reduced form at the back of the book.

Photographs included in the original manuscript have been reproduced xerographically in this copy. Higher quality 6" x 9" black and white photographic prints are available for any photographs or illustrations appearing in this copy for an additional charge. Contact UMI directly to order.

U·M·I

University Microfilms International
A Bell & Howell Information Company
300 North Zeeb Road, Ann Arbor, MI 48106-1346 USA
313/761-4700 800/521-0600

Order Number 1354091

Performance evaluation and multiobjective optimization of passive vehicle suspension systems

Al-Zahrnah, Iyad Talal, M.S.

King Fahd University of Petroleum and Minerals (Saudi Arabia), 1993

U·M·I
300 N. Zeeb Rd.
Ann Arbor, MI 48106

PERFORMANCE EVALUATION AND MULTIOBJECTIVE OPTIMIZATION OF PASSIVE VEHICLE SUSPENSION SYSTEMS

BY

IYAD TALAL AL-ZAHRNAH

A Thesis Presented to the

FACULTY OF THE COLLEGE OF GRADUATE STUDIES

KING FAHD UNIVERSITY OF PETROLEUM & MINERALS

DHAHRAN, SAUDI ARABIA

In Partial Fulfillment of the

Requirements for the Degree of

MASTER OF SCIENCE

In

MECHANICAL ENGINEERING

JANUARY, 1993

KING FAHD UNIVERSITY OF PETROLEUM & MINERALS

DHAHRAN, SAUDI ARABIA

This thesis, written by

IYAD TALAL ALZAHARNAH

under the direction of his thesis committee, and approved by all the members, has been presented to and accepted by the dean, College of Graduate Studies, in partial fulfillment of the requirements for the degree of

MASTER OF SCIENCE IN MECHANICAL ENGINEERING

Thesis Committee:

Chairman (Dr. A. Kerim Kar)

Member (Dr. Rao R. Guntur)

Member (Dr. Moustafa Kamal)

Dr. Muhammad O. Budair
Department Chairman

Dr. Ala H. Rabeh
Dean, College of Graduate Studies

Date:

ACKNOWLEDGEMENT

First and foremost, praise and thanks be to Almighty Allah, the most Gracious, the most Merciful, and peace be upon His Prophet.

Acknowledgement is due to King Fahd University of Petroleum and Minerals for extending all facilities.

I would like to offer my deep and sincere appreciation to my academic advisor and thesis committee chairman, Dr. Abdul Kerim Kar, from whom I learn to be a master's student and who has been a constant source of help and encouragement during this work. I also greatly appreciate the invaluable cooperation and support extended by my thesis committee members: Dr. R.R. Guntur and Dr. K.A.F Moustafa.

Sincere thanks are due to department chairman Dr. Muhammad O. Budair for immeasurable cooperation.

I wish to express my gratitude to my brother and parents, who motivated and guided me through out my career.

Finally, I thank both Mr. P.N. Nair and Aslam Pervaiz who helped me in typing this manuscript.

TABLE OF CONTENTS

LIST OF FIGURES

LIST OF TABLES

NOMENCLATURE

A:	Road roughness factor
a:	Total root mean square acceleration
a_F:	Root mean square acceleration due to external force
a_g:	Root mean square acceleration due to road input
b:	Damping coefficient
B:	Damping coefficient to sprung mass ratio
C:	Constant equal to π.A.V. (V: is defined later)
Δd:	Total root mean square relative displacement
Δd_F:	Root mean square relative displacement due to external force
Δd_g:	Root mean square relative displacement due to road input
k:	Stiffness coefficient
K:	Stiffness coefficient sprung mass ratio
M:	Sprung mass of 1-DOF models
m_1:	Unsprung mass of 2-DOF models
m_2:	Sprung mass of 2-DOF models
V:	Vehicle forward velocity

THESIS ABSTRACT

Name of Student: IYAD TALAL AL-ZAHRNAH

Title of Study: Performance Evaluation and Multiobjective Optimization of Passive Vehicle Suspension Systems.

Major Field: Mechanical Engineering

Date of degree: January 1993

The objective of this study is provide an insight into the behavior of passive vehicle suspension systems in order to obtain a better understanding of their performance limits. In this thesis, responses of different one and two degree of freedom vehicle suspension models are derived and analyzed when subjected to random road and aerodynamic inputs. Comparisons of the behaviors of different one degree of freedom models are made when they are subjected to additional aerodynamic force input. Also comparisons of the behavior of different two degree of freedom models are made when subjected to ground input only. A multiobjective optimization method is applied to a two degree of freedom model and it was shown how it is possible to determine suitable set of suspension parameters to obtain a required vehicle response. These results will improve the understanding of the performance of passive vehicle suspensions.

MASTER OF SCIENCE DEGREE

KING FAHD UNIVERSITY OF PETROLEUM AND MINERALS
Dhahran, Saudi Arabia

January 1993

خلاصة الرسالة

اسم الطالب : إياد طلال الزهارنة
عنوان الدراسة : تقييم أداء والحصول على أفضل أداء متعدد الأغراض للعربات ذات أنظمة التعليق الغير مؤثر بها .
التخصص : هندسة ميكانيكية
تاريخ الشهادة : يناير ١٩٩٣م

الغرض من هذه الدراسة هو الحصول على فهم أكثر لحدود أداء العربات ذات أنظمة التعليق الغير مؤثر بها . في هذه الرسالة يتم اشتقاق وتحليل تجاوب عدة أنظمة تعليق أرضيةوهوائية عشوائية . يتم عقد مقارنات بين أداء عدد من نماذج عربات ذات إتجاه واحد في حرية الحركة عندما تتعرض لإهتزازات إضافية هوائية . أيضاً يتم عقد مقارنات بين أداء عدد من نماذج عربات ذات اتجاهين في حرية الحركة عندما تتعرض لإهتزازات أرضية فقط . يتم تطبيق نظام الحصول على أفضل أداء المتعدد الأغراض على نموذج لعربة ذات اتجاهين في حرية الحركة ويتم تحديد قيم مكونات نظام التعليق المطلوبة للحصول على أداء معين للعربة . نتائج الدراسة ستحسن فهم أداء العربات ذات أنظمة التعليق الغير المؤثر بها .

درجة الماجستير في العلوم
جامعة الملك فهد للبترول والمعادن
الظهران - المملكة العربية السعودية
يناير ١٩٩٣م

CHAPTER 1

INTRODUCTION

Transportation is a basic service for the human society. During this century, the successive developments in transportation facilities have participated considerably in bringing mobility to most segments of the population around the world and accelerated the industrial and commercial successes. To meet the rising need for efficient and fast transportations, several means of transportation system have been either developed or proposed. Among the newly proposed public transportation systems are the air cushion, magnetic suspension and advanced railway systems. The proposed transportation facilities should be built more efficiently, more comfortably and safer apart from being economically feasible. Advanced research is needed in different aspects of transportation such as reliability, maintenance of vehicle structures, vibration and shock effects in transportation.

A major influence on passenger's comfort, and maintenance and repair costs of both vehicles and guideways comes from mechanical vibrations. A vehicle traversing a given road surface is subjected at each wheel to a disturbance which is a random function of time. It is also subjected to aerodynamic forces. To design a vehicle and its suspension so that the vehicle response is at an acceptable level is the objective of a vehicle engineer. Among the requirements are acceptable passenger comfort, small suspension deflections, and good road or track holding ability. A good vibration isolation is required to secure the occupants ride comfort, whereas good road holding is important for vehicle holding and, in general, for enhanced safety. Key design constraints are represented by the acceleration of vehicle body, maximum allowable relative displacement between the vehicle and various suspension components, including wheels, vehicle and other unsprung masses. Additional constraints are imposed by the overall system robustness, reliability, power, and cost requirements.

As suspension becomes softer, it tends to reduce the effects of road disturbances and also requires increased vehicle-road dynamic clearance. External force disturbance act directly on the vehicle and include the effects of aerodynamic forces and tyre-forces developed during the negotiation of hills and curves. The effects of external forces tend to be reduced as a suspension becomes harder and requires less vehicle-road dynamic clearance. The presence of different types of disturbances- the external forces and road disturbances - and the passenger comfort versus suspension dynamic excursion requirements result in a number of competing factors.

The modern approaches in design demand not only acceptable performance but optimal performance. Considerable efforts have been devoted over the last two decades to determine the optimum suspension design for a vehicle travelling on randomly profiled roads, railway tracks or runways. These studies realized that optimum suspension design is essentially a compromise between the several competing requirements of the suspension itself.

Not long ago, road vehicle suspension system were passive devices consisting of energy storage and dissipative elements tuned to one particular design point. The fixed characteristics inherent in the passive suspensions have led to a compromise in performance between sprung mass isolation, suspension travel, and tire-road contact force variation. Recent developments in multivariable control design methodology and microprocessor implementation of modern control algorithms open a new era for the design of electronically controlled vehicle suspension systems, with potential increase in overall performance. Such advanced suspension concepts include actively controlled systems that use sensing devices and servomechanisms, and externally controlled passive systems called semi-active suspensions. However, passive suspensions are found on most of the

conventional vehicles. Roughly, they are characterized by the absence of external power sources, whereas the active suspensions require additional energy sources, such as compressors or pumps to achieve superior ride and/or holding performance. The semi-active suspensions as their name implies, fill the gap between passive and active suspensions since they offer significant performance improvements while requiring relatively small external power sources. Modern optimization methods are heavily used in the design of passive and semi-active suspension systems.

Two approaches are used to solve the optimization problem of suspension systems: a) single objective methods b) multiobjective methods. Single objective methods were heavily employed in the past two decades to optimize the performance of vehicle suspensions and with the wide use of computers, it was possible to employ the optimal control techniques with a single objective method to optimize the performance of suspension systems, especially the actively controlled ones. Recently, the multiobjective approaches, such as the goal programming method, the ϵ-constraint method, and the game theory method have been used to optimize the suspension systems.

In this study, the performances of different passive vehicle suspension systems are evaluated and the multiobjective optimization methods are applied to design suspension systems that will produce desirable dynamic vehicle responses.

CHAPTER 2

LITERATURE REVIEW

There have been many investigations in the area of vehicle suspension design and optimization since 1960's. In this chapter research from the existing literature relating to suspension models, types of inputs and methods used for optimization is reviewed to establish a base for the proposed research.

2.1 Suspension Models

Several suspension models were used in previous literature to study the optimization of vehicle suspension systems. While a multidegree of freedom suspension model is required to describe a vehicle completely, considerable insight may be gained into the basic behavior of a suspension system by focusing attention upon models of small number of degrees of freedom, such as the single degree of freedom models.

Some of the research based on simple one DOF models assume a suspension model with specific form and obtain the optimum suspension parameters under various operating conditions [1,2,3]. They use the suspension forms shown in Figure 2.1.

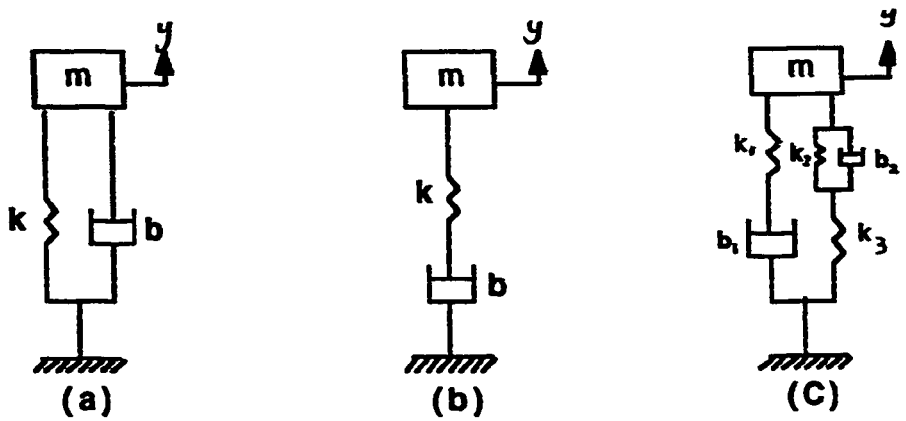

Figure 2.1. One -DOF suspension models.

Other researchers studied one DOF models where the physical form of the suspension is not known, but to be determined from optimization [2,4]. They have obtained a transfer function for the suspension which can be realized, under some conditions, by the suspension models shown in Figure 2.1(b) and (c). However, suspension in Figure 2.1(b) cannot carry static load and its practical usefullness is limited. In some papers, only an actuator force profile is determined in terms of physical variables to provide the necessary suspension properties [3,5].

Some researchers used two DOF suspension models with known physical suspension forms by including primary and secondary suspensions [2,3,6,7,8], as shown in Figure 2.2.

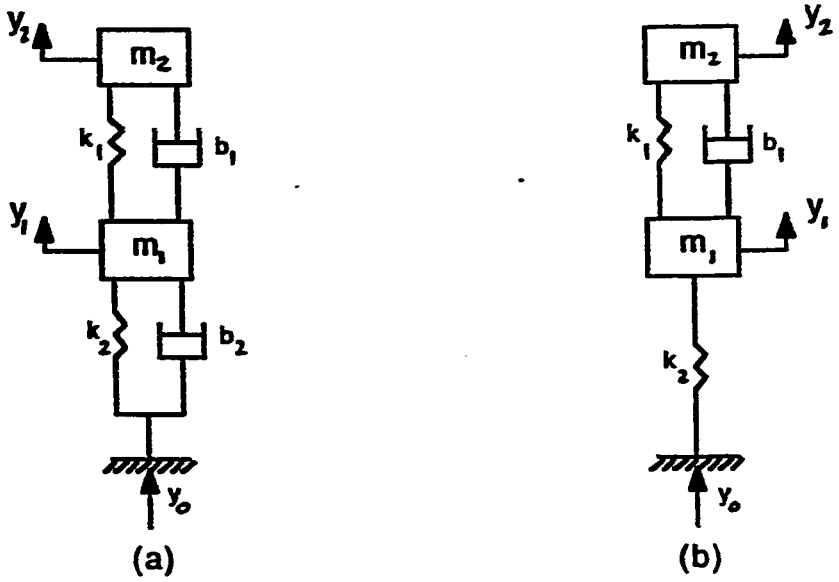

Figure 2.2. Two DOF suspension models.

These two DOF models are also extended into the studies where the form of the suspension force is obtained through optimization and using modern control techniques.

[4,5]. Some kept the primary suspension as a spring and dashpot combination, and obtained the form of secondary suspension by using optimal control techniques [5] or combining the existing secondary suspension (spring and damper) with a force actuator to be determined [5,6,8].

Since a comprehensive understanding of vehicle suspension behavior requires a more complete description of vehicle, higher DOF suspension models were also developed in the literature. Usually vertical and lateral motions were studied separately. Vertical motions are studied for confort and lateral ones for stability. Earlier models have taken the vehicle as having longitudinal symmetry and have described the suspension using two DOF models having heave and pitch motions for vehicle body, as shown in Figure 2.3.[9].

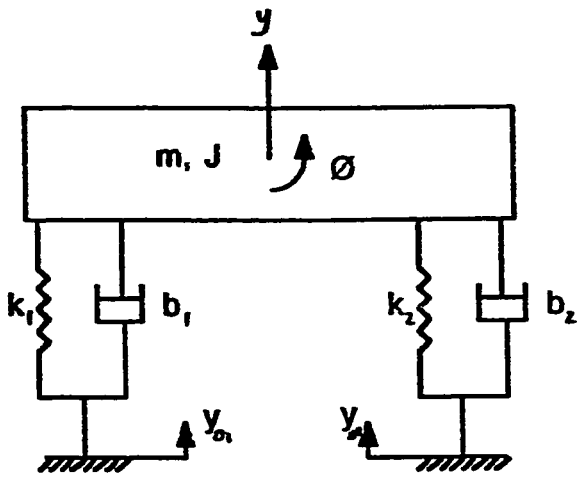

Figure 2.3. Two DOF vehicle model.

Later studies included primary and secondary suspension, as shown in Figure 2.4[10].

More involved studies include three dimensional vehicle suspension models, up to 14 DOF's [1,11,12,13].

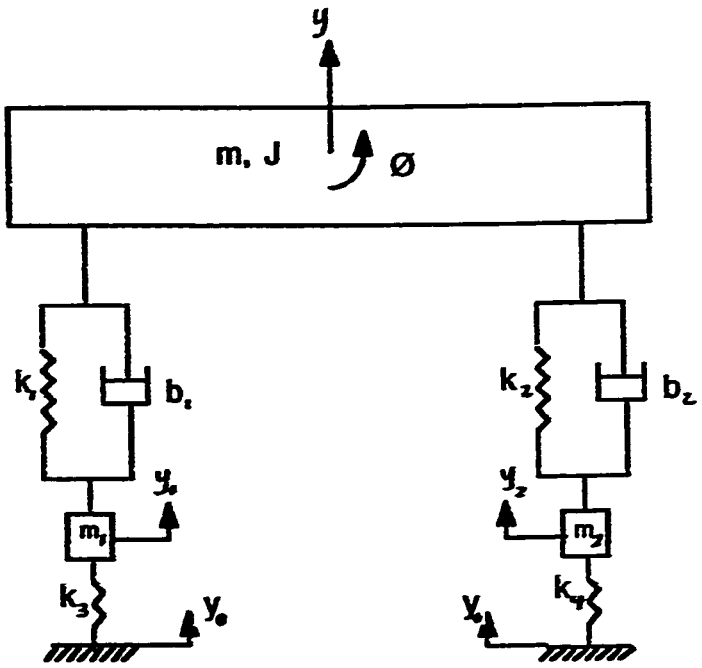

Figure 2.4. Four DOF vehicle model.

2.2 Input Models

Vehicle suspension systems must be designed to function adequately in a wide range of working environments. Suspension models with or without a specific form are optimized using various road and external force inputs.

Deterministic Inputs: Deterministic road inputs are usually taken to be a sinusoidal functions of varying amplitude and frequency or step input of varying amplitude [4,14].

Random Inputs: Real road or external force inputs are modeled using their power spectrum density functions [1,4,10,11,15-19]. A general form used for road power spectrum density function is:

$$S_{y_0}(s) = -\frac{AV}{s^2} \qquad (2.1)$$

where A is roughness factor and V is forward vehicle velocity[1]. Another form is used to represent external forces and is derived from experimental data in terms of body influence coefficient C, the average wind velocity v_o and the wind fluctuation magnitude v_r as:

$$S_f(s) = \frac{\beta_0}{-s^2 + v^2} \qquad (2.2)$$

$$\beta = \frac{4C^2 v_o^2 v_r^2}{\pi}$$

where v is the spectrum characteristic frequency β represents a specific rms disturbance force level [1].

2.3 Single Objective Optimization

The single objective function has been used extensively to solve the optimization problem of suspension systems. In order to choose those parameters which will minimize a specified performance index for a given suspension design, the performance index must first be expressed as a function of the given parameters. There are several ways to describe the performance of a suspension system quantitatively. One way would be in terms of comfort, sizing, power and contact frequency. Comfort criteria are often stated either in terms of mean acceleration levels or in terms of peak acceleration levels. The sizing of the suspension system is a function of mean square or peak relative stroke deflection. Other criteria such as power expended and contact frequency are also important. Reference [2] illustrates an application of parameter optimization using a single performance index to a single DOF system, as shown in Figure.2.5 where y is vertical displacement of the vehicle mass and y_0 is the irregularity of the road.

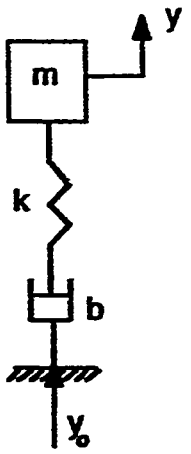

Figure 2.5. One DOF vehicle model.

The problem was solved by finding the parameters k and b to minimize the performance index,

$$J = \overline{\ddot{y}^2} + \rho \overline{(y - y_0)^2} \tag{2.4}$$

where ρ is a numerical weighing constant. The optimal passive system is found to have the following parameters:

$$\left(\frac{k}{m}\right)_{opt} = \sqrt{\rho} \tag{2.5}$$

$$\left(\frac{b}{m}\right)_{opt} = \frac{\rho^{1/4}}{\sqrt{2}} \tag{2.6}$$

As it can be seen, the optimum parameters are functions of the weighing constant, which is specified by the designer. As mentioned earlier, sometimes the suspension system is visualized without a priori specification of the element configuration as in Figure 2.6 where F(t) is an external force disturbance, and G is the transfer function of the suspension system to be determined.

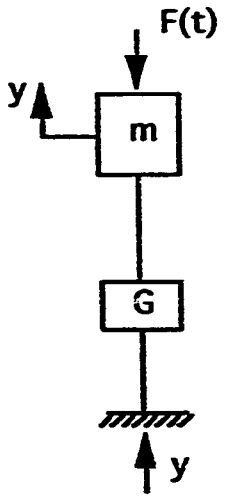

Figure 2.6. One DOF optimization model.

The above transfer function was optimized with regard to the same performance index of Equation (2.4). The power spectral density function of the road is taken as the general form given by Equation (2.1), while the external force model used is based upon which a wind gust spectral density is found in Equation (2.2).

Having the optimum transfer function obtained, the mechanical suspension illustrated in Figure 2.1 (b) is derived as a possible suspension for the case of no external input and Figure.2.1 (c) is derived for the case of external force input [4].

A two DOF vehicle model shown in Figure.2.2 (a) is optimized for an air cushion vehicle, using a single objective function,

$$J=\overline{\ddot{y}_2^2}+\rho_1\,\overline{(y_1-y_0)^2}+\rho_2\,\overline{(y_2-y_1)^2}+\rho_3 h_e^2 \qquad (2.7)$$

where h_e is an equilibrium gap height of a realistic model of a fluid suspension system and ρ_1, ρ_2, and ρ_3 are numerical weighing constants. The performance index was minimized numerically for various values of the numerical constants [2].

Due to the new computer developments and the expanded use of active devices in suspension systems, modern control techniques have been applied in many studies to design actively controlled optimal suspension systems [5,8-11,20,21]. The studies incorporate the use of optimal control laws with a performance index of the general quadratic form:

$$J = \frac{1}{2}\int_0^\infty (x^T Q x + u^T R u)\, dt \qquad (2.8)$$

where x and u are the state and input vectors, respectively, and the matrices Q and R are the weighting matrices. The choice of the optimal active suspension of a single DOF model for a particular application was discussed in some references [2,18]. The suspension form shown in Figure 2.6 was treated as an active system and optimized according to the performance index:

$$J = \frac{1}{2}\int_0^\infty \{u^2 + q\,(y-y_0)^2\}\, dt \qquad (2.9)$$

where u is the control vector and q is a weighing constant. The resulting optimal control vector was found to be

$$u = -\sqrt{q} - \sqrt{2}\,(q)^{\frac{1}{4}}\dot{y} + \sqrt{q}\,y_0 \qquad (2.10)$$

It can be observed that the optimal control vector is a function of the weighing constant and the measured state variables of the system [22]. Sometimes, when it is not convenient to measure all state variables, estimates of state variables from measurements of some output variables can be generated.

Two DOF active vehicle models are commonly faced in the literature [5,6,8,20]. Such a model is shown in Figure 2.7 where the primary suspension is kept as a spring and the actuator controller profile is required to be determined [5].

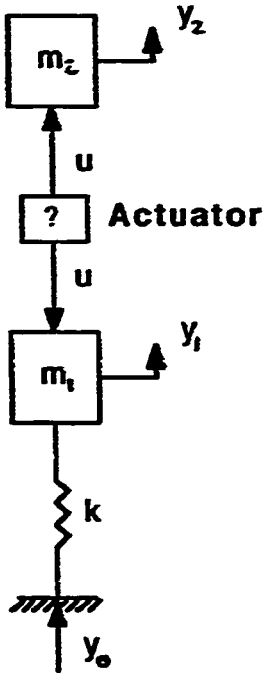

Figure 2.7. Two-DOF active model.

The selected performance index is defined by

$$J = \frac{1}{2}\int_0^\infty \{\rho_1 u^2 + \rho_2 (y_0-y_1)^2 + \rho_3 (y_1-y_2)^2\}\, dt \qquad (2.11)$$

where u is the required control force, and ρ_1, ρ_2, and ρ_3 are the weighing constants. The optimal control force was found to be

$$u = C_1 (y_1-y_2) + C_3 (\dot{y}_1-\dot{y}_2) + (C_1+C_2)(y_2-y_0) + (C_3+C_4)\dot{y}_2 \qquad (2.12)$$

where C_1, C_2, C_3, and C_4 are the coefficients of the feedback gain vector.

Equation (2.12) shows that the control may be realized by an actuator producing a force.

$$f = (C_1+C_2)(y_2-y_0) + (C_3+C_4)\dot{y}_2 \qquad (2.13)$$

in parallel with a spring of stiffness C_1 and a damper with a damping rate C_3 with the absolute body velocity $\dot{y}_2$ and the body displacement relative to the road (y_2-y_0) are required signal inputs to the actuator, [5].

The approaches used to solve the optimization of active suspensions have also dealt with models of higher DOF's [10,11,22]. A four DOF model shown in Figure 2.8, where the random processes λ_1 and λ_2 are modelled as colored noises resulting from the application of first order shaping filters to zero-mean white noise inputs ζ_1 and ζ_2, with their expected values given by:

$$E[\zeta_i(t)\ \zeta_j(t)] = \begin{cases} 2\alpha v\sigma^2 & i=j \\ 0 & i\neq j \end{cases} \qquad i,j=1,2 \qquad (2.14)$$

where E (.) denotes the expected value, σ^2 is the variance of road irregularities, α is a coefficient depending on the shape of road irregularities, and v is vehicle speed.

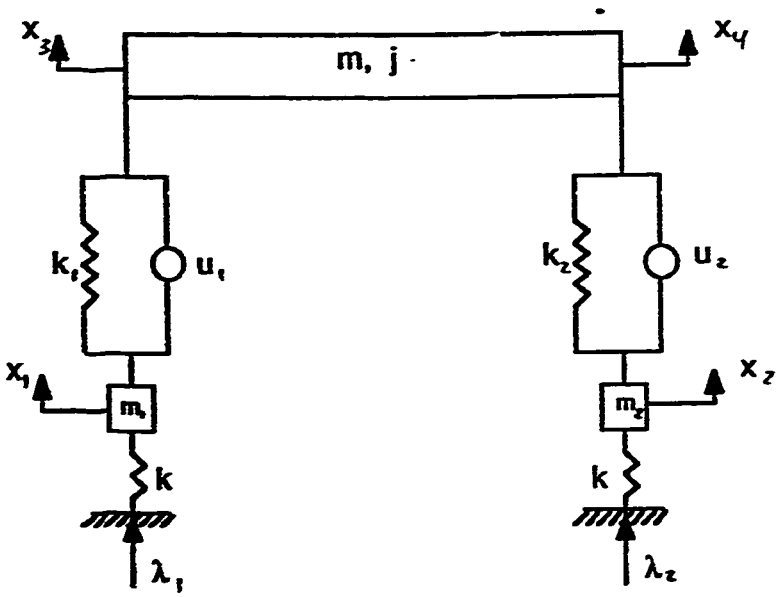

Figure 2.8. Four DOF active model.

The selected performance index is

$$J = E\ [\rho_1 u_1^2 + \rho_2 u_2^2 + \rho_3 (x_1-x_2)^2 + \rho_4 (x_1-\lambda_1)^2 + \rho_5 (x_3-x_4)^2 + \rho_6 (x_3-\lambda_2)^2] \quad (2.15)$$

where ρ_i's refer to the weighing factors. A main result of the study demonstrates that an optimal active suspension system designed as a full state linear regulator can achieve better vibration isolation as compared with passive suspensions, while maintaining comparable levels of suspension deflections and tire force variation [10]. The linear quadratic approach also has been applied to solve the optimization problem of a nine DOF 3-D active model [11].

2.4 Multi-objective Optimization

A suitable choice of the criterion for optimization is a difficult task in the sense that a certain system which is optimum to one criterion may not be optimum with respect to another criterion. Finding solutions which are merely adequate to conflicting objective

problems are no longer possible for the designer in todays competitive industry, and scientists are beginning to devote considerable attention to developing methods for solving such problems. Kuhn and Tucker [23] reported the earliest in-depth work on the formulation of the multiobjective problem. Reviews on the progress in the field have been published in many references [24-26].

The multicriteria techniques are important in the design of complex engineering systems whose quality depends generally on a number of different measures which cannot be combined into a single design criterion. The standard multicriteria optimization problem can be stated as follows:

Minimize: $F_1(x), F_2(x), \ldots\ldots, F_k(x)$

Subject to: $G_i(x) \leq 0, \quad i = 1, 2, \ldots, m$

where $x = (x_1, x_2, \ldots\ldots, x_n)$, are design variables, $F_1(x), F_2(x), \ldots\ldots, F_k(x)$ are the objective functions and $G_i(x)$'s are the constraint functions.

Several methods were proposed by applied mathematicians during the last years for the solution of multicriteria optimization problem. However, most of these methods are suitable for simple linear programming problems and applications to practical design problems faced in the vehicle suspension suspension optimization are still limited.

The multiobjective optimization differs from the single objective optimization since in a multiobjective optimization problem there will be a set of nondominated solutions such that no objective function can be improved without a simultaneous detriment to another objective function. There are many methods to obtain these solutions, such as the Œ - constraint method, the weighing method, the min-max method, the goal programming method and the global criterion method [27-29].

The ϵ-constraint method optimizes one of the objectives subject to the other objectives being constrained for the neighborhood of their respective goals. It is mathematically formulated as:

Find the design vector $x=[x_1, x_2, \ldots, x_n]$ to optimize $F_j(x)$

Subject to: $F_i(x) \leq \epsilon_i$, $i=1, 2, \ldots, n$, $i \neq j$

where ϵ may be varied to generate the Pareto optimal set [27].

The techniques for optimization of single objective problems are well established. It is desirable, therefore, to scalarize the multiobjective problem into a single objective such that a noninferior compromise solution may be found by any standard single objective optimization program. The goal programming method is the most common scalarization method. A preferred solution is defined as the one which minimizes the deviations from a set of goals required by the designer for each of his objectives. Mathematically the method is stated as follows:

$$\text{Minimize} \quad F(x) = \left[\sum_{j=1}^{k} (d_j^+ + d_j^-)^P\right]^{\frac{1}{P}}, \quad P \geq 1$$

$$\text{subject to} \quad F_j(x) - d_j^+ + d_j^- = b_j$$

where b_j is the goal and d_j^+, d_j^- are the respective over or under-achievement of the goal for the jth objective function, $F_j(x)$ [23,27].

Another common scalarization method is the weighted-sum utility function method. The method formulates the objectives into one expression using a product or summation. The most widely used expression is the weighted-sum, where the weights indicate the relative importance of each objective:

$$\text{Minimize} \quad U(x) = \sum_{i=1}^{n} w_i F_i(x)$$

where $\sum_{i=1}^{n} w_i = 1$, and wi is the weight on the ith objective [27,29].

Other methods of scalarization include the global criterion method and the game theory method. The global criterion method finds a compromise solution by minimizing the sum of the squares of the relative deviation of the objectives from their feasible ideal points:

$$\text{Minimize} \quad F(x) = \sum_{i=1}^{n} \left[\frac{F_i(x_i^*) - F_i(x)}{F_i(x_i^*)} \right]^p, \quad P \geq 1$$

$$\text{subject to} \quad G_j(x) \leq 0, \quad j=1, 2, \ldots, m$$

where x_i^* is the optimum vector of the ith objective function, $F_i(x)$ [27,29].

In game theory, the multiobjective optimization problem is viewed as a game problem involving several players, one corresponding to each of the objectives. The system is considered to be under the control of these intelligent adversaries, each seeking to optimize his own gain (objective) at the expense of his opponents, using all the available information [27,29].

The idea of stating the min-max optimum method and applying it to multicriteria optimization problems, was taken from game theory. The min-max optimum compares relative deviations from the separately attainable minima [28].

The mentioned methods have been applied to problems in different areas of engineering and business [28]. In the past two decades, there have been many applications of multiobjective optimization in structural and engineering design fields. The applications include design of mechanisms and dynamic systems [28,30], aircraft and space vehicle

components [22,30], machine tool elements and structures [22,28,31] and engineering design [28,30,32,33].

A multiobjective optimization procedure was applied to design a 5-DOF vehicle suspension system shown in Figure.2.9 [34,35].

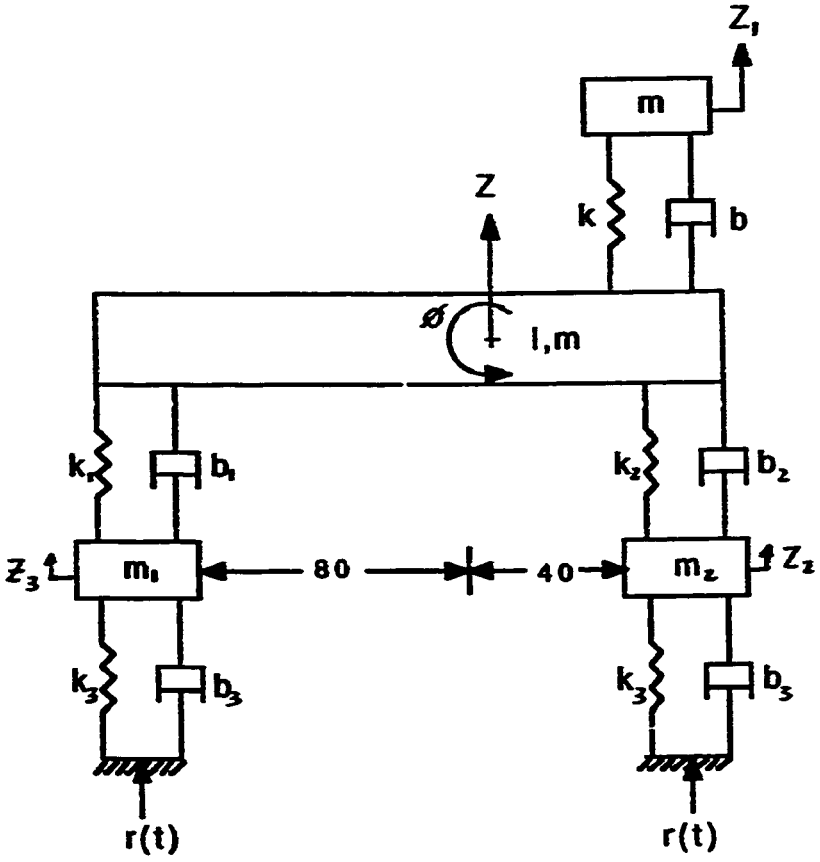

Figure 2.9. Five-DOF vehicle model.

The problem consists of finding stiffness and damping parameters k_1, k_2, k_3, b_1, b_2, and b_3 that optimize the design of the system for a given road condition of the form:

$$r(t) = \begin{bmatrix} x_0\left[1 - \cos w_i(t-t^{i-1})\right], & t^{i-1} \le t \le t^i, \quad i \text{ is odd} \\ x_0\left[1 + \cos w_i(t-t^{i-1})\right], & t^{i-1} \le t \le t^i, \quad i \text{ is even} \end{bmatrix}$$

where x_0 is the amplitude and w_i is the frequency of the sinusoidal waveform input. The satisfactory design is defined as one in which:

i. The acceleration and displacement of the driven seat, $\ddot{Z}_1$, and Z_1, are as small as possible.

ii. The relative displacement between the wheels and the chassis is as small possible.

From these four performance indices a compromised solution was found for stiffness and damping parameters.

In another study a 3-DOF vibration isolation system shown in Figure.2.10 was designed using seven multicriteria methods [29]. The methods used are the method of global criterion method, the utility function method, the bounded objective method, the Lexcicographic method, the goal programming method, the goal attainment method and the game theory method.

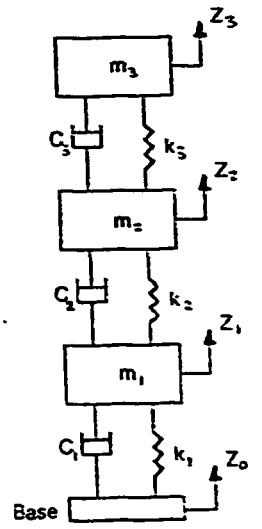

Figure 2.10. Three-DOF vibration isolation system.

The used performance criteria are:

$$J = q \int_0^T [Z_0 - Z_3]^2 dt \qquad (2.16)$$

$$J = \frac{1}{2} \int_0^\infty [k_3 (Z_2 - Z_3)^2 + C_3 (\dot{Z}_2 - \dot{Z}_3)]^2 \, dt \qquad (2.17)$$

where q is a constant, T is duration of the base disturbance which is given by:

$$Z_0 = 21.2\, t^{1.5}\, e^{-4t} \sin (e^{-1.89t} - 1) \qquad (2.18)$$

It was found in the study that the game theory method can be considered to be very efficient in finding a proper balance between the optimum values of the different objective functions even though that the method required the maximum computational effort.

Heavy emphasis was given to the game theory in a study dealing with the same 3-DOF vibration isolation system [36]. Assuming that the two players (objective functions) given by Equation.(2.16) and Equation.(2.17) start bargaining from a reference design vector x_i, a bargaining model or a supercriterion was expressed as:

$$S = [J_1(x_i) - J_1(x_c)]\, [J_2(x_i) - J_2(x_c)] \qquad (2.19)$$

where x_c known as Pareto-optimal solution, is obtained by minimizing a combined objective function:

$$J_c = w_1 J_1 + w_2 J_2 \qquad (2.20)$$

where $w_1 \geq 0$, $w_2 \geq 0$, and $w_1 + w_2 = 1$

It was observed that at the optimum design (with J_1 and J_2 as the objectives), all the damping coefficients are at their lower bounds. It was also found that the minimization of

J_1 indicates that at the optimum design, the stiffness of the first spring (k_1) is very large compared to those of the other two springs while the minimization of J_2 shows that all the springs have approximately the same stiffness at the optimum point. The study demonstrates also the successful application of game theory in finding a best trade-off between the two objectives which optimizes a stated supercriterion.

2.5 Objectives of the Proposed Research

The objective of the proposed research is to investigate the responses of passive vehicle suspension models in order to obtain a better understanding of their performance limits. It is also proposed to apply the multiobjective optimization methods to the vehicle suspension models to determine the suspension parameters that will produce certain desirable responses.

Specifically it is proposed to accomplish the following objectives:

1. An investigation of the responses of different 1-DOF models when subjected to the road input described by Equation (2.1) and when subjected to additional aerodynamic forces described by Equation (2.2). The 1-DOF models include suspensions of the following types:
   i. Maxwell type suspension.
   ii. Maxwell type suspension that is in parallel with a spring.
   iii. Voigt type suspension that is in series with a spring.
   iv. Voigt type suspension that is in series with a spring and both are in parallel with a spring.
   v. Voigt type suspension that is in series with a spring and both are in parallel with Maxwell type suspension.

2. An investigation of the responses of different 2-DOF models when subjected to the road input described by Equation (2.2). The secondary suspensions of the different 2-DOF models are of the same types as those listed in (1) above.

3. Application of multiobjective optimization methods to determine the suspension parameters of a 2-DOF model that can be used to obtain certain desirable responses.

CHAPTER 3

RESPONSE OF 1-DOF SUSPENSION SYSTEMS TO RANDOM EXCITATIONS

This research has been initiated to use the multiobjective optimization methods for passive vehicle suspension optimization. Performance objectives were rms acceleration of vehicle body and rms relative displacement of suspension. They were to be minimized separately in a multiobjective fashion to obtain the optimum suspension parameters. However, preliminary studies have shown that there were multiple values of suspension parameters giving the same levels of rms acceleration and rms relative displacement. This behavior made the optimization program converge to different solutions when the initial starting point changed. Since no satisfactory answer to this problem could be found in the open literature, it has become necessary first to make a detailed study of the performance of various suspension configurations in order to get a detailed knowledge about these suspension systems.

In this chapter, the response of different 1-DOF suspension models are analyzed when subjected to random excitations. First, systems responses are obtained when they are subjected to road inputs as described in Chapter 2. Then they are studied when subjected to additional external force inputs as described in Chapter 2.

3.1 Response of 1-DOF Model with Maxwell Type Suspension to Random Excitations

The 1-DOF suspension model of Maxwell type, shown in Figure 3.1, consists of a vehicle mass m, an equivalent spring with coefficient k and a dashpot with a damping coefficient b. Although this suspension cannot support a static load, it is used as a starting point in our investigations. Since it was shown to be the optimum suspension configuration for a vehicle subjected to random input only [2].

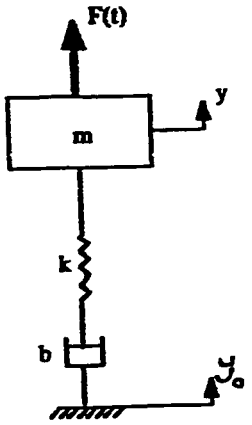

Figure 3.1. 1-DOF suspension system of Maxwell type.

a. The response to the road input only, i.e, F(t) = 0:

The mean square relative displacement and the mean square acceleration responses of the mass owing to the road input only are derived as shown in Appendix A and are given by:

$$\overline{\Delta y_g^2} = C.\left(\frac{m}{b} + \frac{b}{k}\right) \qquad (3.1)$$

and

$$\overline{a_g^2} = C.\frac{k.b}{m^2} \qquad (3.2)$$

where, $C = \pi .A.V$

In order to simplify the analysis of the acceleration and the relative displacement responses, Equations (3.1) and (3.2) are written in the following forms;

$$\overline{\Delta y_g^2} = C.\left(\frac{1}{B} + \frac{B}{K}\right) \qquad (3.3)$$

and

$$\overline{a_g^2} = C.K.B. \tag{3.4}$$

where B = b/m and K = k/m. Above equations show that the responses depend on the ratios of stiffness to mass and damping coefficient to mass. The rms (root mean square) relative displacement Δd_g is given by

$$\Delta d_g = \left[C.\left(\frac{1}{B} + \frac{B}{K}\right)\right]^{1/2} \tag{3.5}$$

and the rms acceleration is given by

$$a_g = [C.K.B]^{1/2} \tag{3.6}$$

To investigate the limits on B and K, based on given levels of acceleration and relative displacement, we obtain the relation (see Appendix B).

$$B = \left(\frac{K}{2}\right)^{1/2} \tag{3.7}$$

for the case where

$$a_g^2(\Delta d_g)^6 = \frac{27}{4}C^4 \tag{3.8}$$

But the limiting performance is $a_g^2.(\Delta dg)^6 \geq \frac{27}{4}C^4$, as shown in Appendix B. There is no feasible solution otherwise.

Some earlier investigations used a performance index of the form [2].

$$J = a_g^2 + \rho \Delta d_g^2 \tag{3.9}$$

to get the optimum K and B values for each ρ, where ρ is a weighing factor. By substituting for a_g and Δd_g in Equation (3.9), it can be written as,

$$J = C.K.B + \rho\left(C.\left(\frac{1}{B} + \frac{B}{K}\right)\right) \qquad (3.10)$$

Minimizing J with respect to K and B gives [2],

$$K = (\rho)^{1/2} \qquad (3.11)$$

$$B = \frac{(\rho)^{1/4}}{(2)^{1/2}} \qquad (3.12)$$

and substituting in Equation (3.12), we get the same relation

$$B = (K/2)^{1/2} \qquad (3.13)$$

This result indicates a damping ratio of 0.707. We also get the optimum relation between $^{a}{}_{g}$ and $^{\Delta d}{}_{g}$ as in Equation (3.8). Minimizing the relative displacement. with respect to B gives,

$$B = K^{1/2} \qquad (3.14)$$

which is shown in Figure 3.2.

To get a better understanding of the performance of suspension, contours are plotted for constant rms acceleration and rms relative displacement values in Figure (3.2). The optimum line given by Equation (3.7) is indicated on the figure. However, for the same values of rms relative displacement, there are two points - one corresponding to an overdamped optimum and the other to an underdamped optimum, such as points P_o and P_u, respectively. Point P has a damping ratio of 0.707.

When the K values are much larger than the B^2 values (where the damping ratio is less than 0.707), the rms relative displacement of Equation (3.5) will have the form

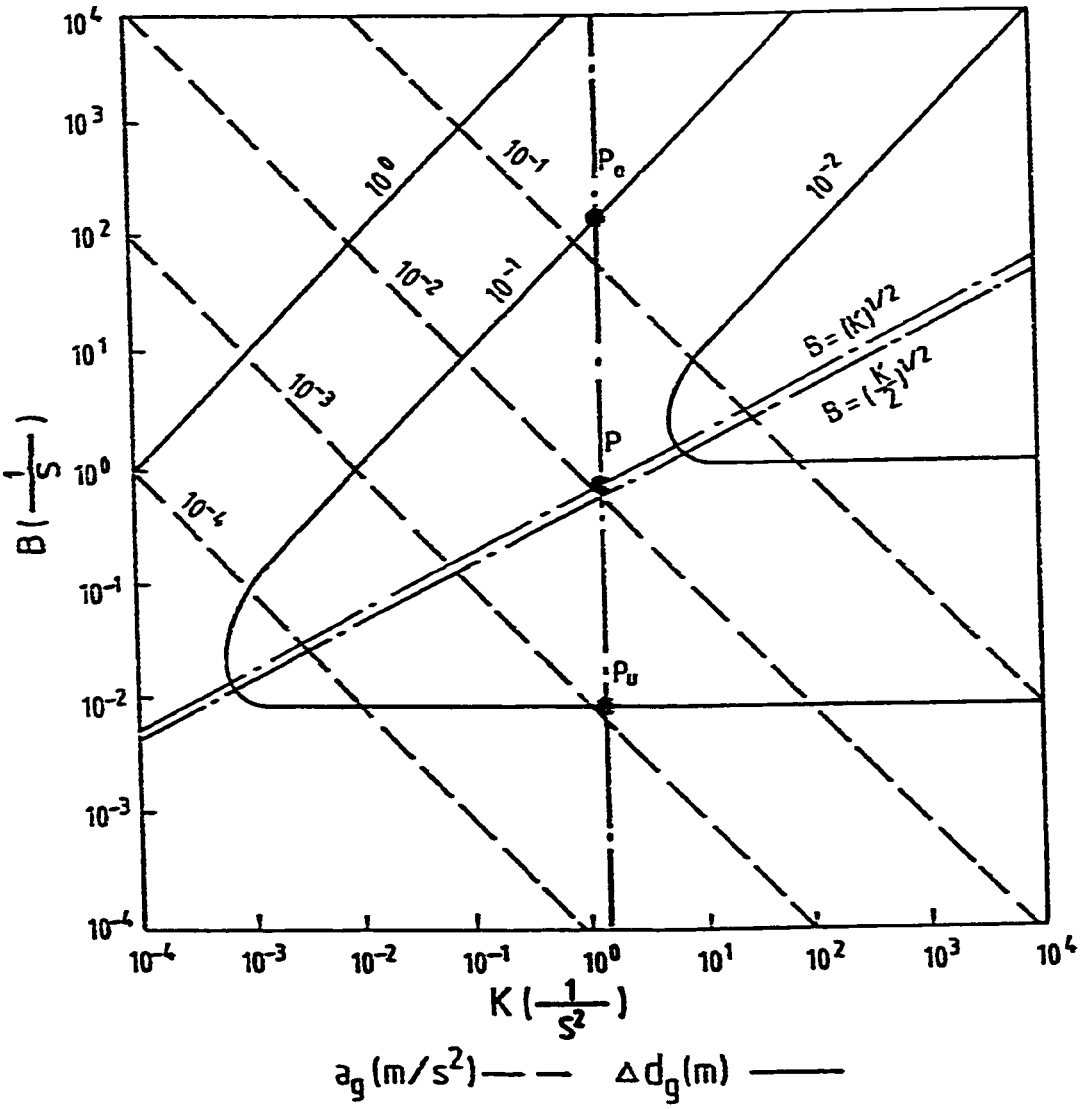

Figure 3.2 Contours of constant rms acceleration and constant rms relative displacement.

$$\Delta d_g \approx \left(\frac{C}{B}\right)^{1/2} \tag{3.15}$$

which indicates that, the rms value of relative displacement is not a function of K. On the other hand, when $B^2 \gg K$ (where the damping ratio is larger than 0.707), the rms relative displacement of Equation (3.5) will have the form;

$$(\Delta d_g)^2 \approx \frac{C B}{K} \tag{3.16}$$

or

$$B \approx \frac{(\Delta dg)^2}{C} . K \tag{3.17}$$

which indicates that K and B will be related linearly for constant Δd_g.

Similarly, writing Equation (3.6) in the form

$$B = \frac{a_g^2}{C K} \tag{3.18}$$

We note that for constant acceleration values, there is a hyperbolic relation relating B and K regardless of the damping ratio, which becomes a linear relation in the log-log scale. Lines of constant acceleration with a slope of (-1) appear on Figure 3.2.

Variation of rms acceleration with rms relative displacement for constant values of K and B are shown in Figure 3.3. There is a limiting line given by relation (3.8), which is also shown on the Figure 3.3.

A closer investigation of Equation (3.5) shows that for low values of B, it can be written as

$$(\Delta d_g)^2 \approx \frac{C}{B} \tag{3.19}$$

Solving Equation (3.6) for B, we also get

$$B = \frac{a_g^2}{(C K)} \tag{3.20}$$

Substituting for B in Equation (3.19), the rms relative displacement of Equation (3.19) can be written in the form;

$$(\Delta d_g)^2 = \frac{C^2 K}{a_g^2} \tag{3.21}$$

or

$$\Delta d_g = C.(K)^{1/2}.\frac{1}{a_g} \tag{3.22}$$

This means that for constant K values, the rms acceleration is inversely proportional for the rms relative displacement. The logarithmic plot of constant values in Figure 3.3 demonstrates this result. However, for large B values, the plot shows that a linear relation exists between the rms relative displacement and the rms acceleration. For large B values Equation (3.5) can be written as

$$(\Delta d_g)^2 = \frac{CB}{K} \tag{3.23}$$

Substituting B Equation (3.6) in Equation (3.23), we can write

$$\Delta d_g = \frac{a_g}{K} \tag{3.24}$$

The linear relation between the rms relative displacement and the rms acceleration explains the linear behavior of the contours for constant values of K in Figure 3.3.

By substituting K in Equation (3.6) into Equation (3.5), we obtain

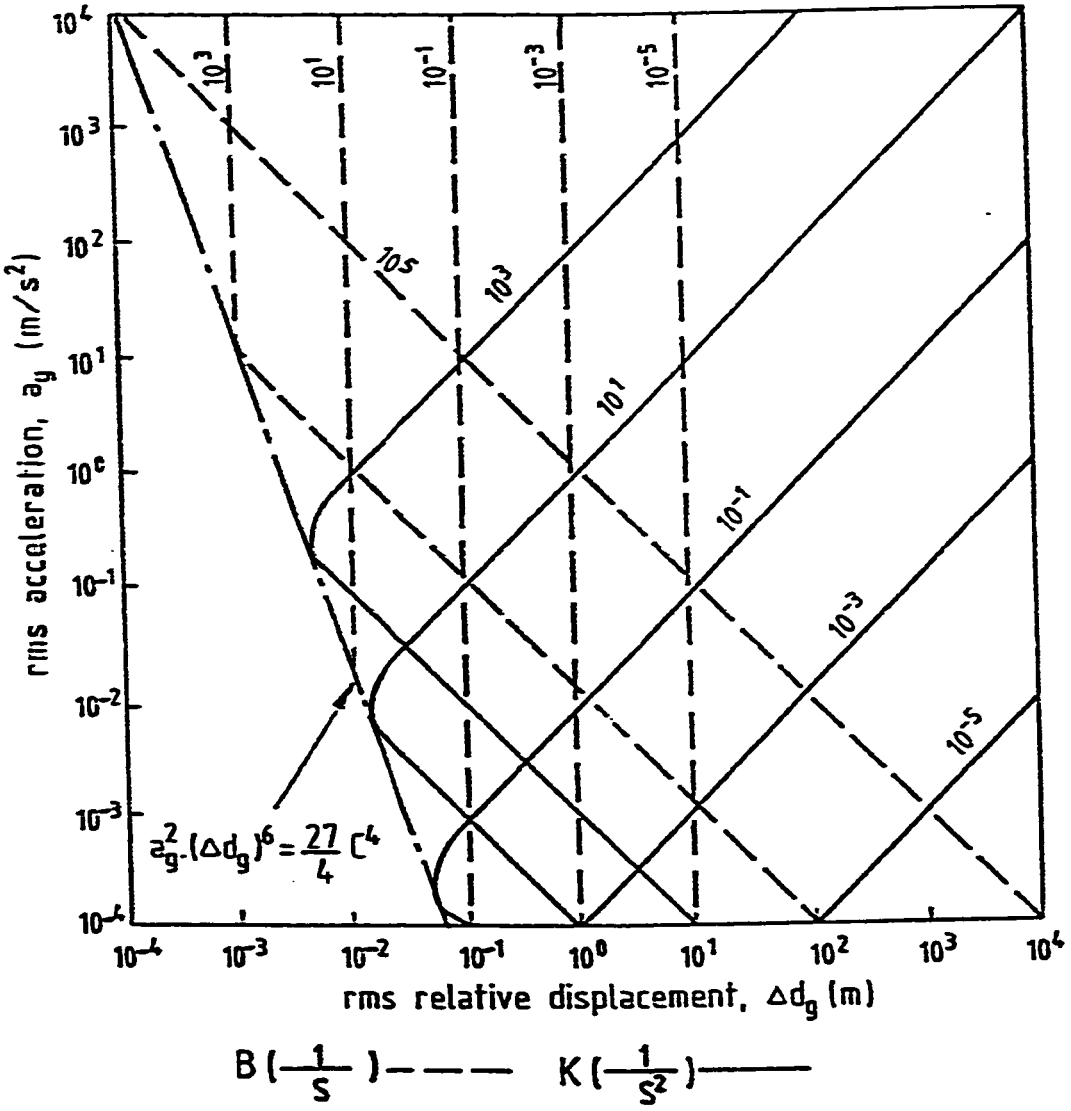

Figure 3.3 Contours of constant B and K values.

$$(\Delta d_g)^2 = \frac{C}{B} + \frac{C^2B^2}{a_g^2} \qquad (3.25)$$

From this equation, we can expect to have a rms value of relative displacement approximately equal to $(C.B/a_g)\ a_g^2$ is less than CB^3. This indicates that for constant B value, rms relative displacement is inversely proportional to rms acceleration as shown in Figure 3.3. On the other hand, when the value of B is very small, rms relative displacement becomes

$$\Delta d_g \approx (\frac{C}{B})^{1/2} \qquad (3.26)$$

Δd_g will be only a function of B explaining the existence of vertical lines in Figure 3.3 when small B values are used.

In Appendix B, it was shown that the relation

$$a_g^2(\Delta d_g)^6 \geq \frac{27}{4}C^4 \qquad (3.27)$$

provides a feasible region for this suspension system. The limiting line in Equation (3.14) is shown on Figure 3.3. It was also found in Appendix B that

$$\Delta d_g > (\frac{C}{B})^{1/2} \qquad (3.28)$$

or rms relative displacement for this suspension can never be less than the value of $(C/B)^{1/2}$. This will put a limit on the value of B during optimization for a required rms relative displacement.

b. The response to the external force and road input:

Since the models used in this study are linear, response of models to different inputs are summed up to obtain the total response. Response to the external force for this model

could not be obtained because of the form of transfer function and the form of force spectrum, as explained in Appendix A. It is evident that the suspension element (Figure 3.1) cannot support a static load, it can only compensate for disturbing perturbations.

3.2 Response of 1-DOF Model with Maxwell Type Suspension in Parallel with a Spring to Random Excitations

The model shown in Figure 3.4 represents a 1-DOF suspension system of Maxwell type in parallel with a spring. It consists of a vehicle mass M with two springs of coefficients k_1 and k_2 and a dashpot of coefficient b_2.

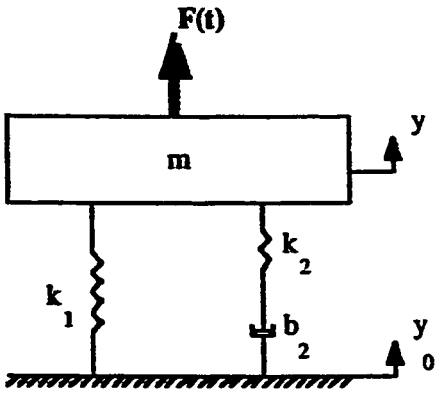

Figure 3.4. 1-DOF suspension system of Maxwell type in parallel with a spring.

a. The response to the road input only, i.e., F(t) = 0:

The mean square relative displacement and the mean square acceleration responses of the mass due to the road input only are derived as shown in Appendix A and are given by:

$$\overline{\Delta y_g^2} = C.\left(\frac{b_2}{k_2^2}(k_1 + k_2) + \frac{m}{b_2}\right) \qquad (3.29)$$

and

$$\overline{a_g^2} = C.\left(\frac{b_2}{m^2 k_2}(k_1 + k_2)^3 + \frac{k_1^2}{m b_2}\right) \qquad (3.30)$$

where, $C = \pi . A.V.$

The analysis is simplified by writing Equations (3.29) and (3.30) in the following form;

$$\overline{\Delta y_g^2} = C.\left(\frac{B_2}{K_2^2}(K_1 + K_2) + \frac{1}{B_2}\right) \qquad (3.31)$$

and

$$\overline{a_g^2} = C.\left(\frac{B_2}{K_2}(K_1 + K_2)^3 + \frac{K_1^2}{B_2}\right) \qquad (3.32)$$

where $B_2 = b_2/m$, $K_1 = k_1/m$ and $K_2 = k_2/m$. The above equations display that the relative displacement and the acceleration responses are dependent on the ratios of stiffness to mass and damping coefficient to mass. The rms relative displacement is given by:

$$\Delta d_g = \left(C.\left(\frac{B_2}{K_2^2}(K_1 + K_2) + \frac{1}{B_2}\right)\right)^{1/2} \qquad (3.33)$$

and the rms acceleration is given by

$$a_g = \left(C.\left(\frac{B_2}{K_2^2}(K_1 + K_2)^3 + \frac{K_1^2}{B_2} \right) \right)^{1/2} \qquad (3.34)$$

An investigation on the limits of B_2 and K_2, based on given levels of relative displacement, we obtain the relations (in Appendix B) as

$$B_2 = \frac{K_2}{(K_1 + K_2)^{1/2}} \qquad (3.35)$$

and

$$\Delta d_g = \left(\frac{2C(K_1 + K_2)^{1/2}}{K_2} \right)^{1/2} \qquad (3.36)$$

The same relation in Equation (3.35) can be obtained if the relative displacement is minimized with respect to B_2. As it is shown in Appendix B, we can obtain the relation

$$B_2 = \frac{K_1 K_2}{(K_1 + K_2)^{3/2}} \qquad (3.37)$$

and

$$a_g = \left(\frac{2CK_1}{K_2}.(K_1 + K_2)^{3/2} \right)^{1/2} \qquad (3.38)$$

when we use Equation (3.34). The same relation (3.37) can be obtained if the acceleration is minimized with respect to B_2. Details of derivation are provided in Appendix B.

If a small value of K_1 is considered, then Equations (3.33) and (3.34) will have the forms,

$$\Delta d_g \approx \left[C.\left(\frac{B_2}{K_2} + \frac{1}{K_2} \right) \right]^{1/2} \qquad (3.39)$$

and

$$a_g \approx [C.\, K_2.\, B_2]^{1/2} \tag{3.40}$$

We note that the rms relative displacement and the rms acceleration have the same forms as those given by Equations (3.5) and (3.6). This result clearly appears in Figure 3.5 where the rms acceleration and the rms relative displacement contours show to be exactly similar to those in Figure 3.2. In this case, the behavior of contour lines is explained in the same manner as those of Figure 3.2 in Section 3.1. The limiting line given by Equation (3.35) is shown on Figure (3.5). From Equation (3.33) we can see that if B_2^2 is much smaller than K_2, then the rms relative displacement can be found as,

$$\Delta d_g \approx \left[C.\, \frac{1}{B_2}\right]^{1/2} \tag{3.41}$$

or

$$B_2 \approx \frac{C}{(\Delta d_g)^2}$$

Equation (3.41) explains the existence of constant B_2 values in Figures (3.5) and (3.6), when constant rms relative displacement levels are used.

Equation (3.33) can be written in the form,

$$K_2^2 = \frac{CB_2^2(K_1 + K_2)}{B_2(\Delta dg)^2 - C} \tag{3.42}$$

If $K_1 \gg K_2$, then K_2 can be solved as,

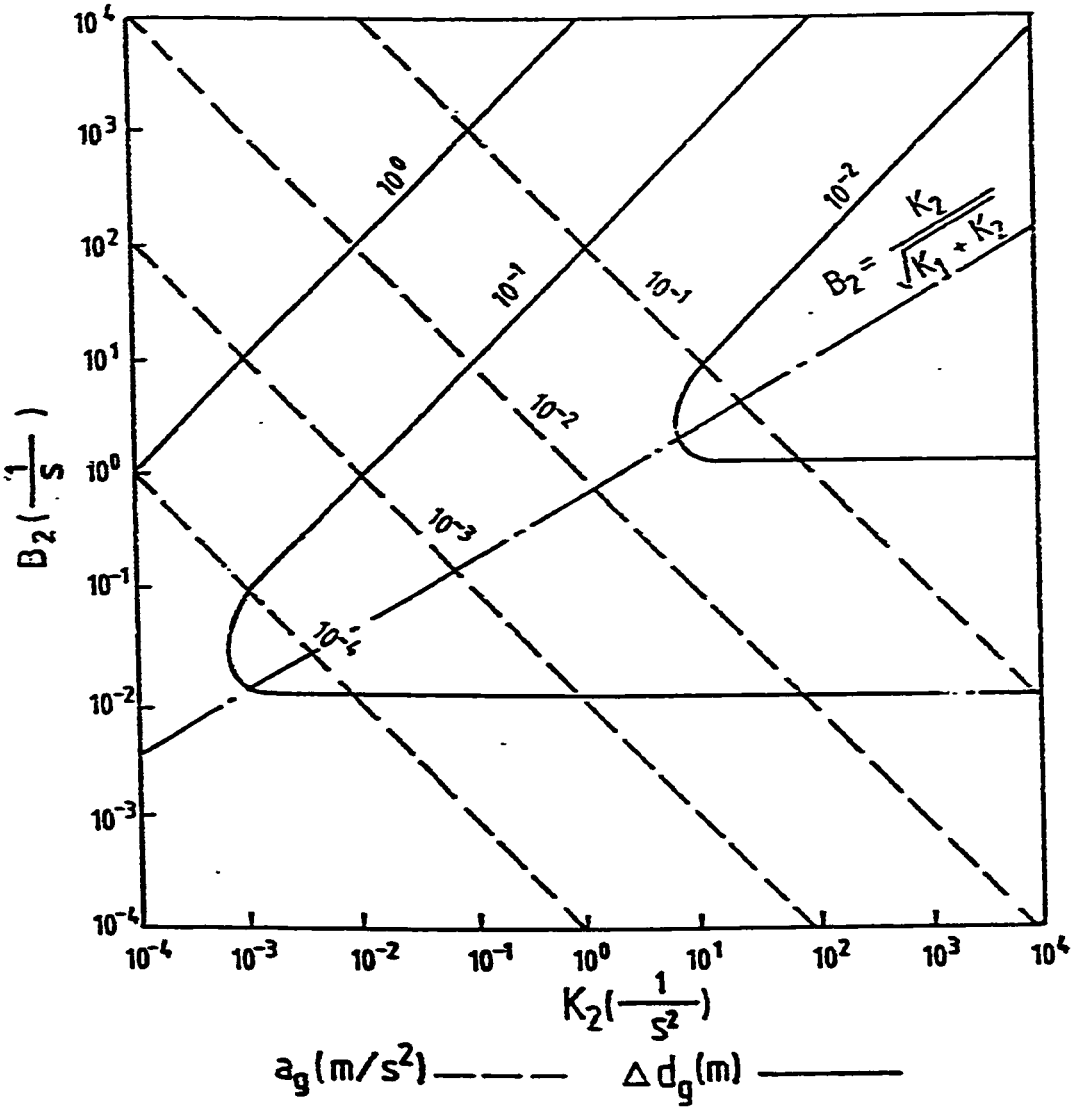

Figure 3.5 Contours of constant rms acceleration and constant rms relative displacement. ($K_1 = 10^{-6}\frac{1}{s^2}$)

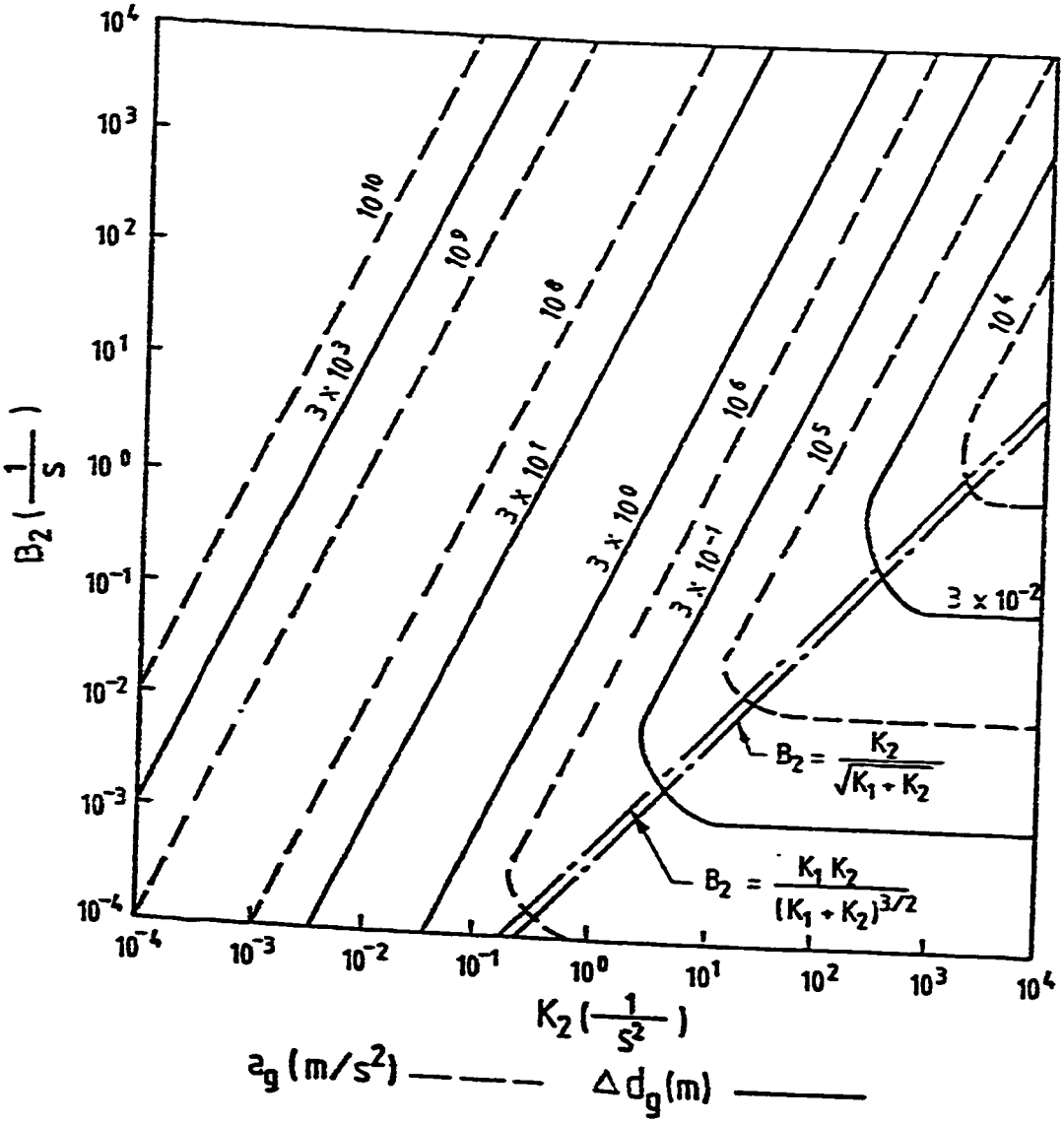

Figure 3.6 Contours of constant rms acceleration and constant rms relative displacement. ($K_1 = 10^6 \frac{1}{s^2}$)

$$K_2 \approx \left(\frac{CB_2^2 K_1}{B_2 (\Delta d_g)^2 - C} \right)^{1/2} \tag{3.43}$$

In Equation (3.43), if

$$B_2 \cdot (\Delta d_g)^2 \gg C \tag{3.44}$$

then, Equation (3.43) could be written as

$$K_2 \approx \left(\frac{CB_2}{(\Delta d_g)^2} \right)^{1/2} \tag{3.45}$$

which is a linear relation between K_2 and B_2 in the log-log scale for constant K_1 constant rms relative displacement values as shown in Figure 3.6.

If $B_2^2 \ll K_2$, when $K_1 \ll K_2$, Equation (3.34) can be approximated by the following relation:

$$a_g^2 \approx C \left(\frac{K_1^2}{B_2} \right) \tag{3.46}$$

If Equation (3.46) is solved for B_2, then

$$B_2 \approx \frac{C \cdot K_1^2}{a_g^2} \tag{3.47}$$

which has a constant value if $^{a}\varepsilon$ is constant, as shown in Figure 3.6.

For $K_1 \gg K_2$, Equation (3.34) can be solved for K_2 as,

$$K_2 \approx \left(\frac{CB_2^2 K_1^3}{B_2 a_g^2 - CK_1^2} \right)^{1/2} \tag{3.48}$$

Then if,

$$B_2 \cdot a_g^2 \gg CK_1^2 \tag{3.49}$$

then Equation (3.48) can be solved as,

$$K_2 \approx \left(\frac{CB_2 K_1^3}{a_g^2} \right)^{1/2} \tag{3.50}$$

Relations (3.48) and (3.50) can be viewed from Figure 3.6. On the figure, also shown the limiting lines given by Equations (3.35) and (3.37).

In Figure 3.7, contours of constant rms acceleration and rms relative displacement values are shown when K_1 has a medium value. B_2 appears to have constant values in some regions when $K_2 \gg K_1$. Two possibilities exist in this case and can be investigated from Equation (3.33). When $K_2 \gg K_1$, Equation (3.33) can be evaluated according to the following relation,

$$(\Delta d_g)^2 \approx \frac{CB_2}{K_2} + \frac{C}{B_2} \tag{3.51}$$

Then, if $B_2^2 \ll K_2$, equation (3.51) will have the form,

$$(\Delta d_g)^2 \approx \frac{C}{B_2} \tag{3.52}$$

else, if $B_2^2 \gg K_2$, then

$$(\Delta d_g)^2 \approx \frac{CB_2}{K_2} \tag{3.53}$$

From Equation (3.52), it is clear that B_2 will have constant values when the rms relative displacement is taken to be constant and from Equation (3.53) we can see that a linear relation exists between B_2 and K_2 for constant rms relative displacement values.

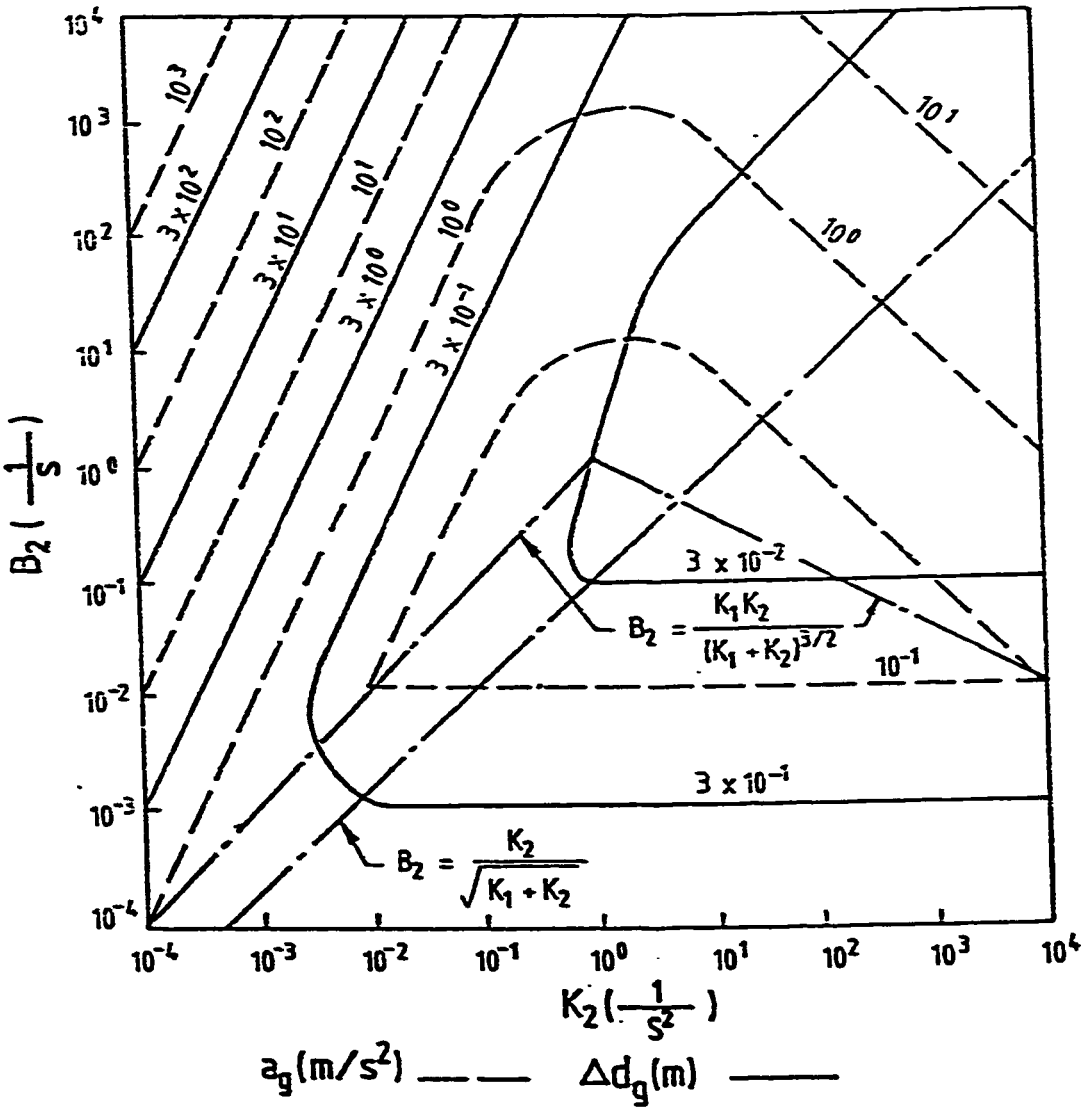

Figure 3.7 Contours of constant rms acceleration and constant rms relative displacement. ($K_1 = 10^0\,\frac{1}{s^2}$)

On the other hand, when $K_1 \ll K_2$, then Equation (3.33) will have the form,

$$(\Delta d_g)^2 \approx \frac{CB_2^2 K_1}{K_2^2} + \frac{C}{B_2} \tag{3.54}$$

or

$$K_2^2 \approx \frac{CB_2^2 K_1}{B_2^2 (\Delta d_g)^2 - C} \tag{3.55}$$

Then, if

$$B_2^2 (\Delta d_g)^2 \gg C \tag{3.56}$$

Equation (3.55) will be

$$K_2^2 \approx \frac{C B_2^2 K_1}{(\Delta d_g)^2} \tag{3.57}$$

This indicates a linear relationship between K_2 and B_2^2, as shown in Figure 3.7.

If $K_2 \gg K_1$, then Equation (3.34) can be written as

$$a_g^2 \approx C B_2^2 K_2 + \frac{CK_1^2}{B_2^2} \tag{3.58}$$

Then if $B_2^2 \gg K_1$, we have

$$a_g^2 \approx C B_2^2 K_2 \tag{3.59}$$

For a constant rms acceleration, this indicates an inverse relation between B_2 and K_2, as shown in Figure 3.7 at the upper right corner. The second case arises if B_2 is very small, then Equation (3.58) will have the form,

$$a_g^2 \approx \frac{C}{B_2} K_1^2 \tag{3.60}$$

This indicates that for constant rms acceleration, B_2 will be constant as shown in Figure 3.7 at the lower right corner.

Solving Equation (3.34) for K_2 when $K_2 \gg K_1$, we get

$$K_2 \approx \left(\frac{C B_2^2 K_1^3}{B_2 a_g^2 - C K_1^2} \right)^{1/2} \tag{3.61}$$

and in addition, if we have

$$B_2 a_g^2 \gg C K_1^2 \tag{3.62}$$

then,

$$K_2 \approx \left(\frac{C B_2 K_1^3}{a_g^2} \right)^{1/2} \tag{3.63}$$

This relation shown in the upper left portion of Figure 3.7 for contours of constant acceleration values. The lines represented by Equations (3.35) and (3.37) can be observed on the figure.

In Figure 3.8, contours of constant K_2 and B_2 values are plotted when K_1 has a very small value. The contours behave exactly similar to those in Figure 3.3 due to the negligible effect of K_1 on the suspension performance in this case.

When the K_2 and B_2 contours are plotted for a larger K_1 value as shown in Figure 3.9, we notice that the rms acceleration and rms relative displacement achieve higher values and there are two limited regions where no rms values appear.

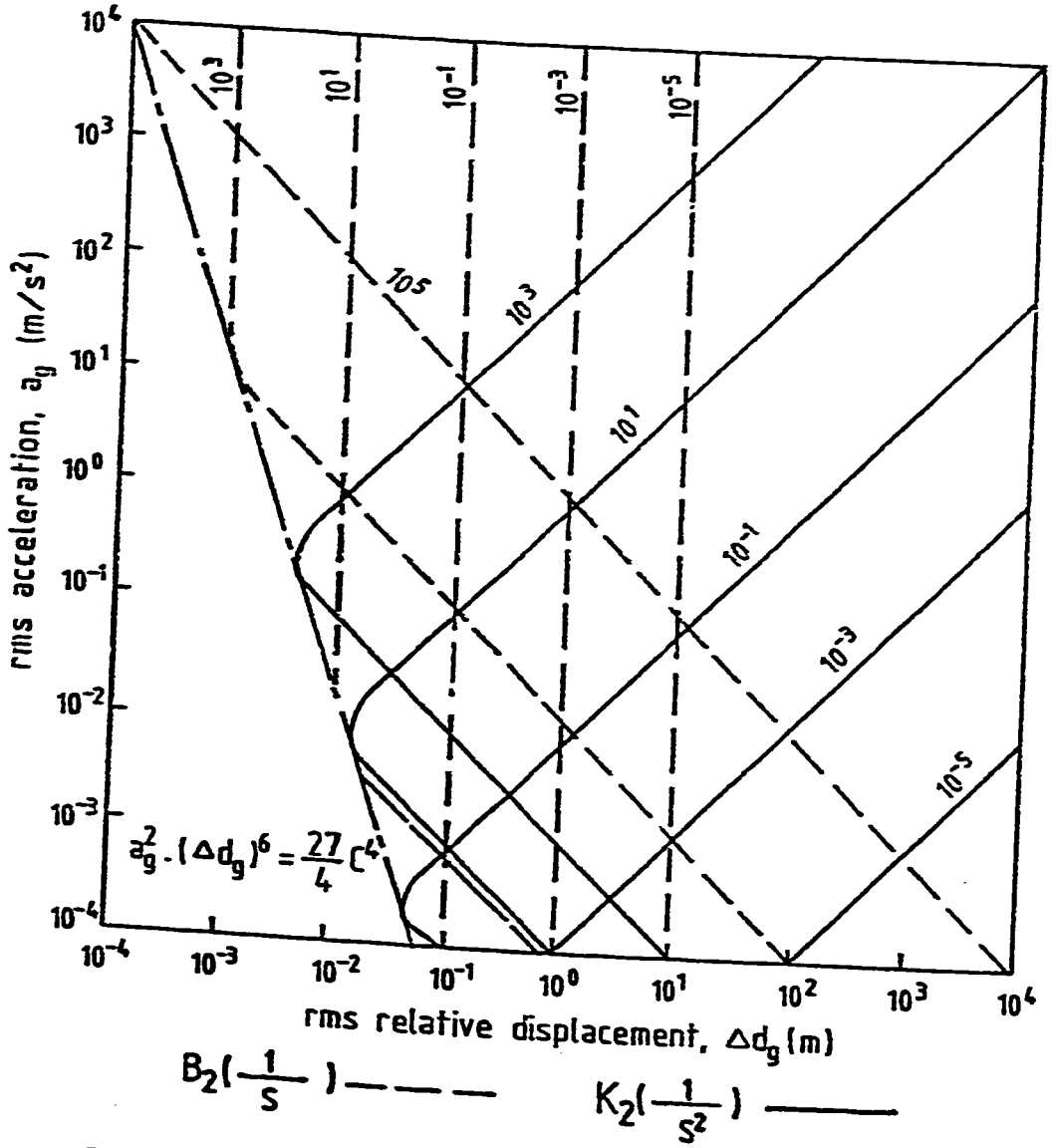

Figure 3.8 Contours of constant B_2 and K_2 values. ($K_1 = 10^{-6} \frac{1}{s^2}$)

The first region is similar to the one in Figure (3.8), where;

$$a_g^2.(\Delta d_g)^6 < \frac{27}{4}C^4 \qquad (3.64)$$

The other limited region exists because of the linear relation between Δd_g and a_g when the smaller K_2 values are used. If K_2 is small and K_1 is equal to ($1/s^2$) as in Figure 3.9, then Equations (3.33) and (3.34) can be written as,

$$\Delta d_g = \left[C.\left(\frac{B_2 K_1}{K_2^2} + \frac{1}{B_2}\right)\right]^{1/2} \quad (K_1 = \frac{1}{s^2}) \qquad (3.65)$$

and

$$a_g = \left[C.\left(\frac{B_2 K_1^3}{K_2^2} + \frac{K_1^2}{B_2}\right)\right]^{1/2} \quad (K_1 = \frac{1}{s^2}) \qquad (3.66)$$

which are equal in value and this behavior explains the availability of the 2nd limited region on the right lower region in the Figure 3.9. Also, in Figure 3.9 we can see that the rms relative displacement becomes constant when K_2 is much larger than B_2^2, and K_1 as indicated by the vertical lines in Figure 3.9. In this case, Equation (3.33) behaves according to the form,

$$\Delta d_g = \left(C.\frac{1}{B_2}\right)^{1/2} \qquad (3.67)$$

which shows that for a constant rms relative displacement, B_2 values can not be less than given by Equation (3.67).

b. The response to the external force and the road input:

The mean square relative displacement and the mean square acceleration of the mass due to the external force only are derived as shwon in Appendix A and given by:

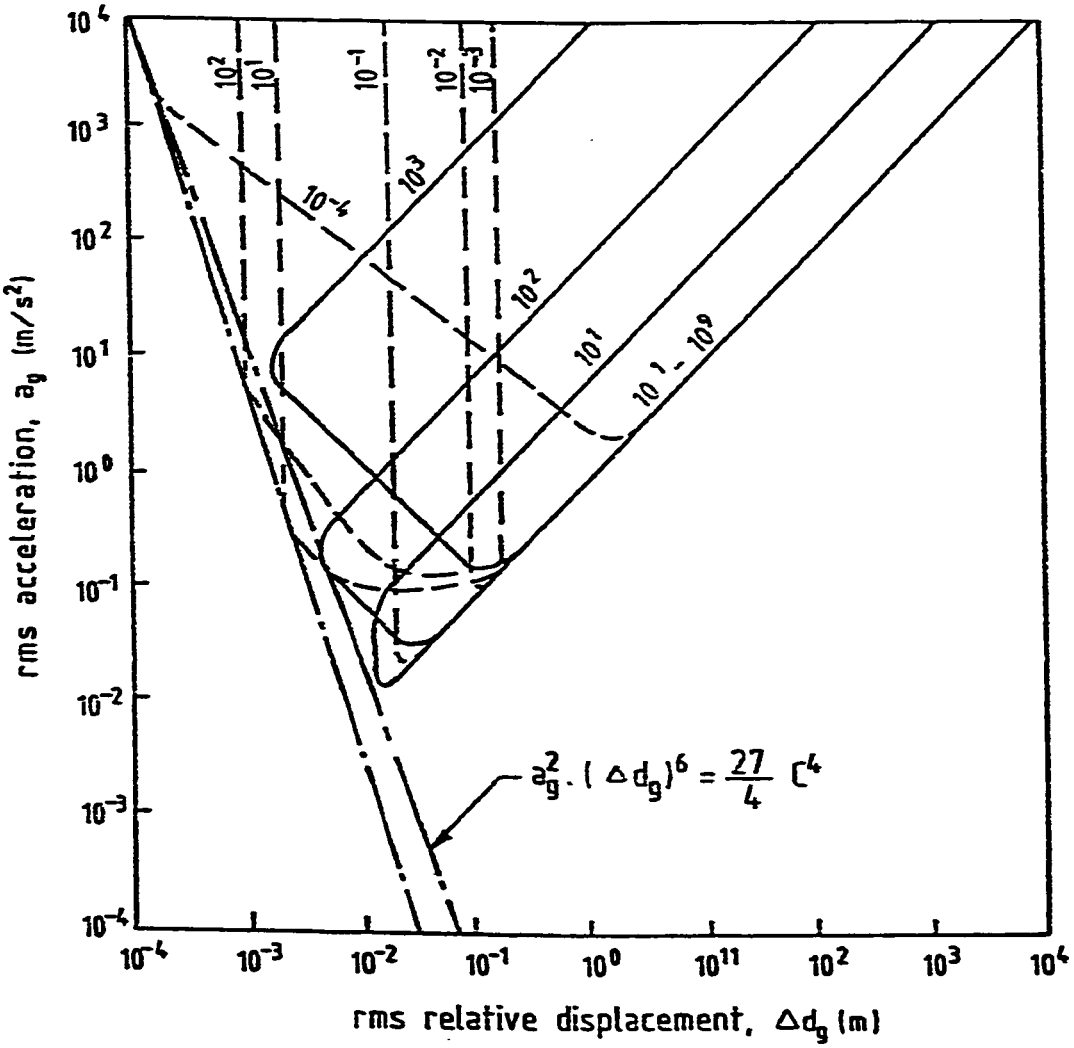

Figure 3.9 Contours of constant B_2 and K_2 values. ($K_1 = 10^0 \frac{1}{s^2}$)

$$\Delta y_F^2 = R.\ \frac{NUM\,1}{DEN\,1} \tag{3.68}$$

where

$$R = \pi \beta.\ \upsilon$$

$$NUM1 = b_2^2 k_1 k_2 um(k_2 + b_2\upsilon) - k_2^2 mb_2(k_1 k_2 + b_2\upsilon)$$
$$(k_1 + k_2) + mk_2^2(k_2 + b_2\upsilon)\left(b_2(k_1 + k_2) + mk_2^2\right) \tag{3.69}$$

and

$$DEN1 = k_1 k_2 \upsilon\left(-k_1 k_2 m^2(k_2 + b_2\upsilon)^2 - mb_2(k_1 k_2 + b_2\upsilon + k_2)\right)^2$$
$$+ m(b_2\upsilon + k_2)\left(b_2(k_1 + k_2) + mk_2\upsilon\right) + \left(k_1 + k_2 + b_2\upsilon(k_1 + k_2)\right) \tag{3.70}$$

and

$$a_F^2 = R.\ \frac{NUM\,2}{DEN\,2} \tag{3.71}$$

where

$$NUM2 = b_2^2 k_1 k_2 um(k_2 + b_2\upsilon) + b_2^2(k_1 k_2 + b_2\upsilon(k_1 + k_2))$$
$$+ mb_2 k_2^2(k_1 k_2 + b_2\upsilon(k_1 + k_2)) \tag{3.72}$$

$$DEN2 = mb_2\left[-k_1 k_2 um^2(k_2 + b_2\upsilon)^2 - mb_2\left(k_1 k_2 + b_2\upsilon(k_1 + k_2)\right)^2\right]$$
$$+ m(b_2\upsilon + k_2)\left(b_2(k_1 + k_2) + mk_2\upsilon\right)\left(k_1 k_2 + b_2\upsilon + b_2\upsilon(k_1 + k_2)\right) \tag{3.73}$$

The analysis of the acceleration and relative displacement is made simpler by writing Equations (3.68) and (3.71) in the following form:

$$\Delta y_F^2 = R.\ \frac{NUM\,3}{DEN\,3} \tag{3.74}$$

where

$$NUM3 = B_2^2K_1K_2\upsilon(K_2 + B_2\upsilon) - K_2^2B_2(K_1K_2 + B_2\upsilon(K_1 + K_2)) + K_2^2 (K_2 + B_2\upsilon)(B_2(K_1 + K_2) + K_2\upsilon) \tag{3.75}$$

and

$$DEN3 = m^2K_1K_2\upsilon(-K_1K_2\upsilon(K_2 + B_2\upsilon))^2 - B_2((K_1K_2 + B_2\upsilon(K_1 + K_2))^2 + (B_2\upsilon + K_2)(B_2(K_1 + K_2) + K_2\upsilon)(K_1K_2 + B_2\upsilon(K_1 + K_2)) \tag{3.76}$$

and

$$a_F^2 = R.\frac{NUM4}{DEN4} \tag{3.77}$$

where

$$NUM4 = B_2^2K_1K_2\upsilon(K_2 + B_2\upsilon) + B_2^2(K_1K_2 + B_2r(K_1 + K_2) (B_2(K_1 + K_2) + K_2\upsilon) + B_2(K_2^2(K_1K_2 + B_2\upsilon(K_1K_2)) \tag{3.78}$$

$$DEN4 = m^2B_2[-K_1K_2\upsilon(K_2 + B_2\upsilon)^2 + B_2(K_1K_2 + B_2\upsilon(K_1 + K_2)]^2 + (B_2\upsilon + K_2)(B_2(K_1 + K_2) + K_2\upsilon)(K_1K_2 + B_2\upsilon(K_1 + K_2)) \tag{3.79}$$

where $B_2=b_2/m$, $K_2 = k_2/m$ and $K_1 = k_1/m$. Equations (3.74) and (3.77) show that the responses to the external force are dependent on the ratios of stiffness to mass, damping coefficient to mass and the mass itself.

The rms response of the relative displacement, Δd_F is given by,

$$\Delta d_F = \left(R.\frac{NUM3}{DEN3}\right)^{1/2} \tag{3.80}$$

and the rms acceleration a_F is given by,

$$a_F = \left(R.\frac{NUM4}{DEN4}\right)^{1/2} \tag{3.81}$$

Since our model is linear, responses of the model to both the road input and the external force are summed up to obtain the total response. Thus, the total rms relative displacement is given by,

$$\Delta d = \left(\Delta d_g^2 + \Delta d_F^2 \right)^{\frac{1}{2}} \tag{3.82}$$

$$a = \left(a_g^2 + a_F^2 \right)^{\frac{1}{2}} \tag{3.83}$$

It is clear that the total responses are mathematically complicated to be analyzed for different values of K_1, K_2 and B_2. In order to investigate the effect of the additional external force on the behavior of the responses, the rms acceleration and relative displacement values were plotted in Figure 3.10 for different K_2 and B_2 values when K_1 is very small. The value of m is taken to be 250 kg [39]. When comparing the behavior of the contours of Figure 3.10 to those in Figure 3.8 where there is no external force applied, we can see that the rms response values are much larger in the case where there is an external force.

A large value of K_1 equal to ($1/s^2$) is used to plot the contours of constant K_2 and B_2 values in Figure 3.11 when an external force disturbance exists. The rms responses are observed to have much larger values in the second case where the external force exists and the feasible solutions region becomes more restricted.

We can note from Figures 3.10 and 3.11 that as the value of K_1 becomes larger, smaller values of relative displacement can be obtained.

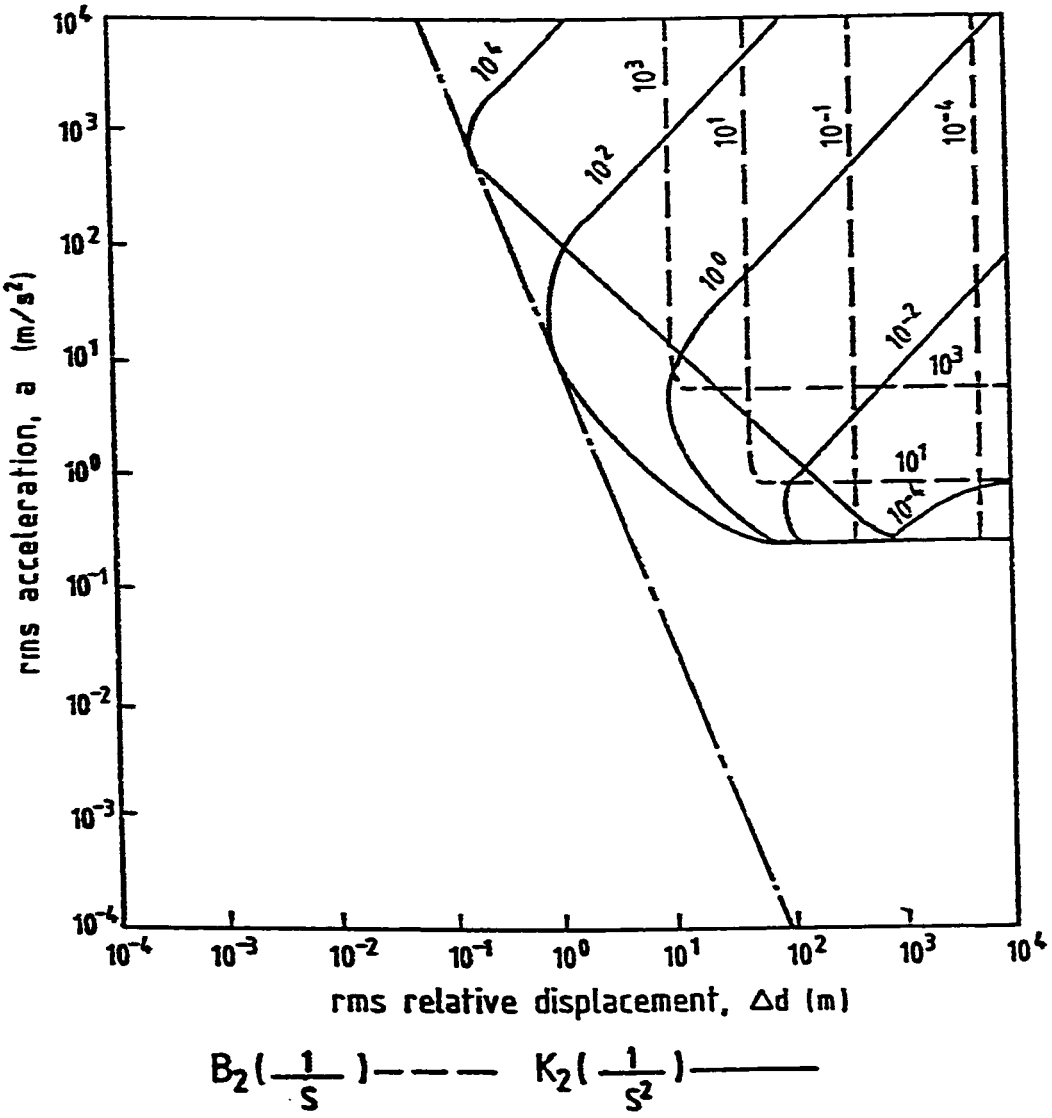

Figure 3.10 Contours of constant B_2 and K_2 values. ($K_1 = 10^{-6}\ \frac{1}{s^2}$)

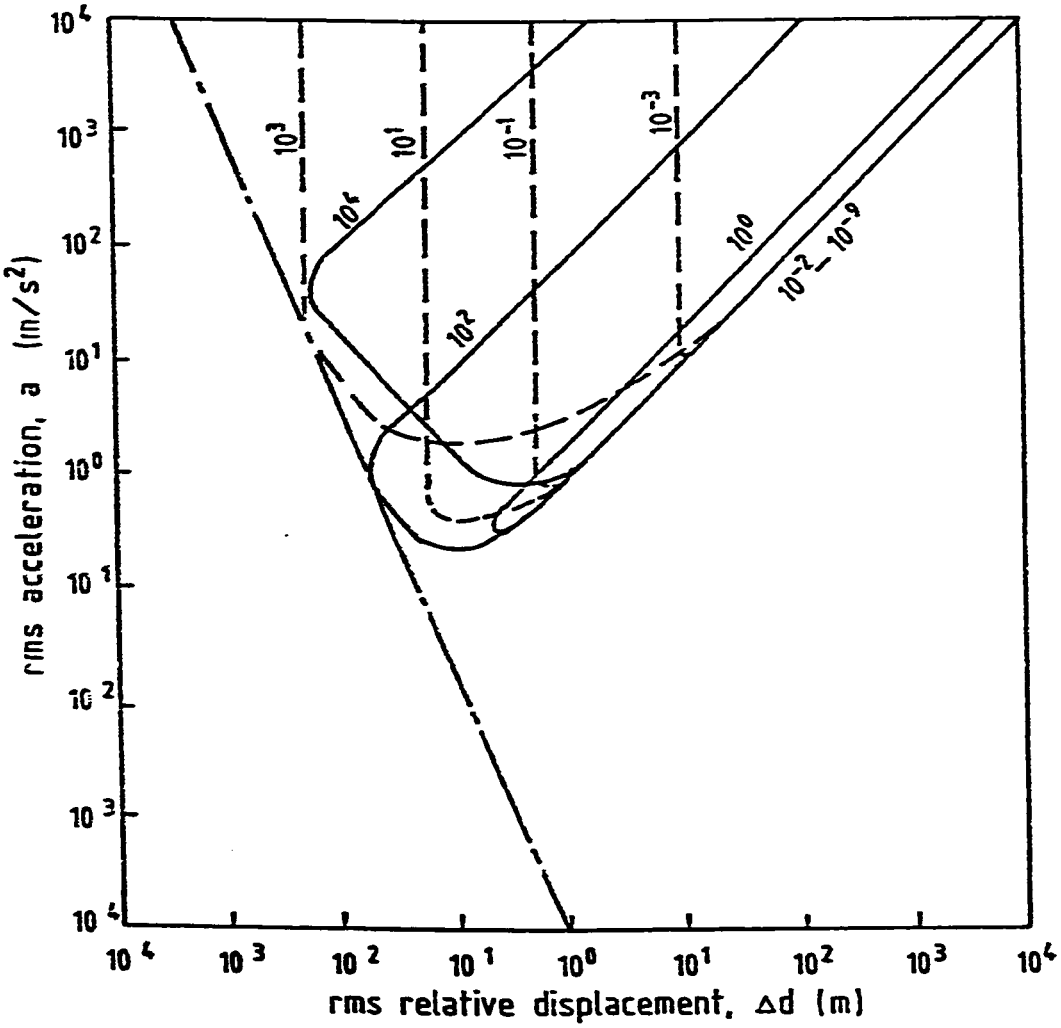

Figure 3.11 Contours of constant B_2 and K_2 values. ($K_1 = 10^0 \frac{1}{S^2}$)

3.3 Response of 1-DOF Model with Voigt Type Suspension in Series with a Spring to Random Vibrations

The model shown in Figure 3.12 represents a 1-DOF suspension system with a vehicle of mass, two springs with coefficients k_2 and k_3 and one dashpot with damping coefficient b_3.

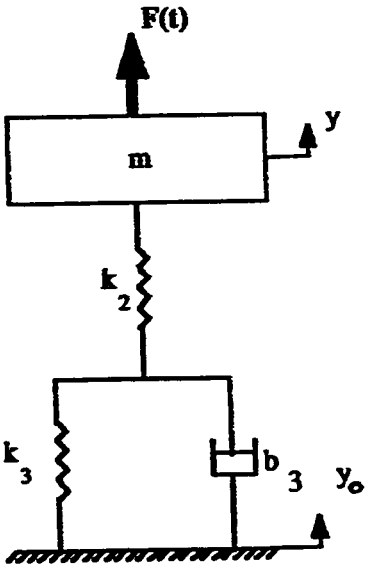

Figure 3.12. 1-DOF model with Voigt type suspension in series with a spring.

a. The response to the road input only i.e., F(t) = 0:

The mean square relative displacement and the mean square acceleration responses of the mass due to the road input only are derived as shwon in Appendix A and are given by:

$$\overline{\Delta y_g^2} = C.\left(\frac{b_3}{k_2} + \frac{m(k_2+k_3)^2}{b_3 k_2^2}\right) \qquad (3.84)$$

and

$$\overline{a_g^2} = C.\left(\frac{k_2 b_3}{m^2} + \frac{k_3^2}{m b_3}\right) \qquad (3.85)$$

where $C = \pi . A.V$

To simplify the analysis of the above equations, they are written in the form,

$$\overline{\Delta y_g^2} = C.\left(\frac{B_3}{K_2} + \frac{(K_2+K_3)^2}{B_3 K_2^2}\right) \qquad (3.86)$$

and

$$\overline{a_g^2} = C.\left(K_2 B_3 + \frac{K_3^2}{B_3}\right) \qquad (3.87)$$

where $B_2 = b_2/m$, $K_2 = k_2/m$, $K_1 = k_1/m$. The above equations show that the acceleration and relative displacement responses are dependent on the ratios of damping coefficient to mass and spring coefficients to mass. The rms relative displacement is given by:

$$\Delta d_g = \left(C.\left(\frac{B_3}{K_2} + \frac{(K_2+K_3)^2}{B_3 K_2^2}\right)\right)^{1/2} \qquad (3.88)$$

and the rms acceleration is given by

$$a_g = \left(C.\left(K_2 B_3 + \frac{K_3^2}{B_3}\right)\right)^{1/2} \qquad (3.89)$$

An investigation on the limits of B_3, based on given levels of relative displacement, K_2 and K_3, obtains the relations

$$B_3 = \frac{K_2 + K_3}{\sqrt{K_2}} \tag{3.90}$$

and

$$\Delta d_g = \left(\frac{2C(K_2 + K_3)}{K_2^{3/2}} \right)^{1/2} \tag{3.91}$$

as shown in Appendix B.

The same result of Equation (3.90) can be obtained if the relative displacement is minimized with respect to B_3 as shown in Appendix B.

Based on given levels of acceleration, K_2 and K_3, we obtain:

$$B_3 = \frac{K_3}{\sqrt{K_2}} \tag{3.92}$$

when

$$a_g = (2CK_2^{1/2}K_3)^{1/2} \tag{3.93}$$

Equation (3.92) can be obtained if the acceleration is minimized with respect to B_3. Details of the above investigation can be found in Appendix B.

Using a small value of K_3 when compared to K_2 and B_3 in Equation (3.88) and (3.89) will result in

$$\Delta d_g \approx \left(C.(\frac{B_3}{K_2} + \frac{1}{B_3}) \right)^{1/2} \tag{3.94}$$

and

$$a_g \approx (C.K_2.B_3)^{1/2} \tag{3.95}$$

Equations (3.94) and (3.95) have the same forms as those of Equations (3.5) and (3.6) due to the very small effect of K_3 on the model response when it has a small value. Shown in Figure 3.13, a plot of the contours of constant rms acceleration and rms relative displacement when K_3 is very small. The contours are the same as those of the Maxwell type suspension shown in Figure 3.2. The line given by Equation (3.90) is shown in the figure.

In Figure (3.14) when K_2 is much larger than B_3^2, then Equation (3.88) can have the form,

$$\Delta d_g = \left(\frac{C}{B_3}\right)^{1/2} \tag{3.96}$$

This approximation explains the constant values of B_3 in some regions in Figure (3.14) where B_3 has a small value for a constant relative displacement. If $B_3^2 > K_2$ and $K_2 < K_3$, then Equation (3.88) can be evaluated as;

$$(\Delta d_g)^2 = \frac{CB_3}{K_2} + \frac{CK_3^2}{B_3 K_2^2} \tag{3.97}$$

then if,

$$B_3^2 \ll \frac{K_3^2}{K_2} \tag{3.98}$$

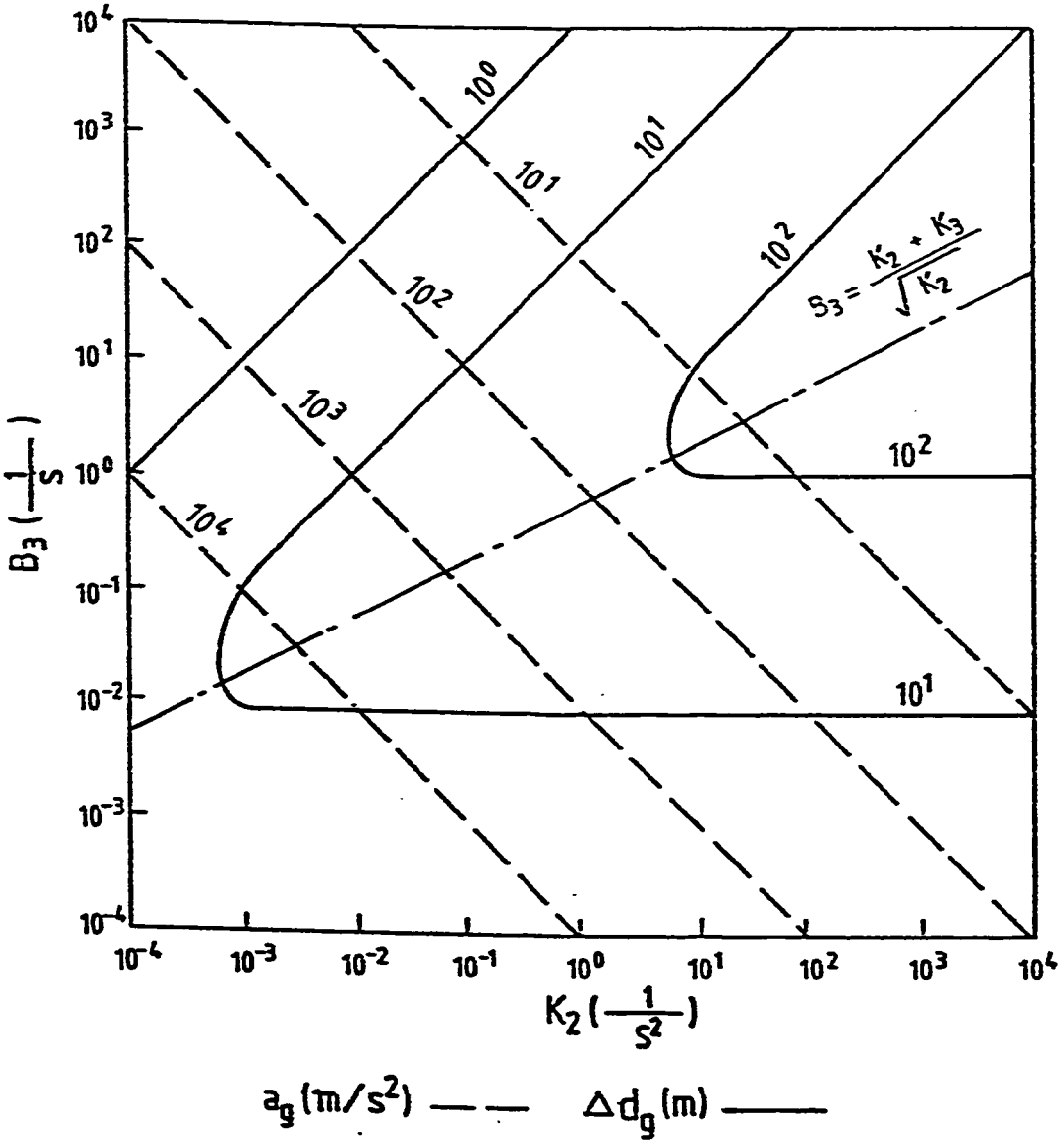

Figure 3.13 Contours of constant rms acceleration and rms relative displacement. ($K_3 = 10^{-6}\frac{1}{s^2}$)

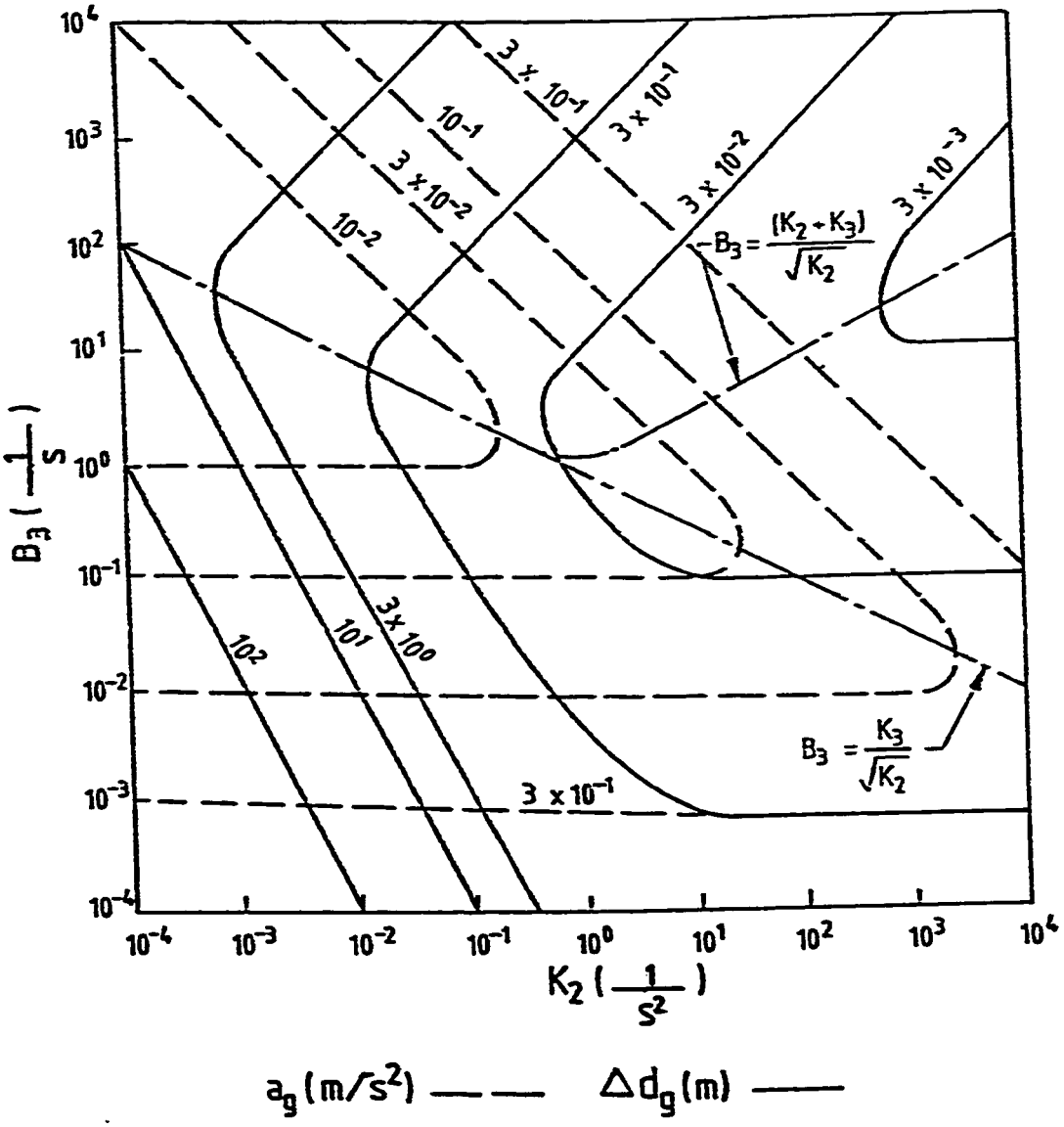

Figure 3.14 Contours of constant rms acceleration and rms relative displacement. ($K_3 = 10^0 \frac{1}{s^2}$)

we have form Equation (3.97);

$$B_3 \approx \frac{CK_3^2}{K_2^2(\Delta d_g)^2} \tag{3.99}$$

This indicates an inversely linear behavior of B_3 with K_2 for constant rms relative displacement as shown in the lower left corner of the Figure 3.14.

If

$$B_3^2 \ll \frac{K_3^2}{K_2} \tag{3.100}$$

then, Equation (3.97) can be solved as,

$$B_3 \approx \frac{K_2(\Delta d_g)^2}{C} \tag{3.101}$$

This indicate a linear relation between B_3 and K_2 as shown in the upper left corner of Figure 3.14.

On the other hand, if $B_3^2 > K_2$, and $K_2 > K_3$, then Equation (3.88) can be written as;

$$K_2 \approx \frac{CB_3^2}{B_3(\Delta dg)^2 - C} \tag{3.102}$$

and if $B_3(\Delta dg)^2 \gg C$, then

$$K_2 \approx \frac{CB_3}{(\Delta dg)^2} \tag{3.103}$$

This relation is shown in Figure 3.14 at the upper right corner for constant rms relative displacement. From Figure 3.14 we can see that small values of constant acceleration

values dominate. The constant B_3 lines appear when B_3 is very small, because in this case Equation (3.89) performs according to the relation;

$$B_3 \approx \frac{CK_3^2}{a_g^2} \tag{3.104}$$

which represents a constant value of B_3 for constant values of acceleration and K_3. On the other hand, when B_3 has larger values, then Equation (3.89) performs according to the relation,

$$B_3 \approx \frac{a_g^2}{CK_2} \tag{3.105}$$

This inverse relation between B_3 and K_2 appears in Figure 3.14 where larger values of B_3 appear.

The lines representing the minimum relative displacement and minimum acceleration with respect to B_3 are shown in Figure (3.14). It is clear that the two lines follow different paths when K_2 has a larger value than K_3 and they exactly match when K_2 has a smaller value than K_3.

The constant acceleration and relative displacement contours when K_3 has a very large value are plotted in Figure (3.15). It is clear that the values of acceleration and relative displacement become very large in this case. The constant relative displacement contours represent an inversely linear relation between B_3^2 and K_2 since Equation (3.88) is of the form given below:

$$B_3 \approx \frac{CK_3^2}{K_2^2 (\Delta d_g)^2} \tag{3.106}$$

when K_3 is very large. Also, the constant acceleration contours represent constant B_3 values because when K_3 is very large, then Equation (3.89) can be written as,

$$B_3 \approx \frac{CK_3^2}{a_g^2} \tag{3.107}$$

In this case, B_3 will be constant for constant acceleration and K_3 values as shown in Figure 3.15. The lines representing the minimum acceleration and relative displacement values with respect to B_3 cannot appear in Figure 3.15 because of the very large value of K_3 used.

Contours of constant B_3 and K_2 values when K_3 is very small are shown in Figure 3.16. The contours behave exactly similar to those in Figure 3.3 representing the Maxwell type suspension because of the negligible value of K_3. When a larger value of K_3 is used, higher acceleration and relative displacement values appear and it can be observed that the feasible region of solution becomes restricted as can be noted from Figure 3.17. When K_2 is much larger than B_3^2 and K_3, then Equation (3.88) can be approximated by

$$\Delta d_g = \left(C.\frac{1}{B_3}\right)^{1/2} \tag{3.108}$$

This means that for some values of B_3, K_2 and K_3, the relative displacement will be constant and this limits the performance of optimization where no smaller relative displacement values can be obtained.

Another limiting constraint can be observed to exist since when B_3 is very small, then Equation (3.89) could be evaluated as:

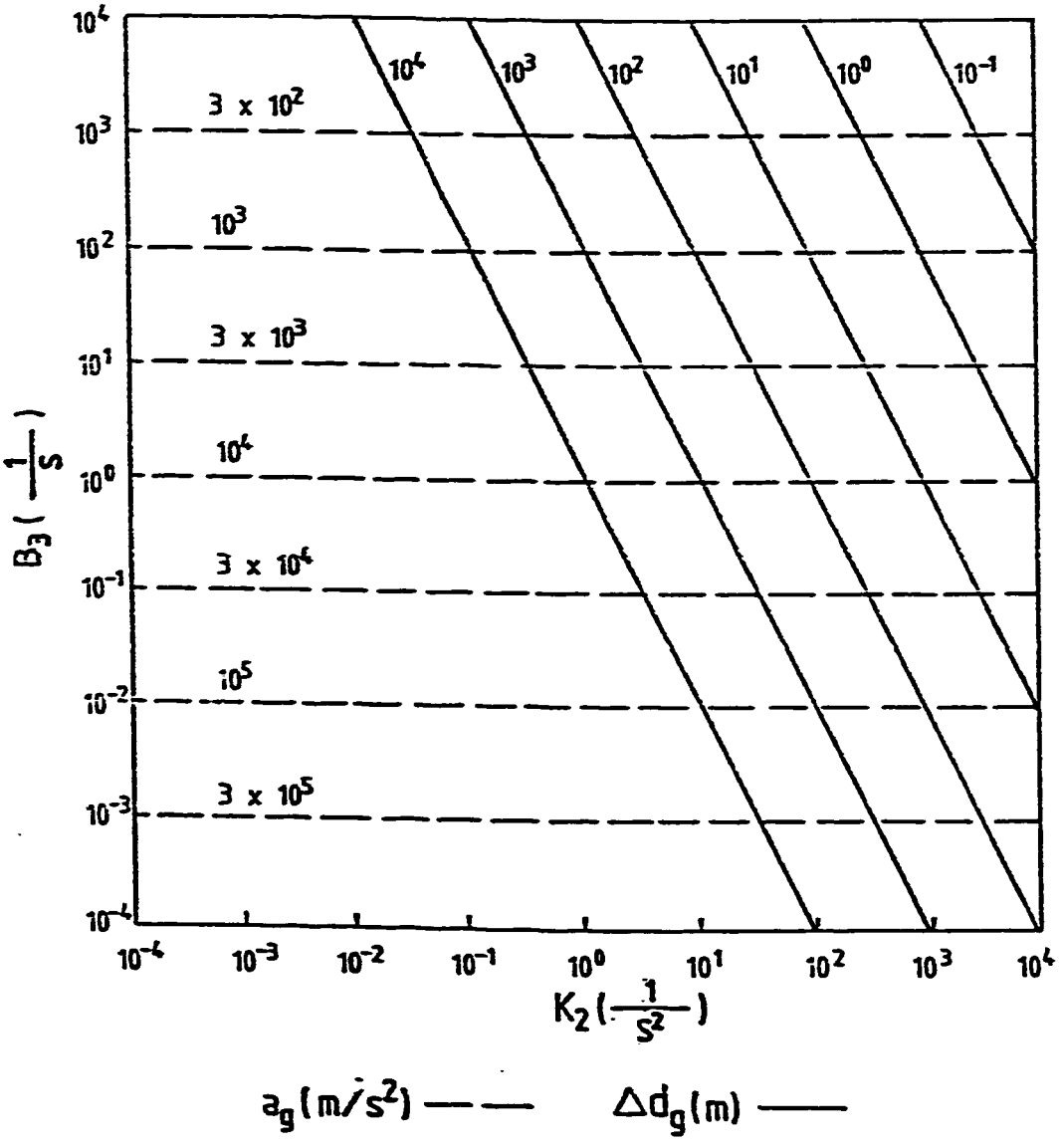

Figure 3.15 Contours of constant rms acceleration and rms relative displacement ($K_3 = 10^6 \frac{1}{s^2}$)

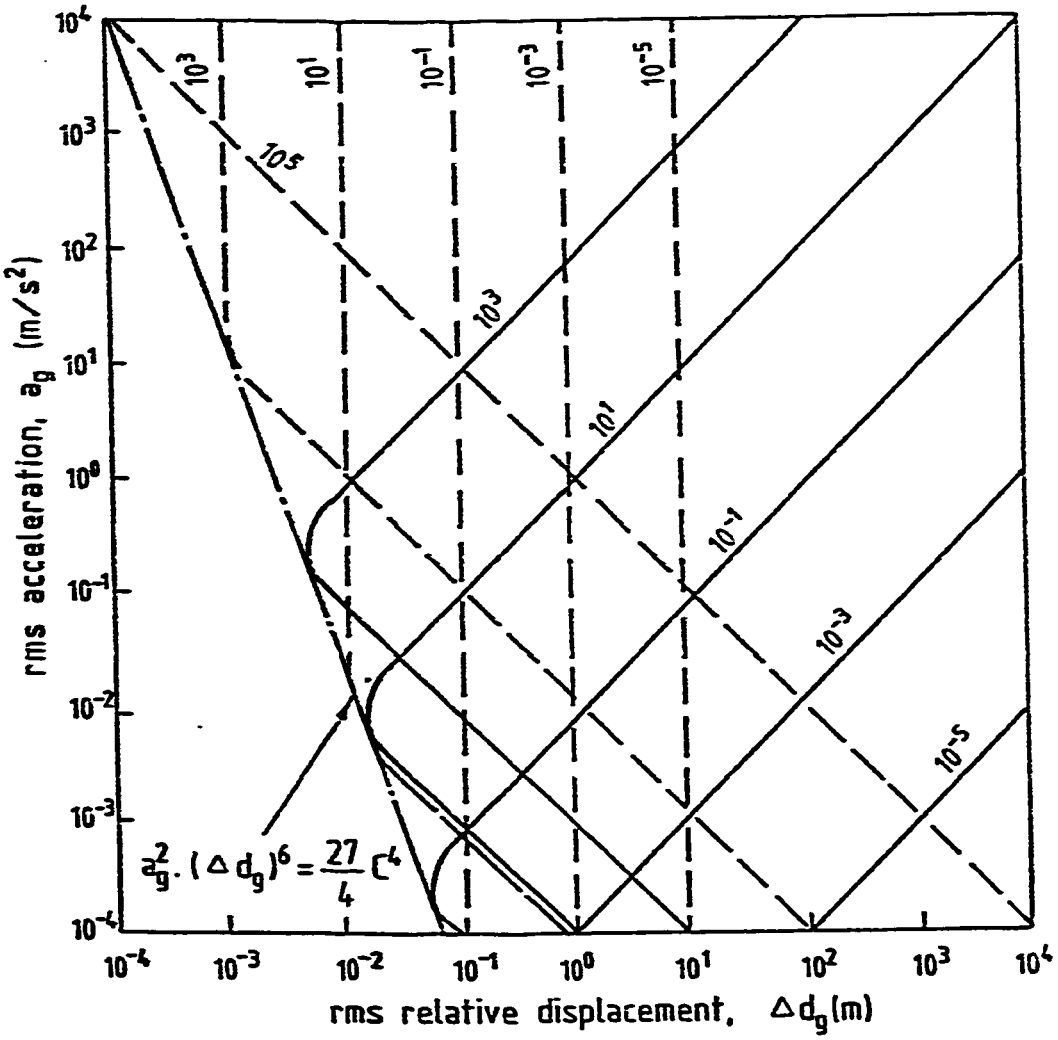

Figure 3.16 Contours of constant B_3 and K_2 values. ($K_3 = 10^{-6}\frac{1}{s^2}$)

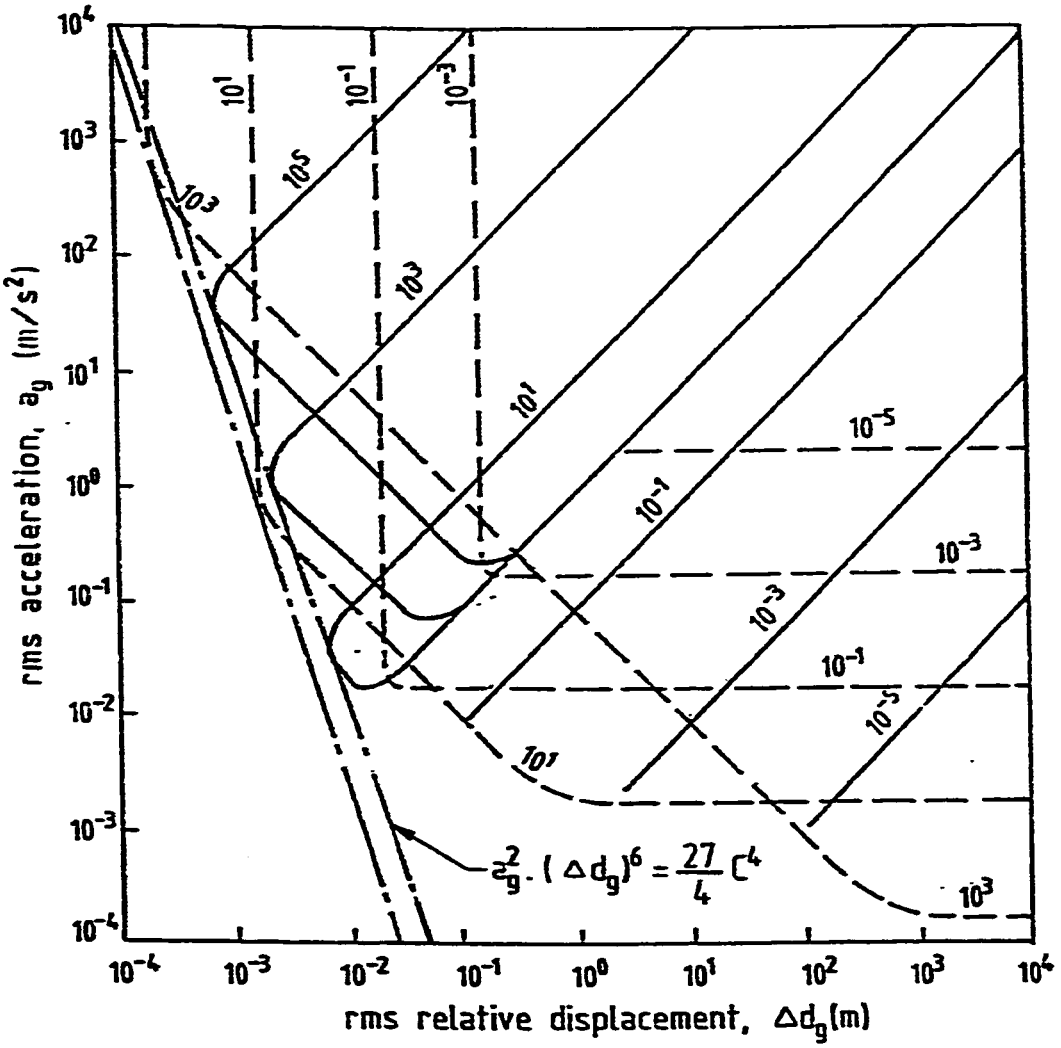

Figure 3.17 Contours of constant B_3 and K_2 values. ($K_3 = 10^0 \frac{1}{s^2}$)

$$a_g \approx \left(\frac{C.K_3^2}{B_3}\right)^{1/2} \qquad (3.109)$$

and in such a case, constant acceleration values appear as shown in Figure 3.17 when small constant B_3 values are used.

In the case where K_2 is much smaller than K_3, then

$$(\Delta d_g)^2 \approx \frac{CB_3}{K_2} + \frac{CK_3^2}{B_3 K_2^2} \qquad (3.110)$$

When comparing Equation (3.110) with Equation (3.89) we can find that

$$a_g \approx K_2 . \Delta d_g \qquad (3.111)$$

This result explains the linear relation between the acceleration and relative displacement in Figure 3.17 when small K_2 values are used.

On the other hand, when the value of K_2 is larger than that of K_3 and when B_3 is very small, Equation (3.88) takes the form:

$$\Delta d_g \approx \frac{CK_3^2}{B_3} \qquad (3.113)$$

Combining Equations (3.112) and (3.113) gives,

$$a_g \approx K_3 . \Delta d_g \qquad (3.114)$$

In case that B_3 is very large, then Equation (3.88) can be obtained as

$$(\Delta d_g)^2 \approx \frac{CB_3}{K_2} \qquad (3.115)$$

and equation (3.89) as,

$$a_g^2 = CK_2B_3 \tag{3.116}$$

from Equation (3.115) and (3.116), we can write

$$a_g = \frac{CB_3}{\Delta d_g} \tag{3.117}$$

This Equation explains why the acceleration and relative displacement are inversely proportional in some regions as displayed in Figure 3.17.

b). The response to the external force and the road input:

The mean square relative displacement and the mean square acceleration of the mass due to the external force only are derived as shown in Appendix A and given by:

$$\overline{\Delta y_F^2} = R.\frac{NUM1}{DEN1} \tag{3.118}$$

where $R = \pi.\beta.\upsilon$,

$$NUM1 = \left(mk_2k_3\upsilon b_3^2(k_2+k_3+b_3\upsilon)\right) - mb_3(k_2+k_3)^2(k_2k_3+k_2b_3\upsilon) + m(k_2+k_3)^2(k_2+k_3+b_3\upsilon)\left(k_2b_3+m(k_2+k_3)\upsilon\right) \tag{3.119}$$

and

$$DEN1 = k_2k_3\upsilon\left(-k_2k_3\upsilon m^2(k_2+k_3+b_3\upsilon)^2\right) - mb_3(k_2k_3+k_2k_3b_3\upsilon)^2 + (k_2k_3+k_2k_3b_3\upsilon)\left(k_2b_3+m(k_2+k_3)\upsilon\right)(k_2+k_3+b_3\upsilon)m) \tag{3.120}$$

and,

$$\overline{a_F^2} = R.\frac{NUM2}{DEN2} \tag{3.121}$$

where

$$NUM2 = -b_3^2 k_2 k_3 \upsilon m(k_2 + k_3 + b_3\upsilon) + b_3^2(k_2k_3 + k_2b_3\upsilon)$$
$$(k_2b_3 + m(k_2 + k_3)\upsilon) + (k_2 + k_3)^2(k_2k_3 + k_2b_3\upsilon)mb_3 \qquad (3.122)$$

and

$$DEN2 = mb_3\begin{pmatrix} -k_2k_3\upsilon m^2(k_2 + k_3 + b_3\upsilon)^2 - mb_3(k_2k_3 + k_2b_3\upsilon)^2 \\ +(k_2k_3 + k_2b_3\upsilon)(k_2b_3m(k_2 + k_3)\upsilon)(k_2 + k_3 + b_3\upsilon)m \end{pmatrix} \qquad (3.123)$$

To simplify the analysis of the responses, Equation (3.122) and (3.123) are written as follows;

$$\Delta y_F^2 = R.\frac{NUM3}{DEN3} \qquad (3.124)$$

where

$$NUM3 = K_2K_3\upsilon B_3^2(K_2 + K_3 + B_3\upsilon) - B_3(K_2 + K_3)^2(K_2 + K_3 + K_2B_3\upsilon)$$
$$+ (K_2 + K_3)^2(K_2 + K_3 + B_3\upsilon)(K_2B_3 + (K_2 + K_3)\upsilon) \qquad (3.125)$$

$$DEN3 = \begin{bmatrix} m^2K_2K_3\upsilon(K_2 + K_3 + B_3\upsilon(K_2K_3 + K_2B_3\upsilon)^2 + \\ (K_2K_3 + K_2B_3\upsilon)(K_2B_3 + (K_2 + K_3)\upsilon)(K_2 + K_3 + B_3\upsilon) \end{bmatrix} \qquad (3.126)$$

and

$$a_F^2 = R.\frac{NUM4}{DEN4} \qquad (3.127)$$

where

$$NUM4 = -B_3^2K_2K_3\upsilon(K_2 + K_3 + B_3\upsilon) + B_3^2(K_2K_3 + K_2B_3\upsilon)$$
$$(K_2B_3 + (K_2 + K_3)\upsilon) + (K_2 + K_3)^2(K_2K_3 + K_2B_3\upsilon)B_3) \quad (3.128)$$

$$DEN4 = m^2B_3(-K_2K_3\upsilon(K_2 + K_3 + B_3\upsilon)^2 - B_3(K_2K_3 + K_2B_3\upsilon)^2$$
$$+ ((K_2K_3 + K_2B_3\upsilon)(K_2B_3 + (K_2 + K_3)\upsilon)(K_2 + K_3 + B_3\upsilon)) \quad (3.129)$$

where $B_3 = b_3/m$, $K_2 = k_2/m$ and $K_3 = k_3/m$. From Equations (3.124) and (3.127), we can see that the responses due to the external force input are dependent on the ratios of stiffness coefficients for mass, damping coefficient to mass as the mass itself.

The rms relative displacement due to the external force is given by;

$$\Delta d_F = \left(R_{\cdot}\frac{NUM3}{DEN3}\right)^{1/2} \quad (3.130)$$

and the rms acceleration is given by:

$$a_F = \left(R_{\cdot}\frac{NUM4}{DEN4}\right)^{1/2} \quad (3.131)$$

Responses of the model to both the road input and the external force together can be added together to obtain the total response since our model is linear. The total rms relative displacement is given by;

$$\Delta d = \left(\overline{\Delta d_g^2} + \overline{\Delta d_F^2}\right)^{\frac{1}{2}} \quad (3.132)$$

and the total rms acceleration is given by;

$$a = \left(\overline{a_g^2} + \overline{a_F^2}\right)^{\frac{1}{2}} \quad (3.133)$$

The two total responses are clearly complicated to be analyzed mathematically for different values of K_2, K_3 and B_3. The rms acceleration and rms relative displacement behavior for different K_2 and B_3 values when K_3 is very small as shown in Figure 3.18. A value of 250 kg for m is used [39].

Comparing the total responses behavior in Figure 3.18 to the behavior when the model is subjected to the road input only as shown in Figure 3.16, we observe that in the case where there is an external force, the feasible region of solution appears where only large values of acceleration and relative displacement exist.

When a larger value of K_3 is used to study the total performance as shown in Figure 3.19 and by comparing the responses to those in Figure 3.17 where there is no external force we can see also that the values of acceleration and relative displacement are much larger in the case where the external force exists. We can notice from Figures 3.18 and 3.19 that as the values of K_3 becomes larger, small values of relative displacement can be obtained.

3.4 Response of 1-DOF Model with Voigt Type Suspension in Series with a Spring and both in Parallel with a Spring

The 1-DOF suspension model shown in Figure 3.20 consists of a vehicle of mass m, three springs with coefficients k_1, k_2, k_3 and a dashpot with damping coefficient b_3.

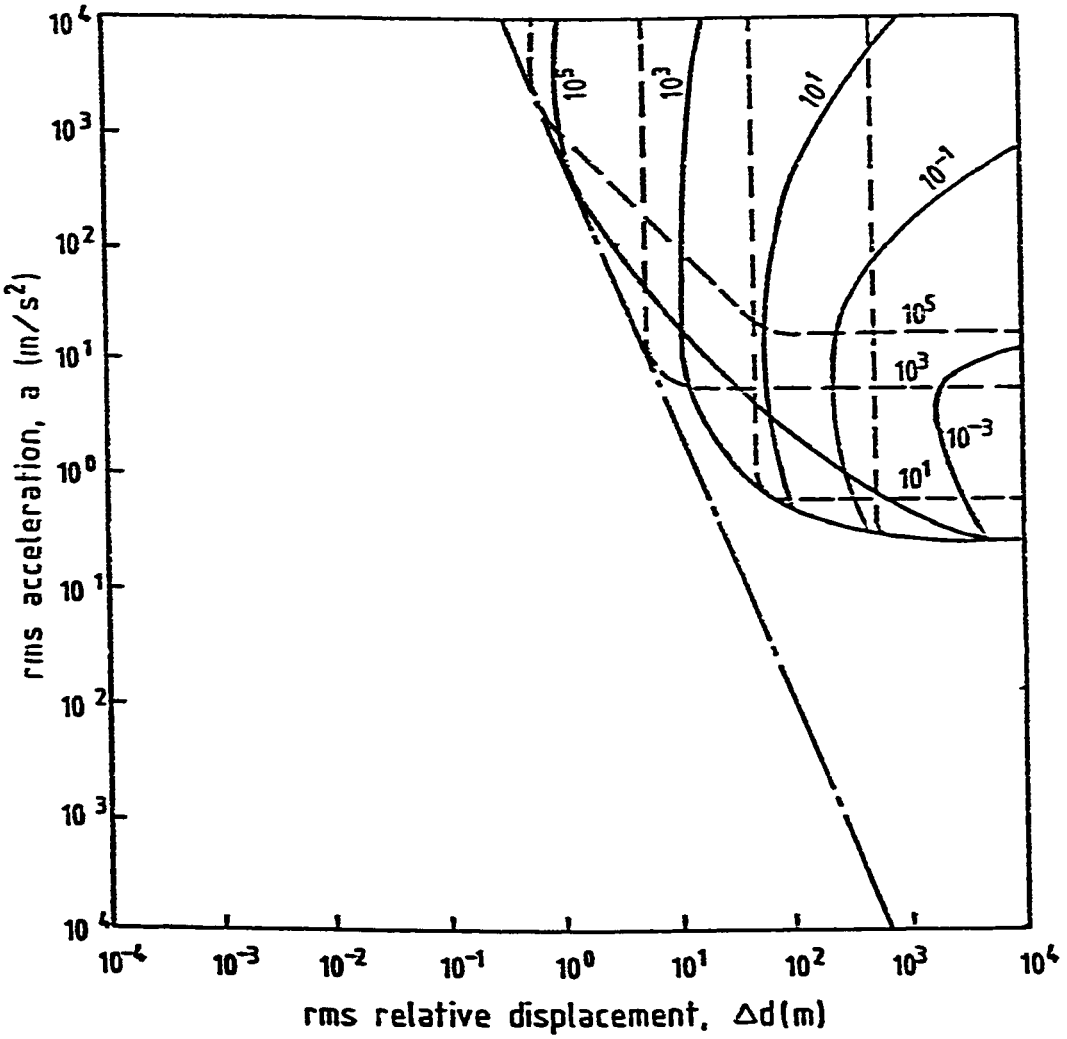

Figure 3.18 Contours of constant K_2 and B_3 values. ($K_3 = 10^{-6}\frac{1}{s^2}$)

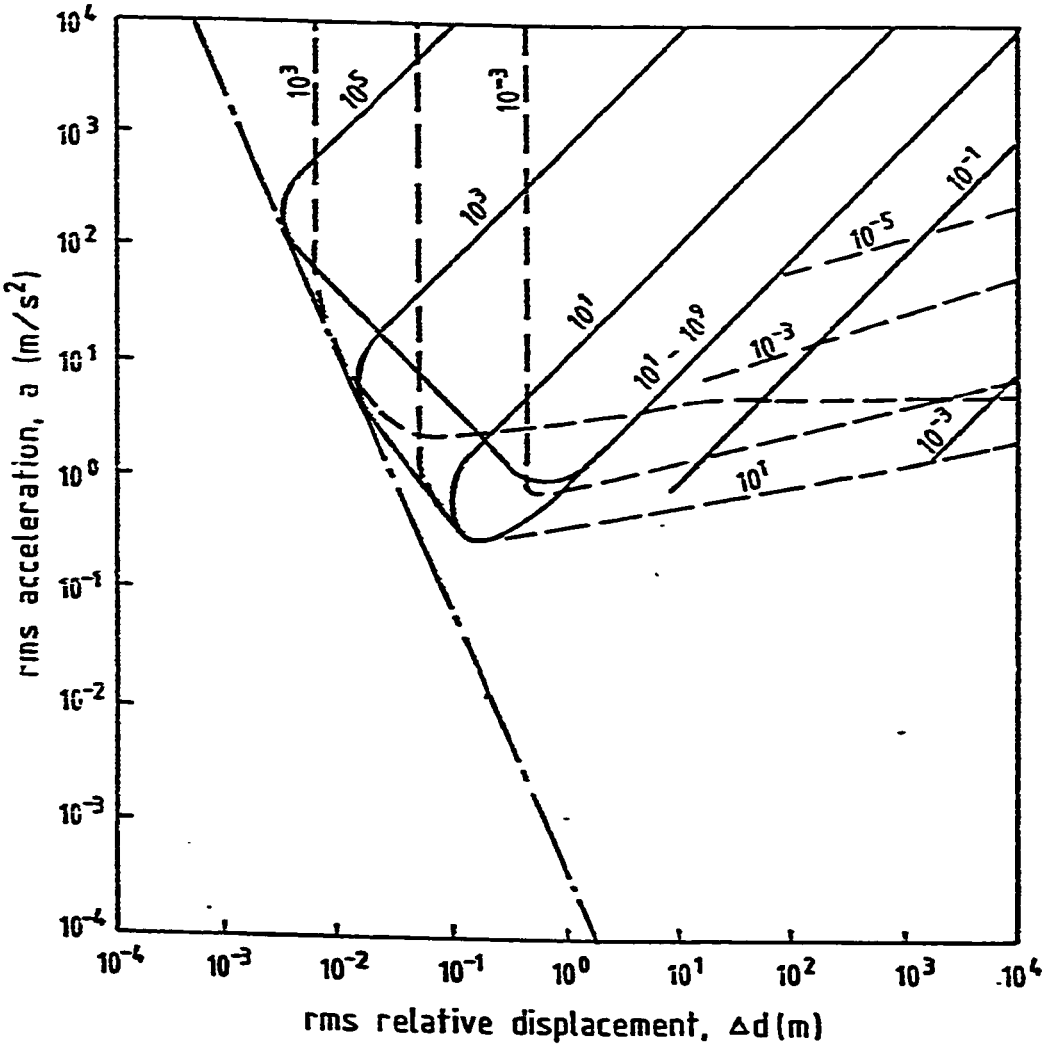

Figure 3.19 Contours of constant K_2 and B_3 values. ($K_3 = 10^0 \frac{1}{s^2}$)

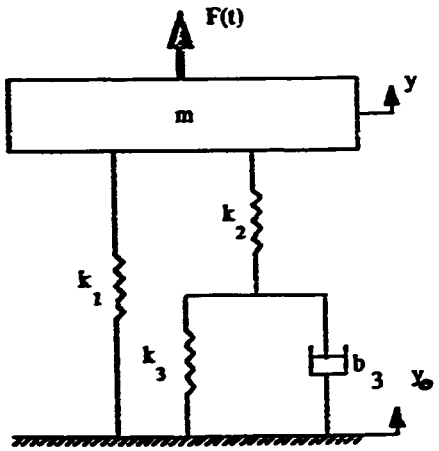

Figure 3.20. 1-DOF model with Voigt type suspension in series with a spring and both in parallel with a spring.

a. The response to the road input only, i.e., F(t)=0:

The mean square relative displacement and the mean square acceleration responses of the mass due to the road input only are derived as shown in Appendix A and given by:

$$\Delta y_g^2 = C\left[\frac{(k_1+k_2)b_3}{k_2^2} + \frac{m(k_2+k_3)^2}{b_3 k_2^2}\right] \qquad (3.134)$$

and

$$a_g^2 = C\left[\frac{(k_1+k_2)^3 b_3}{m^2 k_2^2} + \frac{(k_1k_2+k_1k_3+k_2k_3)^2}{b_3 m k_2^2}\right] \qquad (3.135)$$

where

$C = \pi.A.V.$

The above equations are written in the following form,

$$\overline{\Delta y_g^2} = C\left[\frac{(K_1+K_2)B_3}{K_2^2} + \frac{(K_2+K_3)^2}{B_3K_2^2}\right] \tag{3.136}$$

and

$$\overline{a_g^2} = C\left[\frac{(K_1+K_2)^3B_3}{K_2^2} + \frac{(K_1K_2+K_1K_3+K_2K_3)^2}{B_3K_2^2}\right] \tag{3.137}$$

where $B_3 = b_3/m$, $K_1 = k_1/m$, $K_2 = k_2/m$ and $K_3 = k_3/m$. It is obvious from the above equation that the relative displacement and acceleration responses are dependent on the spring coefficient to mass and the damping coefficient to mass ratios. Then, the rms relative displacement is given by.

$$\Delta d_g = \left[C.\left(\frac{(K_1+K_2)B_3}{K_2^2} + \frac{(K_2+K_3)^2}{B_3K_2^2}\right)\right]^{1/2} \tag{3.138}$$

and the rms acceleration is given by

$$a_g = \left[C.\left(\frac{(K_1+K_2)^3B_3}{K_2^2} + \frac{(K_1K_2+K_1K_3+K_2K_3)^2}{B_3K_2^2}\right)\right]^{1/2} \tag{3.139}$$

Based on given levels of relative displacement, K_1, K_2 and K_3, an investigation is made in Appendix B on the limits of B_3 to obtain;

$$B_3 = \frac{K_2+K_3}{(K_1+K_2)^{1/2}} \tag{3.140}$$

and

$$\Delta d_g = \left[\frac{2C(K_2 + K_3)(K_1 + K_2)^{1/2}}{K_2^2} \right]^{1/2} \tag{3.141}$$

This limit on B_3 can be found if the relative displacement is minimized with respect to B_3 as shown also in Appendix B. Based on given levels of acceleration, K_1, K_2 and K_3, we get;

$$B_3 = \frac{(K_1K_2 + K_1K_3 + K_2K_3)}{(K_1 + K_2)^{3/2}} \tag{3.142}$$

and

$$a_g = \left[\frac{2C(K_1K_2 + K_1K_3)(K_1 + K_2)^{3/2}}{K_2^2} \right]^{1/2} \tag{3.143}$$

When the acceleration is minimized with respect to B_3, then the same result of Equation (3.142) can also be obtained as shown in Appendix B.

In this section, the study of the model responses is performed when K_1 and K_2 have constant and medium values since, small or large values of K_1 or K_2 will reduce the model to either models that have been discussed in previous sections or to models that are not required for study. If K_1 has a small value, then the model will reduce to the 1-DOF model with Voigt type suspension in series with a spring, which has been studied in Section 3.3. If K_1 has a large value, then the effects of the other parameters K_2, K_3 and B_3 on the model responses will be very small and the suspension system could be reduced to an equivalent spring with coefficient K_1. On the other hand, if K_2 has a large value, then, the effect of K_1 will disappear and the model responses will depend only on the values of K_2, K_3 and B_3. If K_2 has a large value, then, the effect of K_1 will disappear and the model responses will depend only on the values of K_2, K_3 and B_3. If K_2 has a small value, then

this will lead us again to the case where only the effect of K_1 will be dominating the suspension performance. So the effect of different medium values on the model responses will be studied while K_3 and B_3 have different values ranging from small to large values.

Contours of constant K_3 and B_3 values are plotted in Figure 3.21 for equal K_1 and K_2 values. It can be observed that a linear relation exists between the relative displacement and the acceleration in the log-log scale. The same behavior can also be seen in Figures 3.22 and 3.23 when higher K1 and K_2 values are used, but with lower relative displacement and higher acceleration values. Equations (3.138) and (3.139) can be combined in the form:

$$\left(\frac{\Delta d_g}{a_g}\right)^2 = \frac{(K_1 + K_2) + \left(\frac{K_2 + K_3}{B_3}\right)^2}{(K_1 + K_2)^3 + \left(\frac{K_2(K_3 + K_1) + K_1 K_3}{B_3}\right)^2} \qquad (3.144)$$

If $K_3 > K_1$ and K_2, then Equation (3.144) can be written as;

$$a_g = (K_1 + K_2).\Delta d_g \qquad (3.145)$$

and for the case where $K_1 = K_2$ as in Figures 3.21, 3.22, and 3.23, then

$$a_g = 2K_1.\Delta d_g \qquad (3.146)$$

or

$$a_g = 2K_2.\Delta d_g \qquad (3.147)$$

If $K_1 > K_2$, then Equation (3.145) can be written as,

$$a_g = K_1.\Delta d_g \qquad (3.148)$$

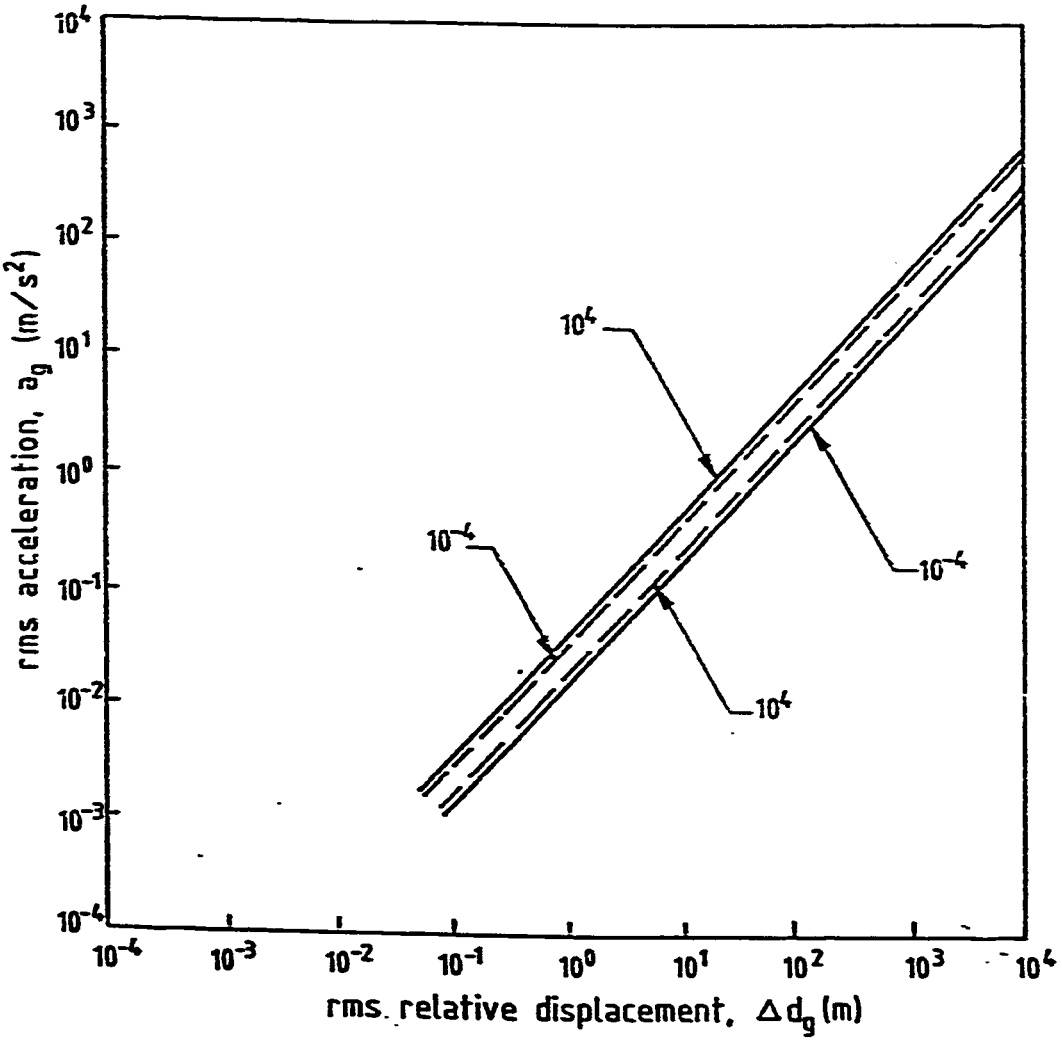

Figure 3.21 Contours of constant K_3 and B_3 values. ($K_1 = K_2 = 10^{-2} \frac{1}{s^2}$)

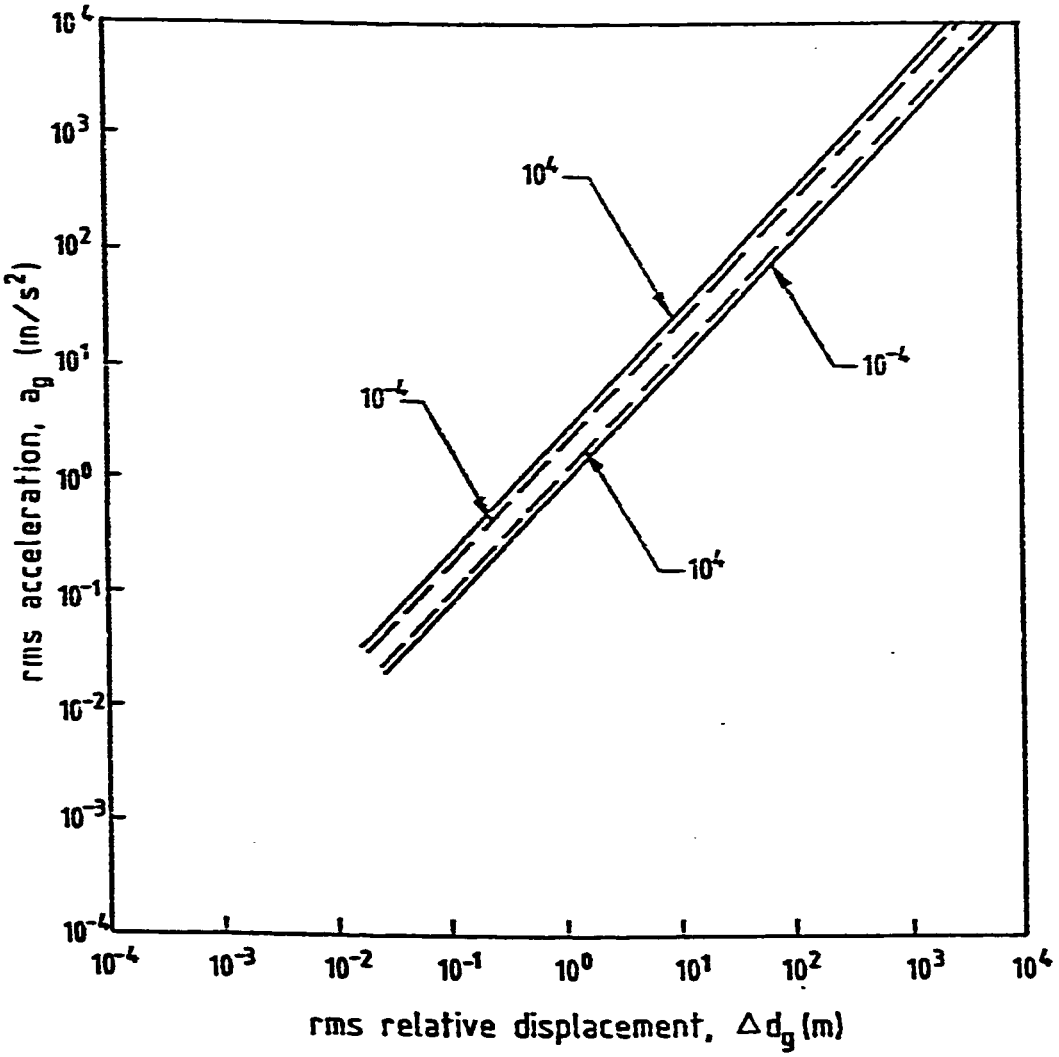

Figure 3.22 Contours of constant K_3 and B_3 values. ($K_1 = K_2 = 10^0 \frac{1}{s^2}$)

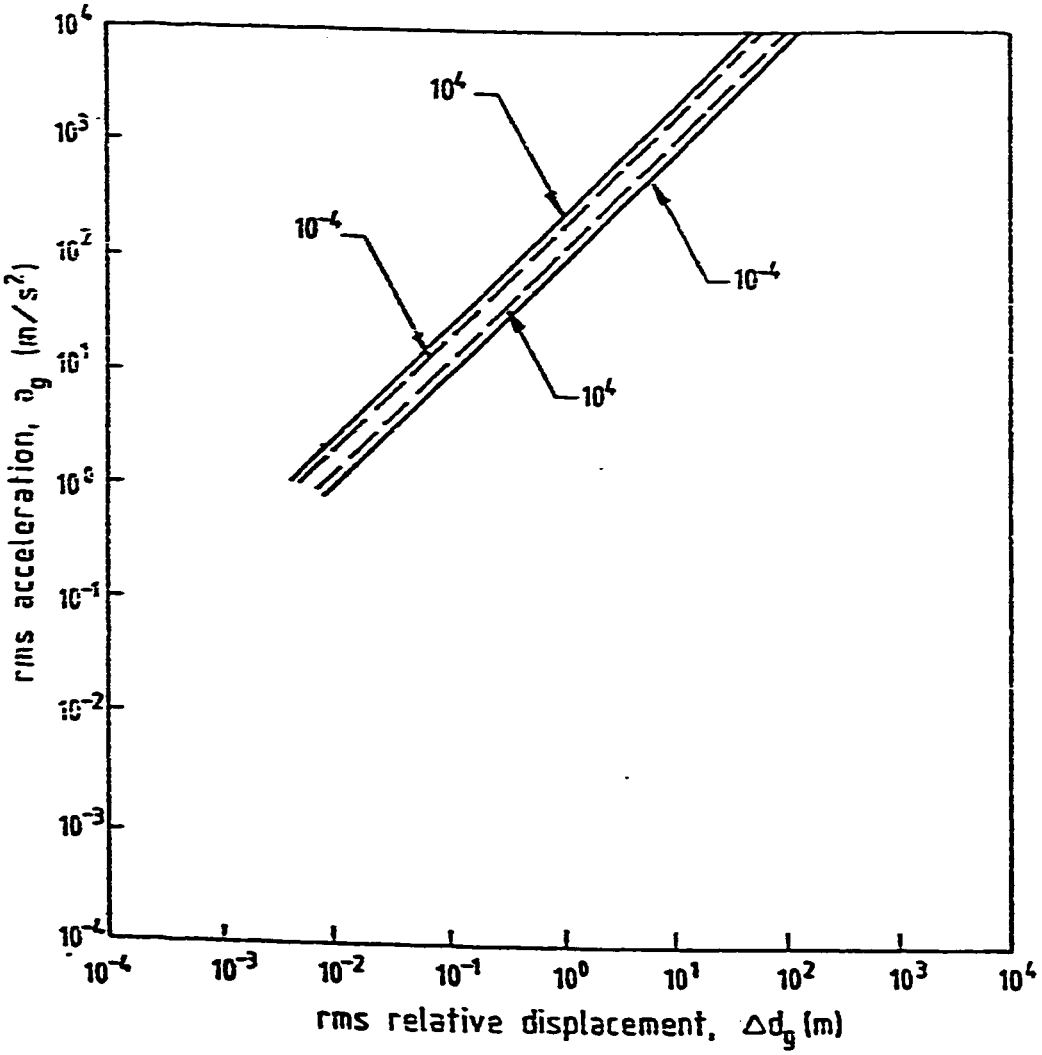

Figure 3.23 Contours of constant K_3 and B_3 values. ($K_1 = K_2 = 10^2 \frac{1}{s^2}$)

On the other hand, if $K_2 > K_1$, then Equation (3.145) can be written as,

$$a_g \approx K_2 \Delta d_g \tag{3.149}$$

If K_3 is smaller than K_2 and K_1, then Equation (3.144) can be simplified to;

$$\left(\frac{\Delta d_g}{a_g}\right)^2 \approx \frac{K_2^2 + \left(\frac{K_2}{B_3}\right)^2}{K_2^3 + \left(\frac{K_2 K_1}{B_3}\right)^2} \tag{3.150}$$

and, when K_1 and K_2 are almost equal then Equation (3.150) reduces to;

$$a_g \approx K_1 . \Delta d_g \tag{3.151}$$

or

$$a_g \approx K_2 \Delta d_g \tag{3.152}$$

Equations (3.146), (3.147), (3.151) and (3.152) explain the linear behavior of the responses as was shown in Figures 3.21, 3.22 and 3.23.

The contours of constant K_3 values plotted in Figures 3.21, 3.22 and 3.23 are combined in Figure 3.24. It can be noted that a limited region of acceleration and relative displacement responses exists and as the values of K_1 and K_2 become larger the values of relative displacement become smaller and the values of acceleration become larger.

Contours of constant rms relative displacement and rms acceleration levels for equal K_1 and K_2 values are shown in Figure 3.25. In Equation (3.138), if

$$B_3 > \frac{K_2 + K_3}{(K_1 + K_2)^{1/2}} \tag{3.153}$$

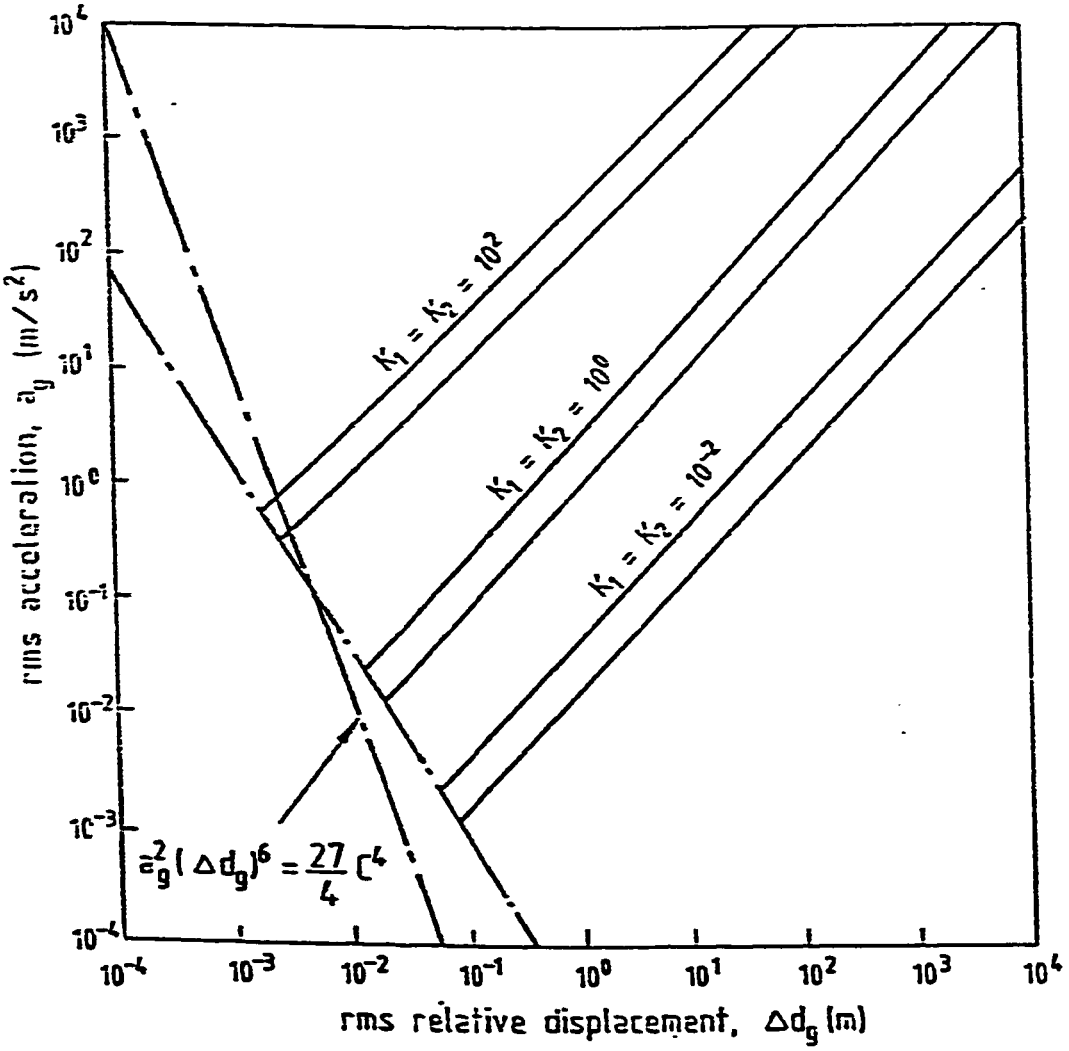

Figure 3.24 Contours of constant K_3 values at different levels of K_1 and K_2.

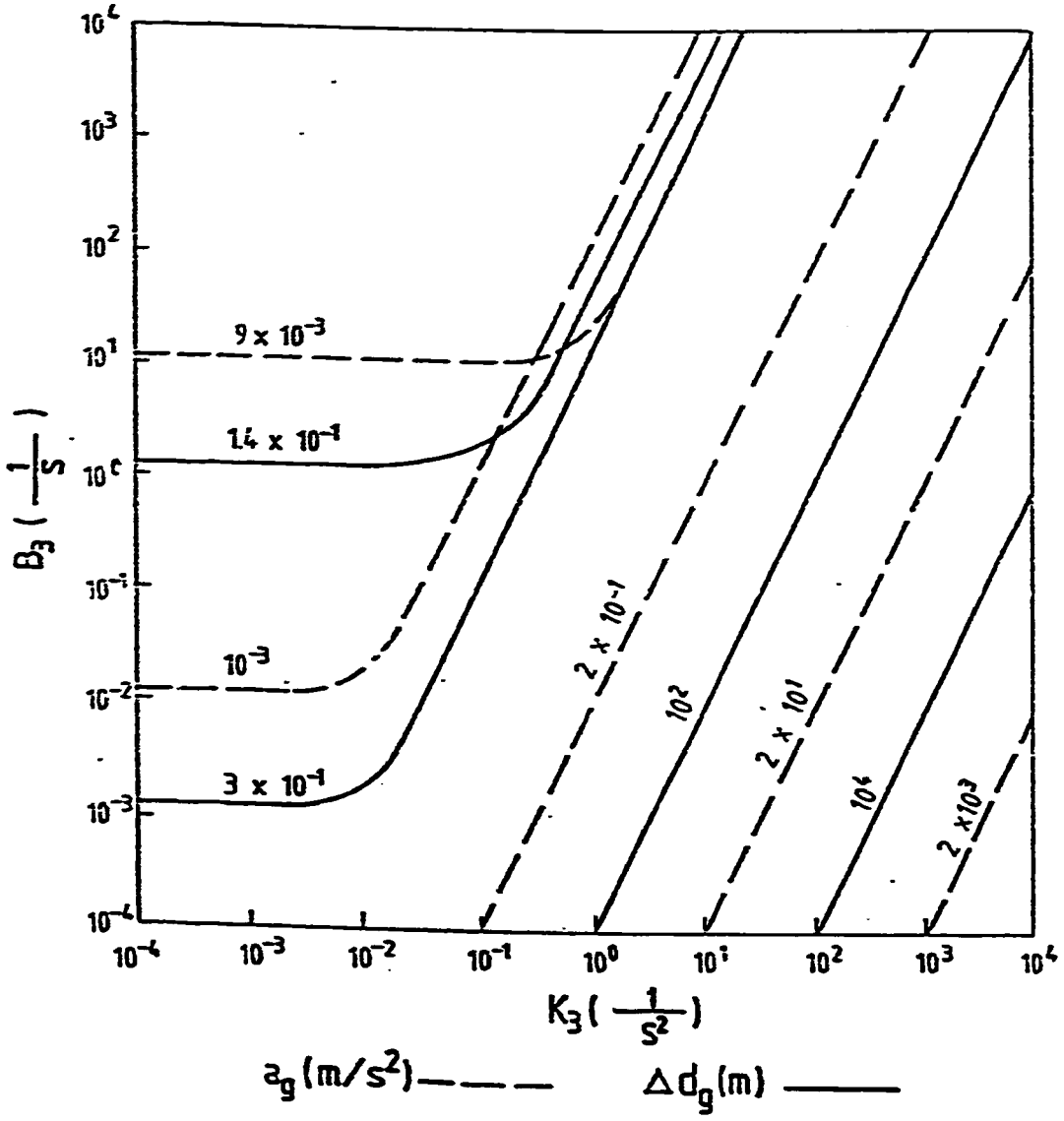

Figure 3.25 Contours of constant rms acceleration and rms relative displacement ($K_1 = K_2 = 10^{-2}\,\frac{1}{s^2}$)

then Equation (3.138) can be solved for B_3 as,

$$B_3 \approx \frac{K_2^2 (\Delta d_g)^2}{C(K_1 + K_2)} \tag{3.154}$$

and it $K_1 = K_2$ as in Figure (3.25), then

$$B_3 \approx \frac{K_2 (\Delta d_g)^2}{C} \tag{3.155}$$

But, when

$$B_3 < \frac{K_2 + K_3}{(K_1 + K_2)^{1/2}} \tag{3.156}$$

then, Equation (3.138) can be solved for B_3, as

$$B_3 = C\left(\frac{K_2 + K_3}{K_2 \cdot \Delta d_g}\right)^2 \tag{3.157}$$

and if $K_2 < K_3$, then

$$B_3 = C\left(\frac{K_3}{K_2 \cdot \Delta d_g}\right)^2 \tag{3.158}$$

Equations (3.154) and (3.155) show that for constant K_1, K_2 and relative displacement values, then B_3 will have a constant value when the condition of Equation (3.153) is satisfied. On the contrary, if the condition of Equation (3.156) is satisfied, then a linear relation exists in the log-log scale between B_3 and K_3 according to Equation (3.158). This explains the behavior of the constant rms relative displacement values in Figure 3.25. The contours of the constant rms acceleration values are observed to follow the same behavior as those of the constant rms relative displacement contours as shown in Figure 3.25. From Equation (3.138) if,

$$B_3 > \frac{(K_1K_2 + K_1K_3 + K_2K_3)}{(K_1 + K_2)^{3/2}} \qquad (3.159)$$

then, Equation (3.138) reduces to

$$B_3 = \frac{K_2^2 a_g^2}{C(K_1 + K_2)^3} \qquad (3.160)$$

and, if $K_1 = K_2$, then

$$B_3 = \frac{a_g^2}{CK_2} \qquad (3.161)$$

Equations (3.160) and (3.161) show that for constant acceleration, K_1 and K_2 values and if the condition of equation (3.159) is satisfied, then B_3 will have constant values as can be seen in Figure 3.25. On the other hand, if

$$B_3 < \frac{(K_1K_2 + K_1K_3 + K_2K_3)}{(K_1 + K_2)^{3/2}} \qquad (3.162)$$

then, Equation (3.139) can be simplified as,

$$B_3 = C\left(\frac{K_1K_2 + K_1K_3 + K_2K_3}{K_2 a_g}\right) \qquad (3.163)$$

If K_1 and K_2 have equal values and they are smaller than K_3, then Equation (3.162) can be written as,

$$B_3 = C\left(\frac{2k_3}{a_g}\right)^2 \qquad (3.164)$$

This equation represents a linear relation between K_3 and B_3 for constant acceleration values. Also, when K_1 and K_2 are equal, but their values are larger than K_3, then Equation (3.163) takes the form,

$$B_3 = C\left(\frac{K_1}{\ddot{z}_g}\right)^2 \tag{3.165}$$

or

$$B_3 = C\left(\frac{K_2}{\ddot{z}_g}\right)^2 \tag{3.166}$$

We can see from Equation (3.165) and (3.166) that B_3 will have constant values for constant acceleration values when K_1 and K_2 are almost equal and they have larger values than K_3. Equations (3.164), (3.165) and (3.166) explain the behavior of constant rms acceleration contours shown in Figure 3.25.

The contours of constant K_2 and B_3 values are plotted in Figures 3.26 and 3.27 for equal K_1 and K_3 values in order to find whether it is possible to obtain values of relative displacement or acceleration that will break the limiting line produced when constant and medium K_1 and K_2 values are used to study the behavior of the model as shown in Figure 3.24. From Figure 3.26, we can notice that it is possible to obtain values of acceleration and relative displacement that will be as small as the values produced by the Maxwell type suspension when the values of K_1 and K_3 are equal small. Also, we can notice from Figure 3.26 that there is a limited region where no values of acceleration or relative displacement can be obtained and it is produced because of the linear relation that exists between the acceleration and the relative displacement. It can be observed that two acceleration values can correspond to the same relative displacement value for the same K_2 value and this happens due to the existence of both a linear and an inversely linear relation between the acceleration and the relative displacement. The appearance of lines representing constant relative displacement values for constant B_3 values as shown in Figure 3.26 provides another limiting behavior for the optimization of the suspension performance since no small relative displacement values can be obtained for a certain B_3 value.

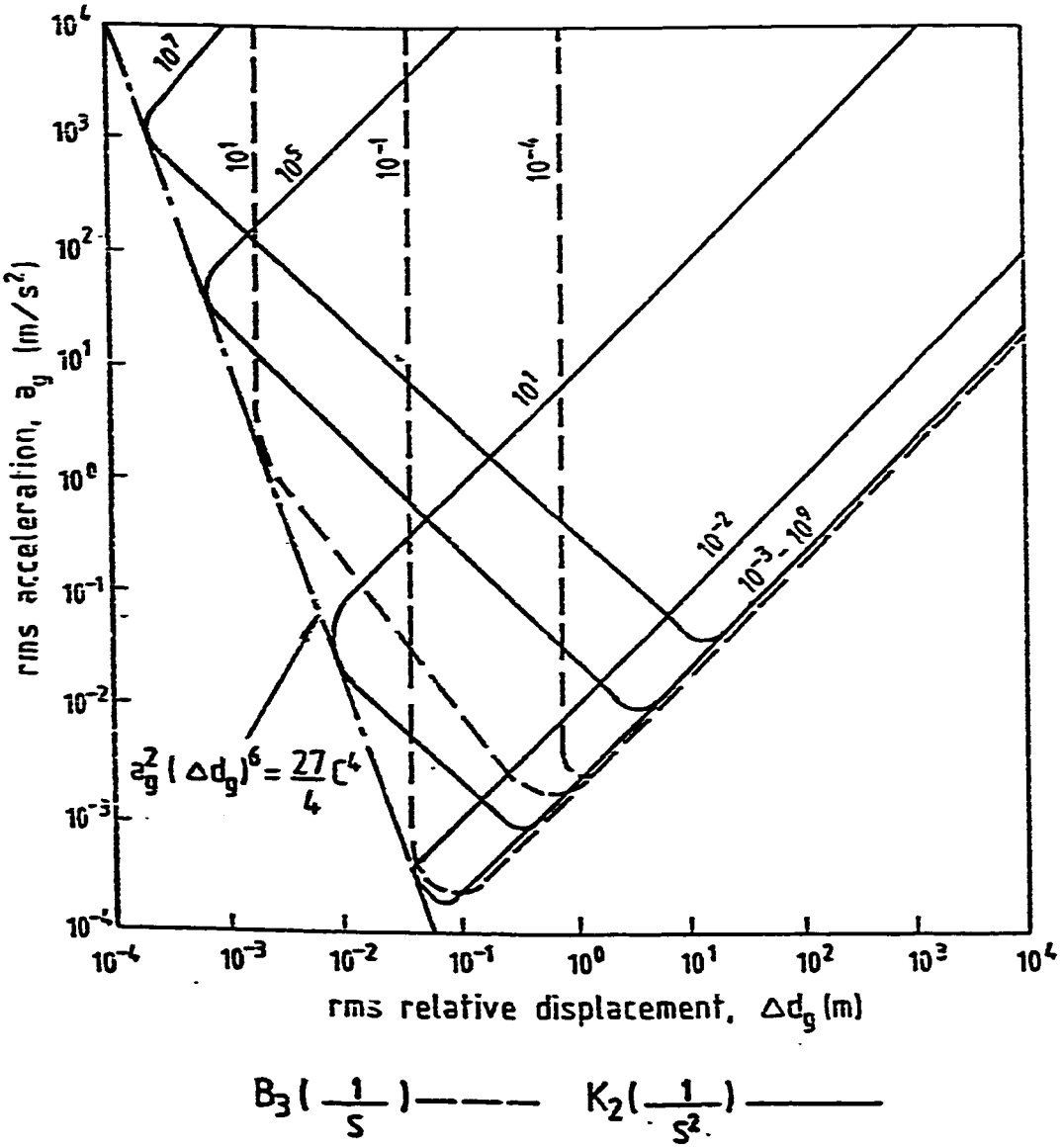

Figure 3.26 Contours of constant K_2 and B_3 values ($K_1 = K_2 = 10^{-3} \frac{1}{s^2}$)

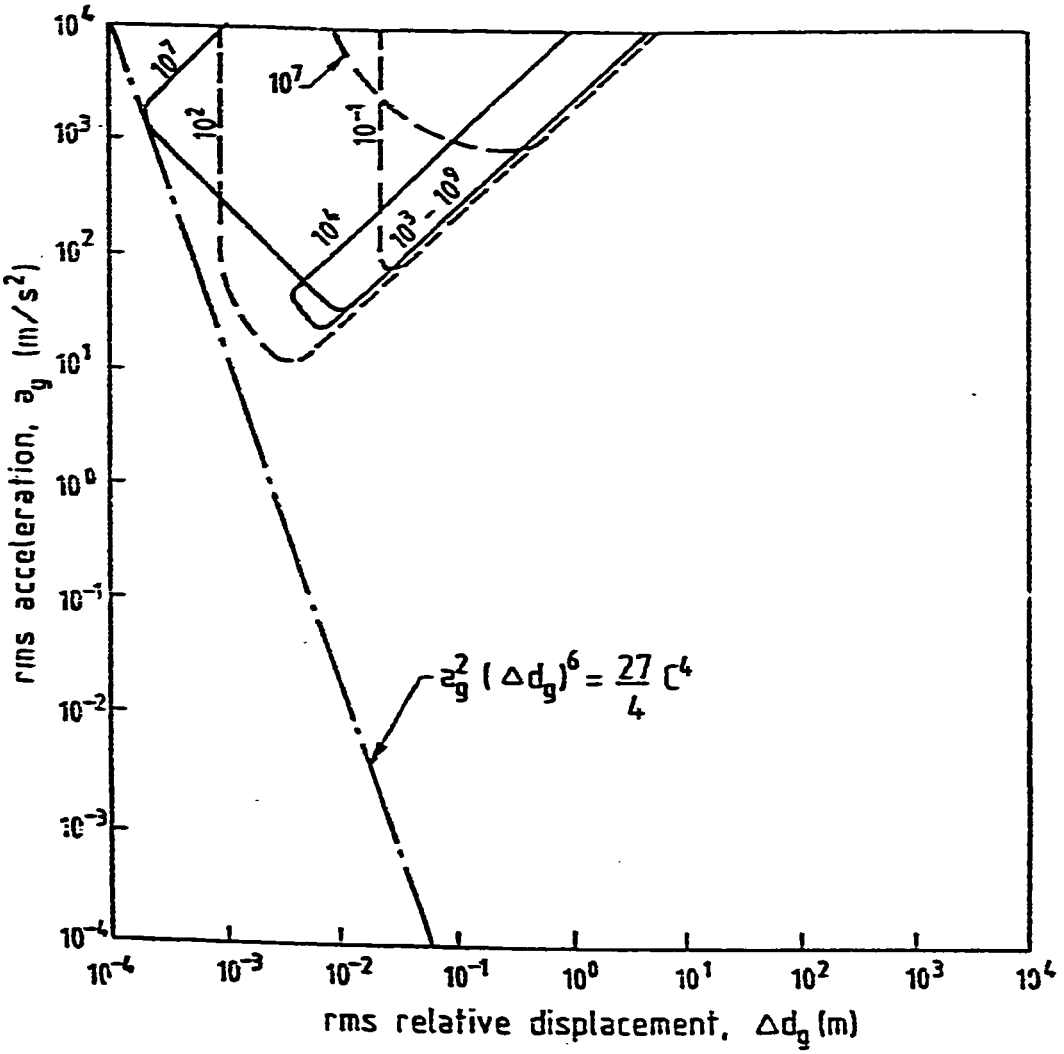

Figure 3.27 Contours of constant K_2 and B_3 values ($K_1 = K_3 = 10^3 \frac{1}{s^2}$)

It can be noted from Figure 3.27 that using larger K_1 and K_3 in the suspension will produce a similar behavior to the one shown in Figure 3.26 but with a very large increase in the acceleration values.

b). The response to the external force and road input:

The mean square relative displacement and the mean square acceleration of the mass due to the external force only are derived as shown in Appendix A and given by:

$$\overline{\Delta y_F^2} = R. \frac{NUM1}{DEN1} \tag{3.167}$$

and

$$\overline{a_F^2} = R. \frac{NUM2}{DEN2} \tag{3.168}$$

where,

$$R = \pi. \beta. \upsilon,$$

$$NUM1 = C_1^2 d_0 d_3 + C_0^2(-d_1 d_4 + d_2 d_3) \tag{3.169}$$

$$DEN1 = d_0(-d_0 d_3^2 - d_1^2 d_4 + d_1 d_2 d_3) \tag{3.170}$$

$$NUM2 = C_3^2(-d_0 d_3 + d_1 d_2) + C_2^2 d_3 d_4 \tag{3.171}$$

$$DEN2 = d_4(-d_0 d_3^2 - d_1^2 d_4 + d_1 d_2 d_3) \tag{3.172}$$

and

$$
\begin{aligned}
C_0 &= k_2 + k_3 \\
C_1 &= b_3 \\
C_2 &= k_2 + k_3 \\
C_3 &= b_3 \\
d_0 &= (k_1k_2+k_1k_3+k_2k_3)\,\upsilon \\
d_1 &= b_3\,\upsilon\,(k_1+k_2)+k_1k_2+k_1k_3+k_2k_3 \\
d_2 &= m\,\upsilon\,(k_2+k_3)+b_3(k_1+k_2) \\
d_3 &= m(k_2+k_3+b_3\,\upsilon) \\
d_4 &= mb_3
\end{aligned}
\qquad (3.173)
$$

To simplify the analysis, Equations (3.166) and (3.167) are written in the forms,

$$\overline{\Delta y_F^2} = \frac{R\ NUM\ 1}{m^2\ DEN\ 1} \qquad (3.174)$$

and

$$\overline{a_F^2} = \frac{R\ NUM\ 2}{m^2\ DEN\ 2} \qquad (3.175)$$

but where,

$$
\begin{aligned}
C_0 &= K_2 + K_3 \\
C_1 &= B_3 \\
C_2 &= K_2 + K_3 \\
C_3 &= B_3 \\
d_0 &= (K_1K_2+K_1K_3+K_2K_3)\,\upsilon \\
d_1 &= B_3\,\upsilon\,(K_1+K_2)+K_1K_2+K_1K_3+K_2K_3 \\
d_2 &= \upsilon\,(K_2+K_3)+B_3(K_1+K_2) \\
d_3 &= (K_2+K_3+b_3\,\upsilon) \\
d_4 &= B_3
\end{aligned}
\qquad (3.176)
$$

and where $B_3 = b_3/m$, $K_1 = k_1/m$, $K_2 = k_2/m$, $K_3 = k_3/m$. It is clear from Equations (3.173) and (3.174) that the acceleration and relative displacement responses are dependent on the mass itself as on the stiffness coefficients to mass and damping coefficient to mass ratios.

The rms relative displacement due to the external force is given by;

$$\Delta d_F = \left(R_{\cdot} \frac{NUM\,1}{DEN\,1}\right)^{1/2} \tag{3.177}$$

and the rms acceleration is given by;

$$a_F = \left(R_{\cdot} \frac{NUM\,2}{DEN\,2}\right)^{1/2} \tag{3.178}$$

Since our model is linear, the rms responses due to the road input and the external force input are summed-up to obtained the total rms response. The total rms relative displacement is given by

$$\Delta d = \left(\Delta d_g^2 + \Delta d_F^2\right)^{\frac{1}{2}} \tag{3.179}$$

and the total rms acceleration is given by

$$a = \left(a_g^2 + a_F^2\right)^{\frac{1}{2}} \tag{3.180}$$

Shown in Figure 3.28 a plot of the total rms relative displacement and the total rms acceleration behavior for different K_3 and B_3 values and with different levels of K_1 and K_2 values when they are equal and with a value of m equal to 250 kg[38]. When comparing the behavior of total responses in Figure 3.28 to the ground input responses in Figures 3.21 and 3.22, where the same K_1 and K_2 values are used, it can be observed that

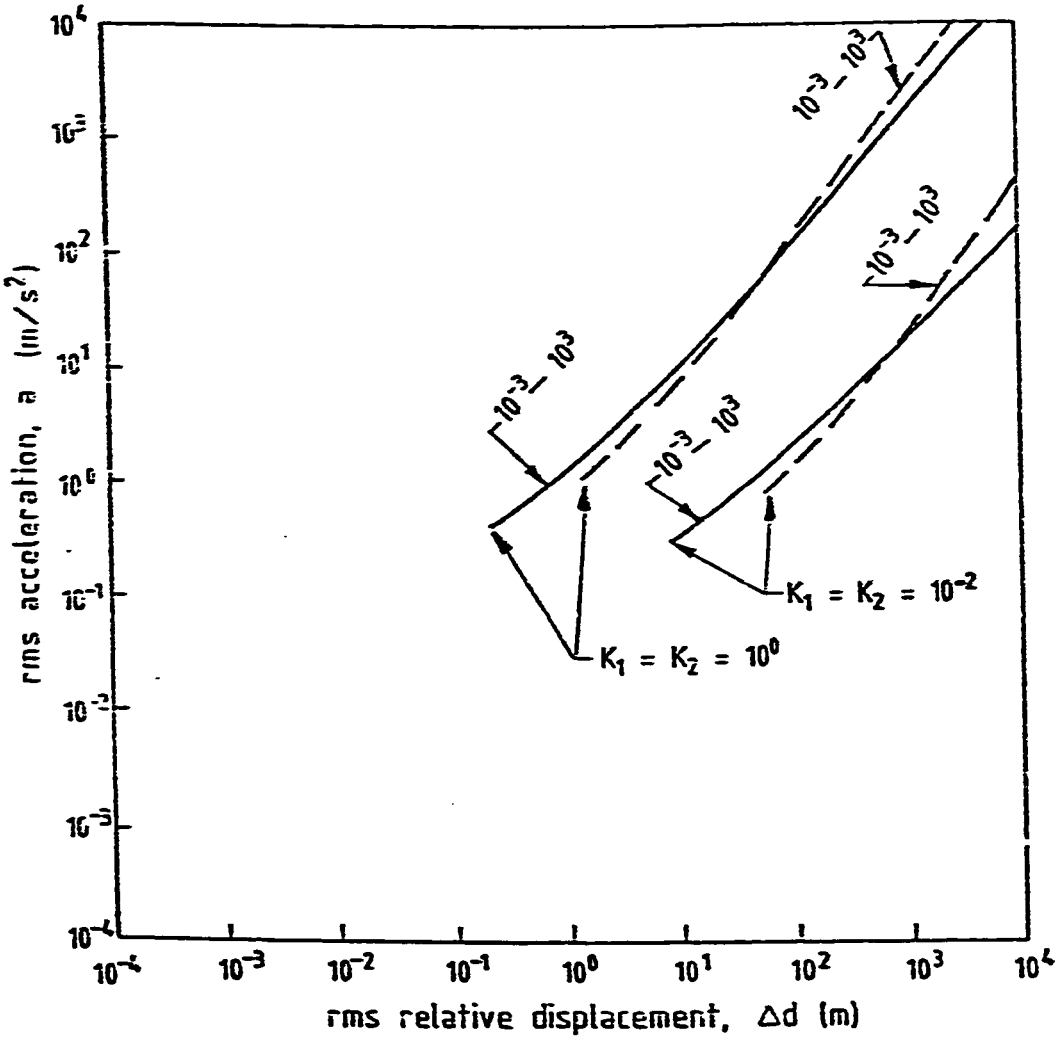

Figure 3.28 Contours of constant K_3 and B_3 values.

larger values of rms relative displacement and rms acceleration values appear in the case of total responses due to the effect of external force. Also, it can be noted that some kind of linear relation exists between the total rms acceleration and the total rms relative displacement when constant K_3 and B_3 values are used, which is a similar behavior to the one of the road input only. We can note from Figure 3.28 that as the values of K_1 and K_2 become larger, smaller values of relative displacement can be obtained.

The contours of constant K_2 and B_3 values for equal K_1 and K_3 values are plotted in Figures 3.29 and 3.30 to display the behavior of total responses. From Figure 3.29, it can be observed that using small K_1 and K_3 values results in both large relative displacement and acceleration values when compared to the behavior shown in Figure 3.26 where only the road input is applied. From Figure 3.30, it can be noted that using larger K_1 and K_3 values results in lower relative displacement values but without much effect on the acceleration values.

3.5 Response of 1-DOF Model with Maxwell Type Suspension in Parallel with a Viogt Type Suspension that is in Series with a Spring to Random Excitations

In this section, both the suspension systems of Maxwell type and the Voigt type that is in series with a spring, are combined to produce the suspension system represented by the model shown in Figure 3.31. The model consists of a vehicle mass m, three springs with coefficients k_1, k_2 and k_3 and two dashpots with damping coefficients b_1 and b_3.

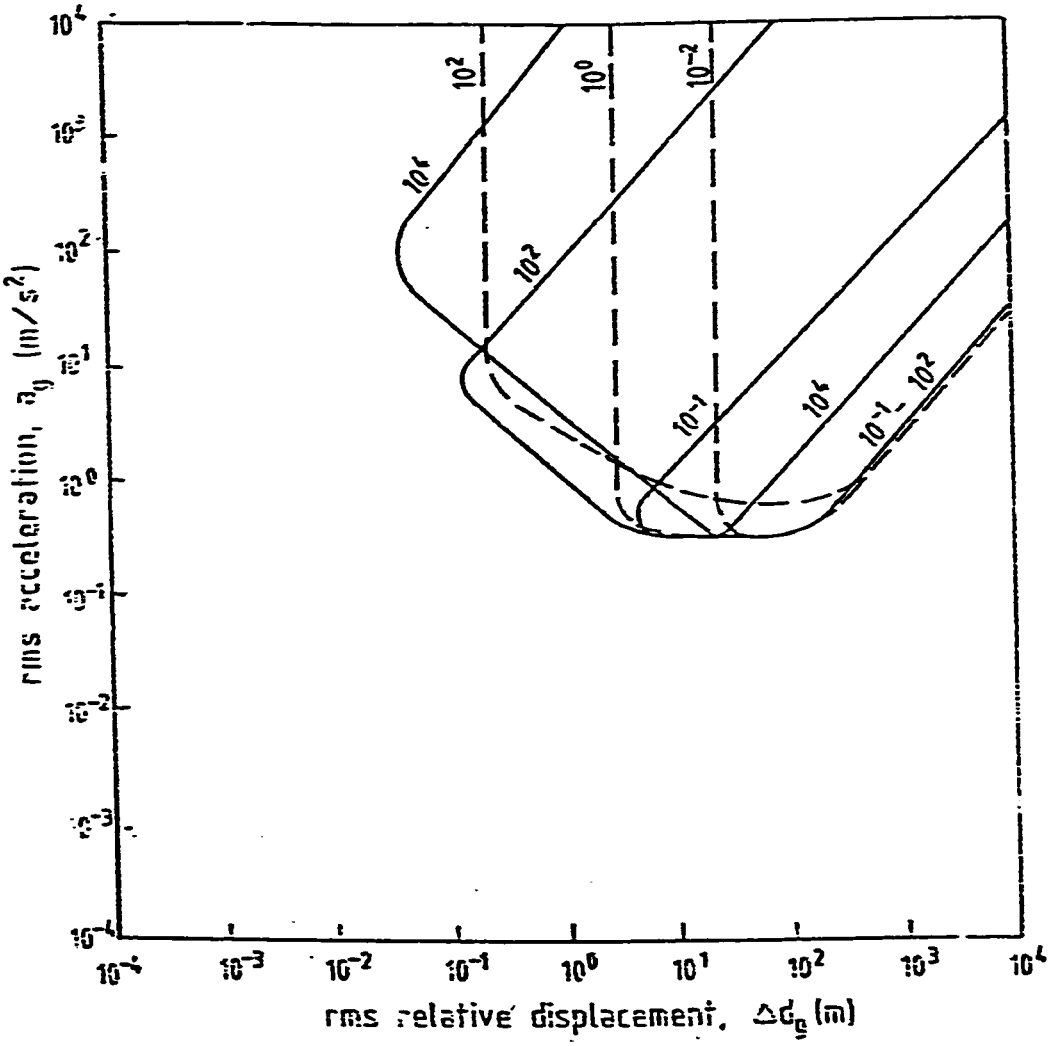

Figure 3.29 Contours of Constant K_2 and B_3 values ($K_1 = K_3 = 10^{-3}\frac{1}{s^2}$)

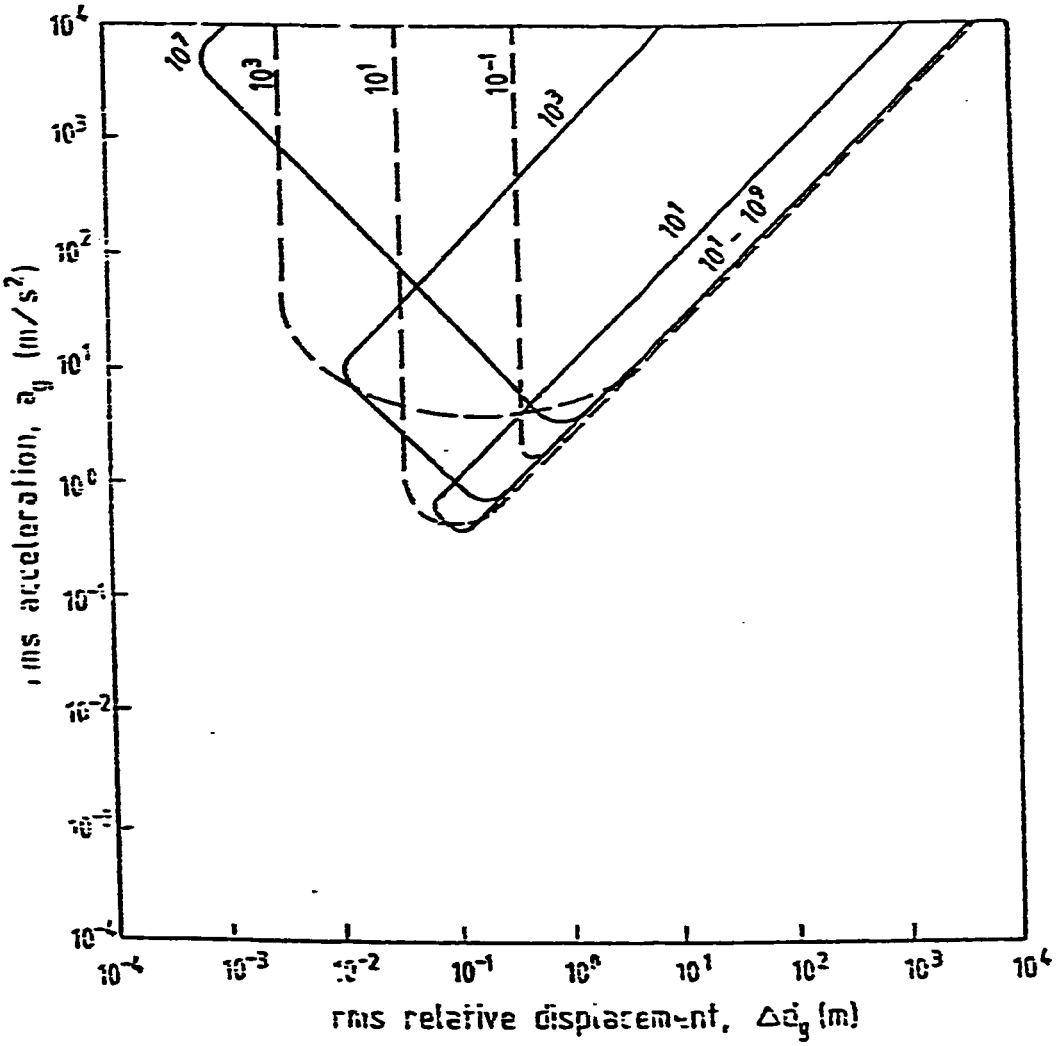

Figure 3.30 Contours of constant K_2 and B_3 values ($K_1 = K_3 = 10^0 \frac{1}{s^2}$)

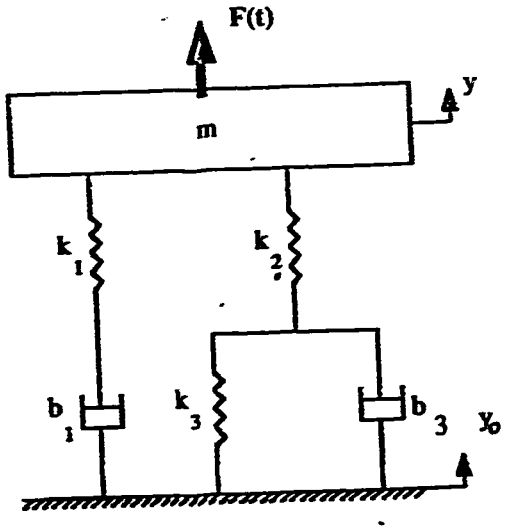

Figure 3.31. 1-DOF model with Maxwell type suspension in parallel with a Voigt type suspension that is in series with a spring

a. The response to the road input only, i.e., (F(t)=0):

The mean square relative displacement and the mean square acceleration of the mass due to the road input only are derived as shown in Appendix A. The mean square relative displacement is given by:

$$\overline{\Delta y_g^2} = C.\frac{NUM1}{DEN1} \tag{3.181}$$

where

$$C = \pi.A.V,$$

$$NUM1 = C_3^2(d_1d_2 - d_0d_3) + (C_2^2 - 2C_1C_3)d_1d_4 + C_1^2d_3d_4 \tag{3.182}$$

and

$$DEN1 = d_4(d_1d_2d_3 - d_1^2d_4 - d_od_3^2) \tag{3.183}$$

where,

$$\begin{aligned} C_1 &= -mk_1(k_2+k_3) \\ C_2 &= -m\,(b_1k_2+b_1k_3+k_1b_3) \\ C_3 &= -m\,b_1b_3 \\ d_o &= k_1k_2k_3 \\ d_1 &= K_1b_1(k_2+k_3)+k_2(k_1b_3+k_3b_1) \\ d_2 &= mk_1\,(k_2+k_3) + b_1b_3\,(k_1+k_2) \\ d_3 &= m\,(k_3b_1+k_2b_1+k_1b_3) \\ d_4 &= mb_1b_3 \end{aligned} \tag{3.184}$$

The mean square acceleration is given by:

$$a_z^2 = C\,\frac{NUM\,2}{DEN\,2} \tag{3.185}$$

where,

$$NUM2 = C_3^2(d_1d_2 - d_od_3) + (C_2^2 - 2C_1C_3)d_1d_4 + C_1^2d_3d_4 \tag{3.186}$$

$$DEN2 = d_4(d_1d_2d_3 - d_1^2d_4 - d_od_3^2) \tag{3.187}$$

where,

$$\begin{aligned} C_1 &= k_1k_2k_3 \\ C_2 &= k_1k_2b_1+k_1k_3b_1+k_1k_2b_3+k_3k_2b_1 \\ C_3 &= b_1b_3(k_1+k_2) \end{aligned} \tag{3.188}$$

and d_o,d_1,d_2,d_3 and d_4 are as given by Equation (3.184).

The analysis of the relative displacement and acceleration is simplified by writing the coefficient given in Equation (3.184) in the form,

$$
\begin{aligned}
C_1 &= K_1(K_2+K_3) \\
C_2 &= (B_1K_2+B_1K_3+K_1B_3) \\
C_3 &= B_1B_3 \\
d_o &= K_1K_2K_3 \\
d_1 &= K_1B_1(K_2+K_3)+K_2(K_1B_3+K_3B_1) \\
d_2 &= K_1\,(K_2+K_3) + B_1B_3\,(K_1+K_2) \\
d_3 &= K_3B_1+K_2B_1+K_1B_3 \\
d_4 &= B_1B_3
\end{aligned}
\qquad (3.189)
$$

and the coefficients of Equation (3.188) in the form,

$$
\begin{aligned}
C_1 &= K_1K_2K_3 \\
C_2 &= K_1K_2B_1+K_1K_3B_1+K_1K_2B_3+K_3K_2B_1 \\
C_3 &= B_1B_3\,(K_1+K_2)
\end{aligned}
\qquad (3.190)
$$

where $K_1 = k_1/m$, $K_2 = k_2/m$, $K_3 = k_2/m$, $B_3 = b_3/m$ and $B_1 = b_1/m$. It can be noted that the relative displacement and the acceleration responses are dependent on the damping coefficient and stiffness coefficients to mass ratios.

In this section, the responses of the model are investigated when different medium values of K_2,K_3 and B_3 values are used, and with a wide range of K_1 and B_1 values. The reason behind this that if large values of K_2 or K_3 and B_3 values are used, then the effects of K_1 and B_1 values on the suspension performance will be small, and it is expected that the obtained responses will be similar to those of the Voigt type suspension which is in series with a spring, such a model was studied in Section 3.3. On the other hand, if small values of K_2 or K_3 and B_3 values are used, then their effect will be small when compared to the effect of the K_1 and B_1 values which leads us to the performance of Maxwell type suspension that was discussed in Section 3.1.

In Figure 3.32, the contours of constant K_1 and B_1 values are plotted for a medium value equal to 10^{-2} for K_2, K_3 and B_3. We can observe that for small and constant B_1 values, the relative displacement is constant regardless of the value of K_1. At larger constant values of B_1 we note that the relative displacement is constant for small values of K_1 and then as the K_1 values increase, we find that the acceleration and the relative displacement are inversely proportional in the log-log scale and again, we obtain constant values of relative displacement at large values of K_1. The availability of constant relative displacement values for constant B_1 values imposes a limitation on the optimization of the suspension performance where no smaller values of relative displacement can be obtained. The contours of constant K_1 values show that for small B_1 values, the relative displacement is constant and as the B_1 values increase, the acceleration and the relative displacement become inversely proportional in the log-log scale and at larger B_1 values, they become linearly proportional which shows that it is possible to have two acceleration values for one K_1 value. The existence of the constant relative displacement values at small B_1 values and for constant K_1 values also imposes a constraint on the optimization of the suspension performance.

For larger K_2, K_3 and B_3 medium values the contours of constant K_1 and B_1 values are plotted in Figure 3.33. When comparing the behavior of the suspension responses in this case to the previous case shown in Figure 3.32, we observe that the acceleration values become larger for the later case where larger K_2, K_3 and B_3 values are used and at the same time we see that we could have small relative displacement values as

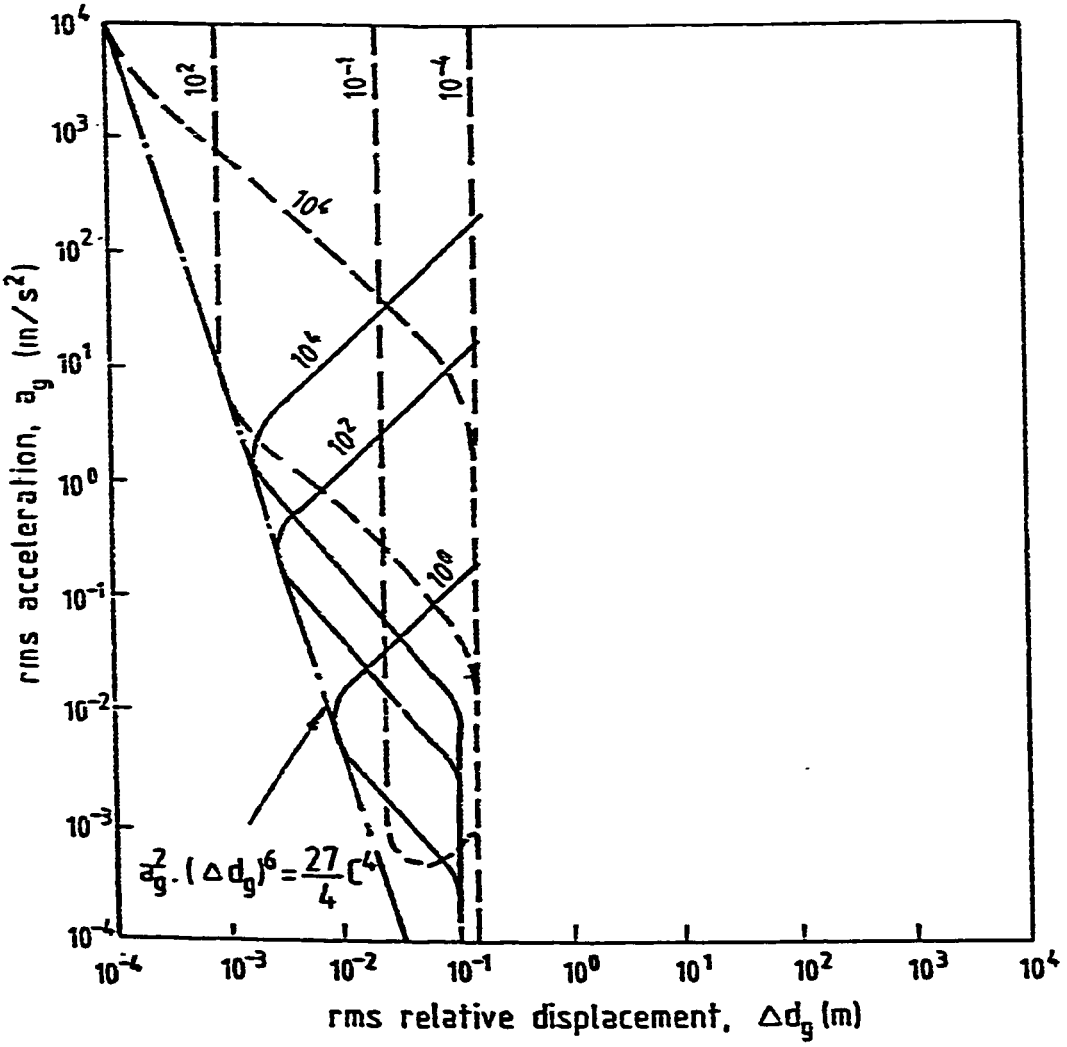

Figure 3.32 Contours of constant K_1 and B_1 values ($K_2 = K_3 = 10^{-2}\frac{1}{S^2}$ and $B_3 = 10^{-2}\frac{1}{S}$)

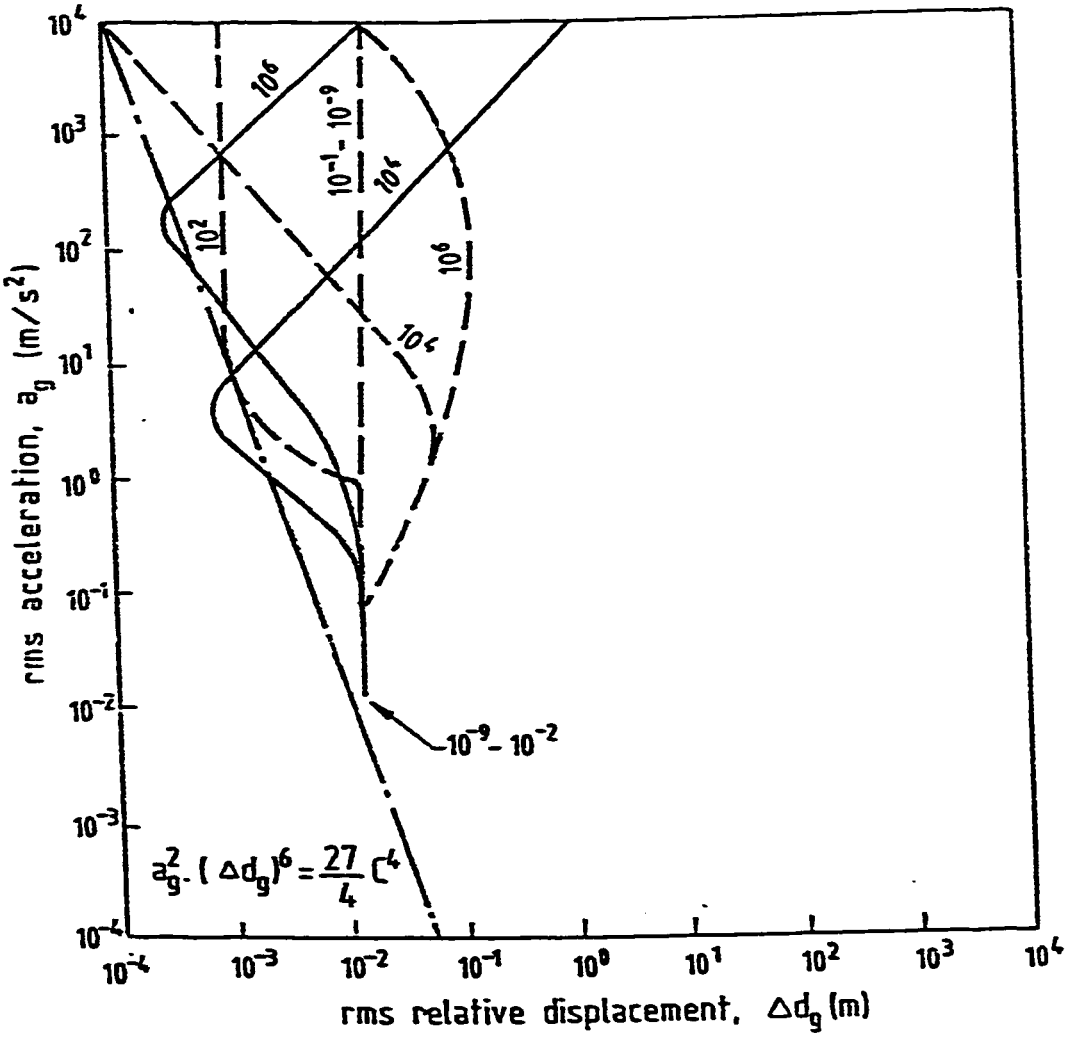

$B_1(\frac{1}{S})$ ——— $K_1(\frac{1}{S^2})$ ———

Figure 3.33 Contours of constant K_1 and B_1 values. ($K_2 = K_3 = 10^0 \frac{1}{S^2}$ and $B_3 = 10^0 \frac{1}{S}$)

in the case of smaller medium values. In the case of larger medium values, it can be observed that obtaining more than one acceleration value for a constant K_1 value is possible, and we can see that it is also possible to have more than one acceleration value for a constant B_1 value. The acceleration values become large in the case we use larger values of K_2,K_3 and B_3 as shown in Figure 3.34.

b. The response to the external force and the road input:

The mean square relative displacement and the mean square acceleration of the mass due to the external force only are derived as shown in Appendix A. The mean square acceleration is given by:

$$\overline{\Delta y_F^2} = R.\frac{NUM1}{DEN} \tag{3.191}$$

where,

$R = \pi.A.V,$

$$NUM1 = C_2^2 M_2 + (C_1^2 - 2C_oC_2)M_3 + C_o^2 M_4 \tag{3.192}$$

$$DEN = d_o(d_1 M_4 - d_3 M_3 + d_5 M_2) \tag{3.193}$$

where,

$$M_4 = \frac{1}{d_o}(d_2 M_3 - d_4 M_2) \tag{3.194}$$

$$M_3 = \frac{1}{d_o}(d_2 M_2 - d_4 M_1) \tag{3.195}$$

$$M_2 = d_1 d_4 - d_o d_5 \tag{3.196}$$

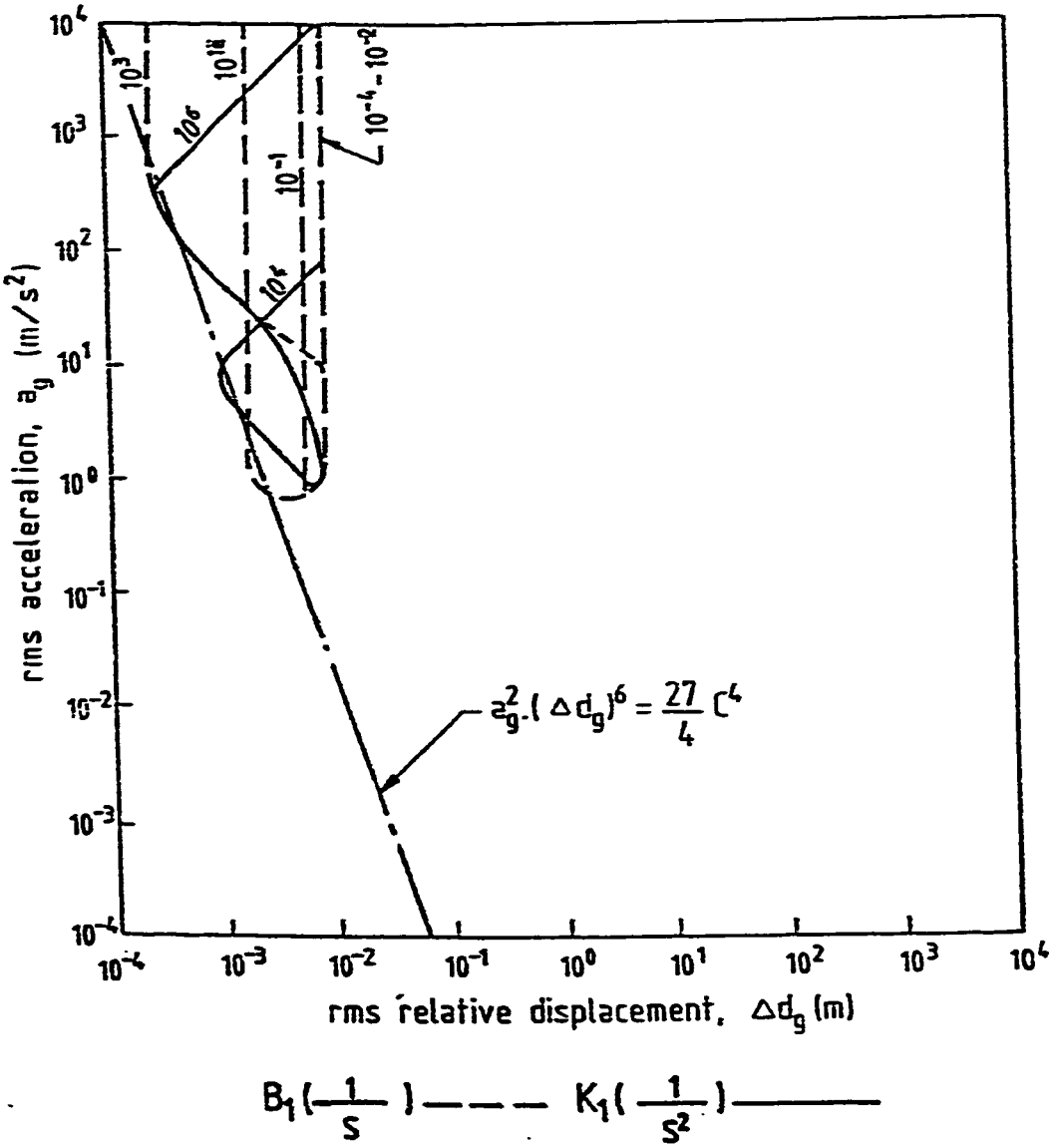

Figure 3.34 Contours of constant K_1 and B_1 values ($K_2 = K_3 = 10^2 \frac{1}{S^2}$ and $B_3 = 10^2 \frac{1}{S}$)

and,

$$C_1 = k_1(k_2+k_3)$$
$$C_2 = k_1b_3+k_2b_1+k_3b_1)$$
$$C_3 = b_1b_3$$
$$d_0 = \upsilon\, k_1k_2k_3$$
$$d_1 = k_1k_2k_3 + \upsilon k_1k_2b_1 + \upsilon k_3b_1 + \upsilon k_1k_2b_3 + \upsilon k_2k_3b_1 \qquad (3.197)$$
$$d_2 = m\,\upsilon\, k_1k_2 + m\,\upsilon k_1k_3 + \upsilon\, k_1b_1b_3 + \upsilon k_2b_1b_3 + k_1k_2b_1 + k_1k_3b_1 + k_1k_2b_3 + k_2k_3b_1$$
$$d_3 = mk_1k_2 + mk_1k_3 + k_1b_1b_3 + k_2b_1b_3 + m\,\upsilon k_1b_3 + m\,\upsilon k_2b_1 + m\,\upsilon k_3b_1$$
$$d_4 = mk_1b_3 + mk_2b_1 + mk_3b_1 + m\,\upsilon b_1b_3$$
$$d_5 = mb_1b_3$$

The mean square acceleration is given by,

$$\overline{a_F^2} = R.\ \frac{NUM2}{DEN} \qquad (3.198)$$

where

$$NUM2 = C_4^2M_o + (C_3^2 - 2C_2C_4)M_1 \qquad (3.199)$$

and,

$$C_2 = k_1\,(k_2+k_3)$$
$$C_3 = k_1b_3+k_2b_1+k_3b_1 \qquad (3.200)$$
$$C_4 = b_1b_3$$

and the coefficient d_0 to d_5 are given by Equation (3.197). To simplify the analysis of the relative displacement response, Equation (3.191) is written in the form,

$$\overline{\Delta y_F^2} = \frac{R}{m^2}.\ \frac{NUM1}{DEN} \qquad (3.201)$$

where NUM1 and DEN are as given by Equations (3.192) and (3.193), but the coefficients given by Equation (3.197) are written in the form,

$$C_0 = K_1(K_2+K_3)$$
$$C_1 = K_1B_3+K_2B_1+K_3B_1$$
$$C_2 = B_1B_3$$
$$d_0 = \upsilon K_1K_2K_3$$
$$d_1 = K_1K_2K_3+\upsilon K_1K_2B_1+\upsilon K_3B_1+\upsilon K_1K_2B_3+\upsilon K_2K_3B_1 \qquad (3.202)$$
$$d_2 = \upsilon K_1K_2+\upsilon K_1K_3+\upsilon K_1B_1B_3+K_1K_2B_1+K_1K_3B_1+K_1K_2B_3+K_2K_3B_1$$
$$d_3 = K_1K_2+K_1K_3+K_1B_1B_3+K_2B_1B_3+\upsilon K_1B_3+\upsilon K_2B_1+\upsilon K_3B_1$$
$$d_4 = K_1B_3+K_2B_1+K_3B_1+\upsilon B_1B_3$$
$$d_5 = B_1B_3$$

where $K_1 = k_1/m$, $K_2 = k_2/m$, $K_3 = k_3/m$, $B_1 = b_1/m$ and $B_3 = b_3/m$ similarly, the acceleration response is simplified by writing Equation (3.198) in the form,

$$\overline{a_F^2} = \frac{R}{m^2}\cdot\frac{NUM\,2}{DEN} \qquad (3.203)$$

where NUM2 and DEN are as given by Equations (3.199) and (3.193) and where,

$$C_2 = K_1(K_2+K_3)$$
$$C_3 = K_1B_3+K_2B_1+K_3B_1 \qquad (3.204)$$
$$C_4 = B_1B_3$$

and the coefficients d_0 to d_5 as given by Equation (3.202). From Equations (3.201) and (3.203) we can see that the obtained responses are dependent on the stiffness coefficients to mass and the damping coefficients to mass ratios as on the mass itself. The total rms relative displacement is given by

$$\Delta d = \left(\overline{\Delta y_g^2}+\overline{\Delta y_F^2}\right)^{\frac{1}{2}} \qquad (3.205)$$

and the total rms acceleration is given by;

$$a = \left(\overline{a_g^2}+\overline{a_F^2}\right)^{\frac{1}{2}} \qquad (3.206)$$

To study the total responses of the model, contours of constant K_1 and B_1 values are plotted in Figures 3.35 and 3.36 for medium values of K_2, K_3 and B_3 values and an m value equal to 250 [38]. When comparing the behavior of total responses shown in Figure 3.35, where a value of 10^{-2} ($1/s^2$) is given for K_2, K_3 and 10^{-2} (1/s) for B_3, with the behavior of the responses due to the road input only shown in Figure 3.32 where the same value of K_2, K_3 and B_3 is used, we can see that the rms relative displacement and the rms acceleration values become very large in the case when the external force is applied. The total responses of the model, shown in Figure 3.36, are again compared to the ground input responses shown in Figure 3.33 where the same value of $K_1 = K_2 = 10^{\circ}$ ($1/s^2$) and $B_3 = 10^{\circ}$ (1/s) is used in both cases and it can be observed that small relative displacement values due to both inputs can be comparable to the relative displacement values obtained due to the ground input only. The same result also applies to the acceleration values in both cases, but we can see that in the case where only the road input is applied, it is possible to get small values of acceleration and relative displacement that we can never approach when the external force is added.

We can note from Figures 3.35 and 3.36 that as the value of K_2, K_3 and B_3 becomes larger, smaller values of relative displacement can be obtained.

3.6 Comparison of the Responses of the 1-DOF Models

In the previous sections of this chapter, the responses of five different 1-DOF suspension models were studied and analyzed separately when subjected to road input as described in and external force disturbance as described in Chapter 2. In this section, the different responses of the models to the road input are compared to anticipate the model that will produce the optimum values of relative displacement and acceleration. Then, the model responses to both the road input and the external force disturbances

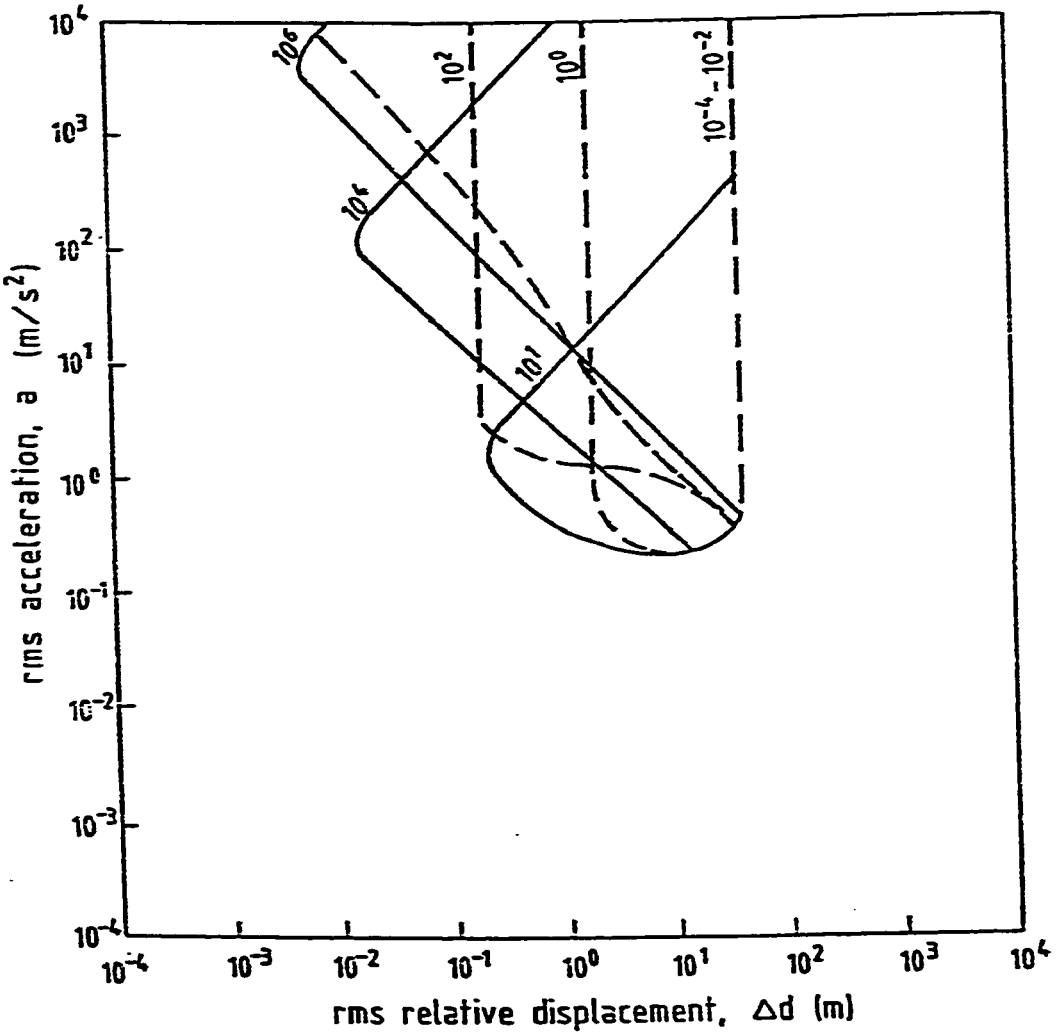

Figure 3.35 Contours of constant K_1 and B_1 values ($K_2 = K_3 = 10^{-2}\frac{1}{s^2}$ and $B_3 = 10^{-2}\frac{1}{s}$)

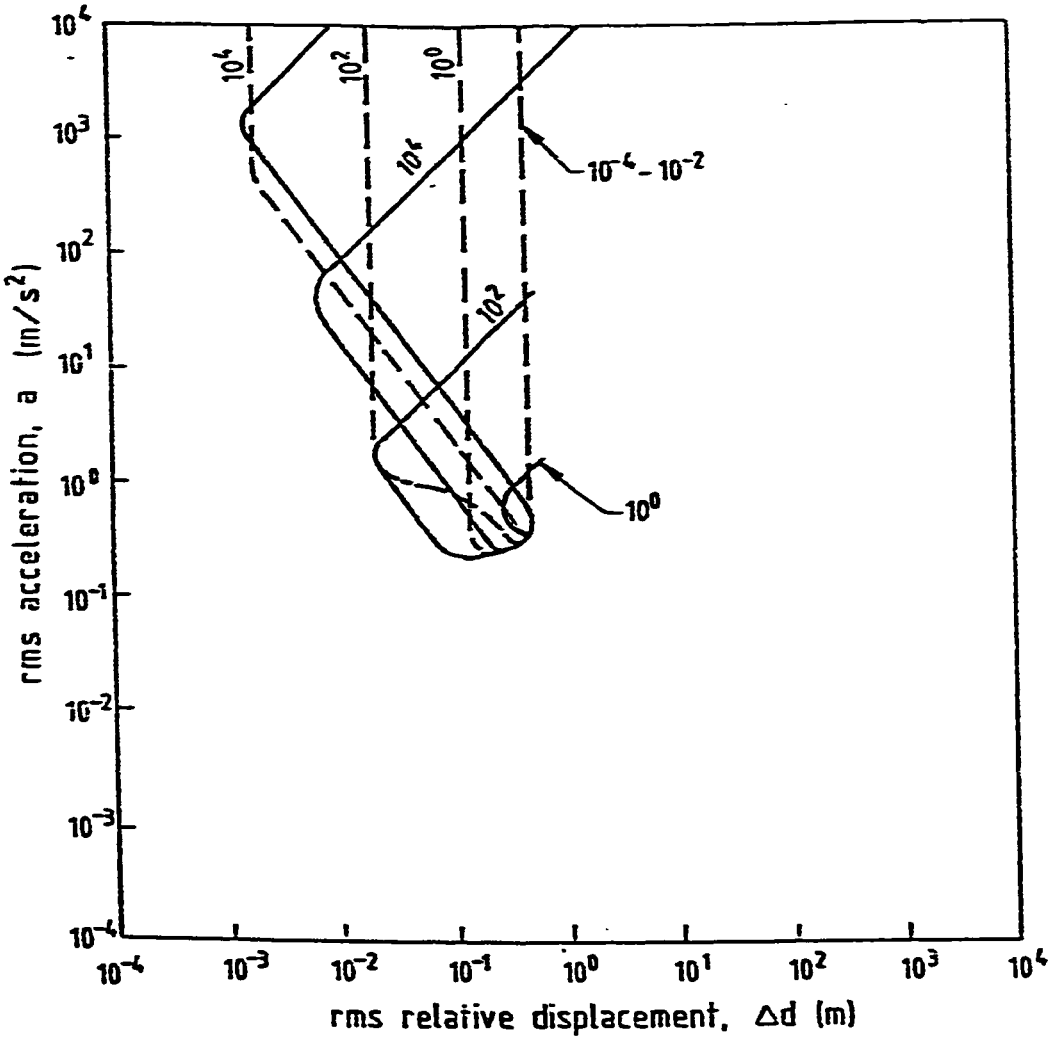

Figure 3.36 Contours of constant K_1 and B_1 values ($K_2 = K_3 = 10^0 \frac{1}{S^2}$ and $B_3 = 10^0 \frac{1}{S}$)

are compared to predict the model that will produce the optimum acceleration and relative displacement values.

a. Comparing the responses of the models when subjected to the road input only (F(t)=o)

It is shown in the analysis of the responses of the Maxwell type suspension (Figure 3.1) in Section 3.1 that there is a limit to the minimization of both the relative displacement and acceleration values and it is given by:

$$a_g^2.(\Delta d_g)^6 \geq \frac{27}{4}C^4 \qquad (3.207)$$

The line representing this limit was shown in Figure 3.3 where a simulation of the model responses has been made.

There is a doubt, i.e., whether it is possible to break this limit and to achieve both smaller values of relative displacement and acceleration or either one of them by other models.

It was shown in Figure 3.8 that the responses of the Maxwell type suspension that is in parallel with a spring (Figure 3.4), when a small value of K_1 is used, can behave exactly the same as the responses at the Maxwell type suspension and the same boundary limit is produced. When a larger K_1 value was used, it was shown in Figure 3.9 that it is possible to obtain some smaller values of relative displacement than the ones obtained by the Maxwell type suspension, but at the same time the acceleration values can be seen to be much larger than the ones that could be obtained by the Maxwell type suspension. The physical reason behind this behavior is that using a spring with larger stiffness value adds more rigidity to the suspension system and thus making it less able to deflect and more

forceful to vibrate the vehicle mass. It is clear that using a spring in parallel to a Maxwell type suspension will not provide regions of acceleration and relative displacement that could be produced by the Maxwell type suspension.

The responses behavior of a Voigt type suspension that is in series with a spring (Figure 3.12) was shown in Figure 3.16 when a very small value of K_3 is used. It is clear in this case that the suspension responses behave exactly the same as the responses of the Maxwell type suspension. It was shown in Figure 3.17 that using a larger value of K_3 produces some smaller relative displacement values will break the limit of Equation (3.207), but on the other hand the corresponding acceleration values are much larger than the ones that could be produced by the Maxwell type suspension. Here, it is also clear that adding more stiffness to the suspension could produce some smaller relative displacement values, but this occurs at the expense of the acceleration values which become large.

The relative displacement and acceleration responses of a Voigt type suspension that is in series with a spring and both are in parallel with a spring (Figure 3.20) are analyzed in Section 3.4 for different medium and equal K_1 and K_2 values. It was shown in Figure 3.24 that a certain limit exists for the minimization of both relative displacement and acceleration for the different equal K_1 and K_2 values. From the same figure also, we can note that as the K_1 and K_2 values become larger, the relative displacement values become smaller and the acceleration values become larger and it is clear that it is possible to obtain much smaller values of relative displacement than those that could be obtained by the Maxwell type suspension, but unfortunately these small values of relative displacement occur where it is not possible to obtain small acceleration values as those of the Maxwell type suspension. On the other hand, we can obtain a similar behavior to the behavior of the Maxwell type suspension when small and equal K_1 and K_3 values are used to plot the

contours of constant K_2 and B_3 values as shown in Figure 3.26. It is shown in Figure 3.27 that increasing the values of K_1 and K_3 will produce large acceleration values.

In Section (3.5), both the Maxwell type suspension and the Voigt type suspension that is in series with a spring are placed in parallel to each other to produce one suspension system (Figure 3.31). From Figures (3.33) and (3.34) we can see that using larger K_2, K_3 and B_3 values could produce values of relative displacement that are smaller than the values that were obtained by the Maxwell type suspension. As before, these smaller values of relative displacement exist in the regions where unacceptably large values of acceleration occur due to the increased stiffness of the suspension system.

From the above comparisons of the acceleration and relative displacement responses of the different 1-DOF suspension models with the responses of the Maxwell type suspension we can conclude that the only model that will be able to produce both smaller and acceptable acceleration and relative displacement values is the Maxwell suspension model.

b. Comparing the responses of the models when subjected to both the road input and the external force disturbance.

We have seen in Section 3.1 that the Maxwell type suspension is not suitable for the case where the external force disturbance is applied. On the other hand, there was no limit on the application of the external force disturbance to the other force different models. In Sections 3.2-3.5, we have seen that the application of external force disturbance in addition to the road input will result in larger acceleration and relative displacement values that can be obtained when the road input is applied only.

In the simulation of the Maxwell type suspension that is parallel with a spring (Figure 3.4) when a small value of K_1 is used and when an external force is applied, we

can see that the possible acceleration and relative displacement values are very large, but from Figure 3.11 we can see that a larger K_1 value could achieve substantial improvement in obtaining smaller relative displacement values, but without any improvement in the minimization of the acceleration values.

Similar conclusions can be made for the responses of the Voigt type suspension that is in series with a spring (Figure 3.12). When analyzing the acceleration and relative displacement responses shown in Figures 3.18 and 3.19 and where the model has been subjected to additional external force disturbance. It can be seen from Figure 3.18 that very large values of acceleration and relative displacement can be obtained when a small stiffness value of K_3 is used and by increasing the value of K_3, as shown in Figure 3.19, smaller values of relative displacement could be obtained without any minimization of the acceleration values.

From Figure 3.28, where the responses to both the road input and the external force disturbance have been applied to the Voigt type that is in series with a spring and both are in parallel with a spring (Figure 3.20), we can see that using small values of stiffness for K1 and K_2 will produce large relative displacement values and by increasing the stiffness values, we will be able to reduce the relative displacement values. From Figure 3.29 it is possible to observe that using small K_1 and K_3 values results in large acceleration and relative displacement values and from Figure 3.30, we can see that using larger K_1 and K_3 values will result in smaller relative displacement values.

In Section 3.5, both the Maxwell type suspension and the Voigt type suspension that is in series with a spring (Figure 3.31) are combined in parallel to produce one suspension model. The model responses are analyzed when subjecting it to both external force disturbance and road input as shown in Figures 3.35 and 3.36 for two medium values. By

investigating both the figures simultaneously, we can observe that increasing the K_2, K_3 and B_3 values will reduce the relative displacement values without much influence on the acceleration values.

From the above analysis of the different 1-DOF model responses when subjected to both the road input and the external force disturbance, we conclude that a similar behavior is observed for all models in the sense that using small stiffness values will produce very large relative displacements. As the stiffness values increase, it is more likely to obtain smaller values of relative displacement and they are even comparable to the values that could be obtained for the Maxwell type suspension when subjected only to the road input. The effect of the stiffness values on the minimization of acceleration values seems to be very little, but at larger stiffness values, it is less likely to obtain small acceleration values.

It can be seen from the provided figures that generally there are multiple suspension parameters for any set of performance measures. This point is very important for design and optimization of vehicle suspension systems.

CHAPTER 4

RESPONSE OF 2-DOF SUSPENSION SYSTEMS TO RANDOM EXCITATIONS

The behaviors of the acceleration and relative displacement responses of different 1-DOF suspension systems were studied in Chapter 3. The conducted studies have lead to better understanding of suspension systems in terms of their performance limits. In this chapter, the studies are expanded to 2-DOF vehicle models in order to obtain results closer to realistic performance systems. The system responses are studied here when subjected to the road input described in Chapter 2.

4.1 Response of 2-DOF Model with Maxwell Type Secondary Suspension to Random Excitations

The 2-DOF vehicle model shown in Figure 4.1 consists of a sprung mass m_2, an unsprung mass m_1, a primary suspension and a secondary suspension. The Secondary suspension is of Maxwell type and consists of a spring with stiffness coefficient k_2 and a dashpot with damping coefficient b_2. The Primary suspension consists of a spring with a stiffness coefficient k_1.

The mean square responses of the model are derived as shown in Appendix A. The mean square relative displacement of the secondary suspension in given by,

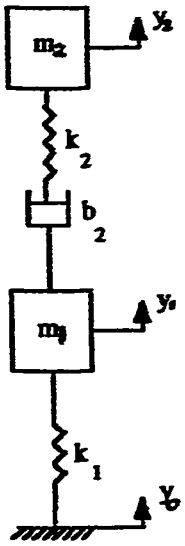

Figure 4.1. 2-DOF vehicle model with Maxwell type secondary suspension.

$$\overline{(y_2 - y_1)^2} = C \cdot \frac{NUM1}{DEN} \tag{4.1}$$

where,

$C = \pi \cdot A.V._n$

$$NUM1 = C_1^2 d_o d_3 + C_o^2(-d_1 d_4 + d_2 d_3) \tag{4.2}$$

$$DEN = d_o(-d_o d_3^2 - d_1^2 d_4 + d_1 d_2 d_3) \tag{4.3}$$

where,

$$\begin{aligned} C_o &= k_1 k_2 m_2 \\ C_1 &= -k_1 b_2 m_2 \\ d_o &= k_1 k_2 b_2 \\ d_1 &= k_1 k_2 m_2 \\ d_2 &= m_2 b_2 (k_1 + k_2) + m_1 k_2 b_2 \\ d_3 &= m_1 m_2 k_2 \end{aligned} \tag{4.4}$$

$$d_4 = m_1 m_2 b_2$$

The mean square relative displacement of the primary suspension is given by,

$$\overline{(y_1 - y_o)^2} = C \cdot \frac{NUM2}{DEN} \qquad (4.5)$$

where,

$$NUM2 = C_3^2(-d_o d_3 + d_1 d_2) + (C_2^2 - 2C_1 C_3) d_1 d_4 + C_1^2 d_3 d_4 \qquad (4.6)$$

where,

$$C_1 = -m_2 k_2 b_2 - m_1 k_2 b_2$$
$$C_2 = -m_1 m_2 k_2 \qquad (4.7)$$
$$C_3 = -m_1 m_2 b_2$$

and the coefficients d_o to d_4 are as given by Equation (4.4). The mean square acceleration of the sprung mass, m_2 is given by,

$$\overline{a_s^2} = C \cdot \frac{NUM3}{DEN} \qquad (4.8)$$

where,

$$NUM3 = C_1^2 d_3 \qquad (4.9)$$

where,

$$C_1 = k_1 k_2 b_2 \qquad (4.10)$$

and the coefficient d_3 is as given by Equation (4.4).

To simplify the analysis of the three responses, the coefficients in Equation (4.4) can be written in the form,

$$C_o = -K_1 K_2$$
$$C_1 = -K_1 B_2$$
$$d_o = K_1 K_2 B_2 \qquad (4.11)$$
$$d_1 = K_1 K_2$$
$$d_2 = B_2 (K_1 + K_2) + MK_2 B_2$$
$$d_3 = MK_2$$
$$d_4 = MB_2$$

and the coefficient of Equation (4.7) can be written in the form,

$$C_1 = -K_2 B_2 - MK_2 B_2$$
$$C_2 = -MK_2 \qquad (4.12)$$
$$C_3 = -MB_2$$

and C_1 that is given by Equation (4.10) can be written in the form,

$$C_1 = K_1 K_2 B_2 \qquad (4.13)$$

where $K_1 = k_1/m_2$, $K_2 = k_2/m_2$, $B_2 = b_2/m_2$ and $M = m_1/m_2$. In this way the responses can be shown to be dependent on the stiffness and damping coefficients to the unsprung mass ratios and on the mass ratio M.

The rms responses of the model are given by,

$$(y_2 - y_1)_{rms} = \sqrt{C_o \frac{NUM1}{DEN}} \qquad (4.14)$$

$$(y_1 - y_o)_{rms} = \sqrt{C_o \frac{NUM2}{DEN}} \qquad (4.15)$$

$$a_s = \sqrt{C_o \frac{NUM3}{DEN}} \qquad (4.16)$$

In order to analyze the respons of the model, contours of constant K_2 and B_2 values are plotted in Figures 4.2 and 4.3. From Figure 4.2, we can note that there is a

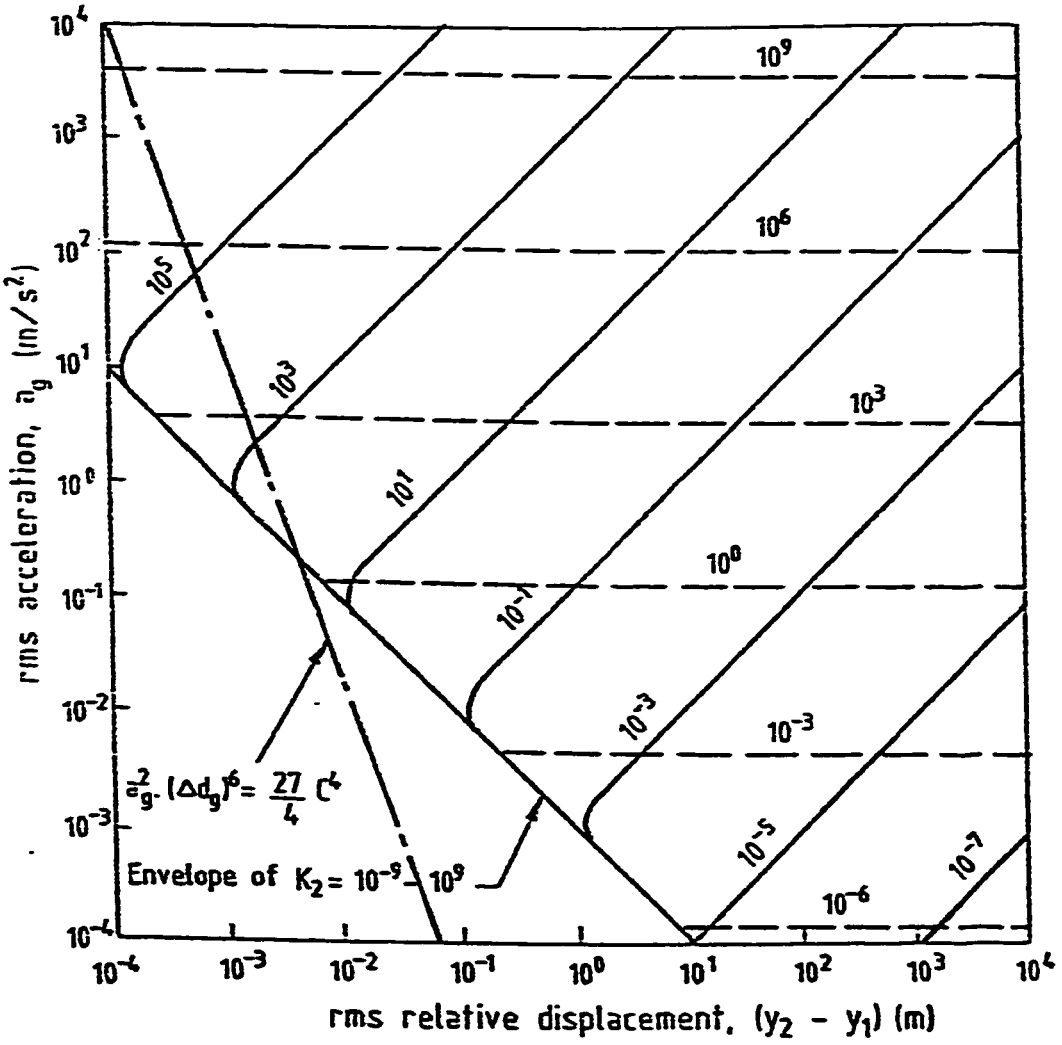

Figure 4.2. Contours of constant K_2 and B_2 values.

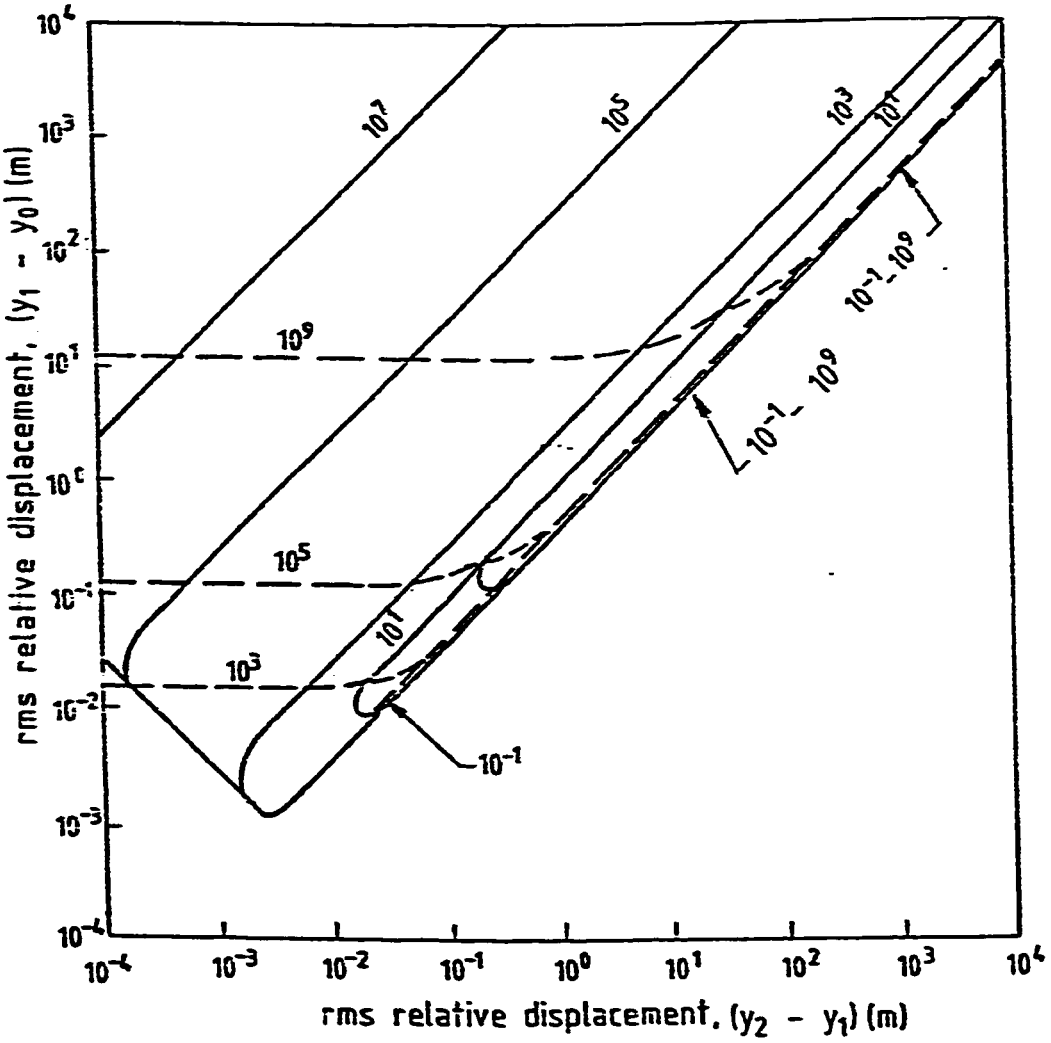

Figure 4.3 Contours of constant K_2 and B_2 values.

limited region where no acceleration or secondary relative displacement values could be obtained. The contours of constant K_2 values show that the relation between the secondary relative displacement and the acceleration is linear in certain regions and inversely linear in other regions. This makes it possible to obtain more than one acceleration value for the same K_2 value. Another limiting behavior is also shown in Figure 4.2 where the lines of constant acceleration values appear for constant B_2 values. It is shown that by lowering the B_2 values, it becomes possible to obtain lower acceleration values, but it becomes less possible to obtain smaller secondary relative displacement values. We can note also that it is possible to have low secondary relative displacement values at the large K_2 values with an increase in the values of the sprung mass acceleration.

From Figure 4.3, we can observe that there is a limit to the optimization of both the primary suspension displacement and the secondary suspension displacement. The contours of constant K_2 values show that it is possible to obtain two primary relative displacement values for one K_2 value. From the same figure also, we can note that it is possible to obtain one value for the primary suspension displacement by using either a smaller or a larger B_2 value. But, when the smaller B_2 value is used, it is noted that a larger secondary suspension displacement is obtained, whereas using the larger B_2 value makes it possible to obtain smaller secondary relative displacement values at the same level of the primary relative displacement value. It can be also observed that by lowering the B_2 values, it becomes possible to lower the primary relative displacement values.

From Figure 4.4, where the contours of constant acceleration, primary relative displacement and secondary relative displacement are plotted, we can observe that the

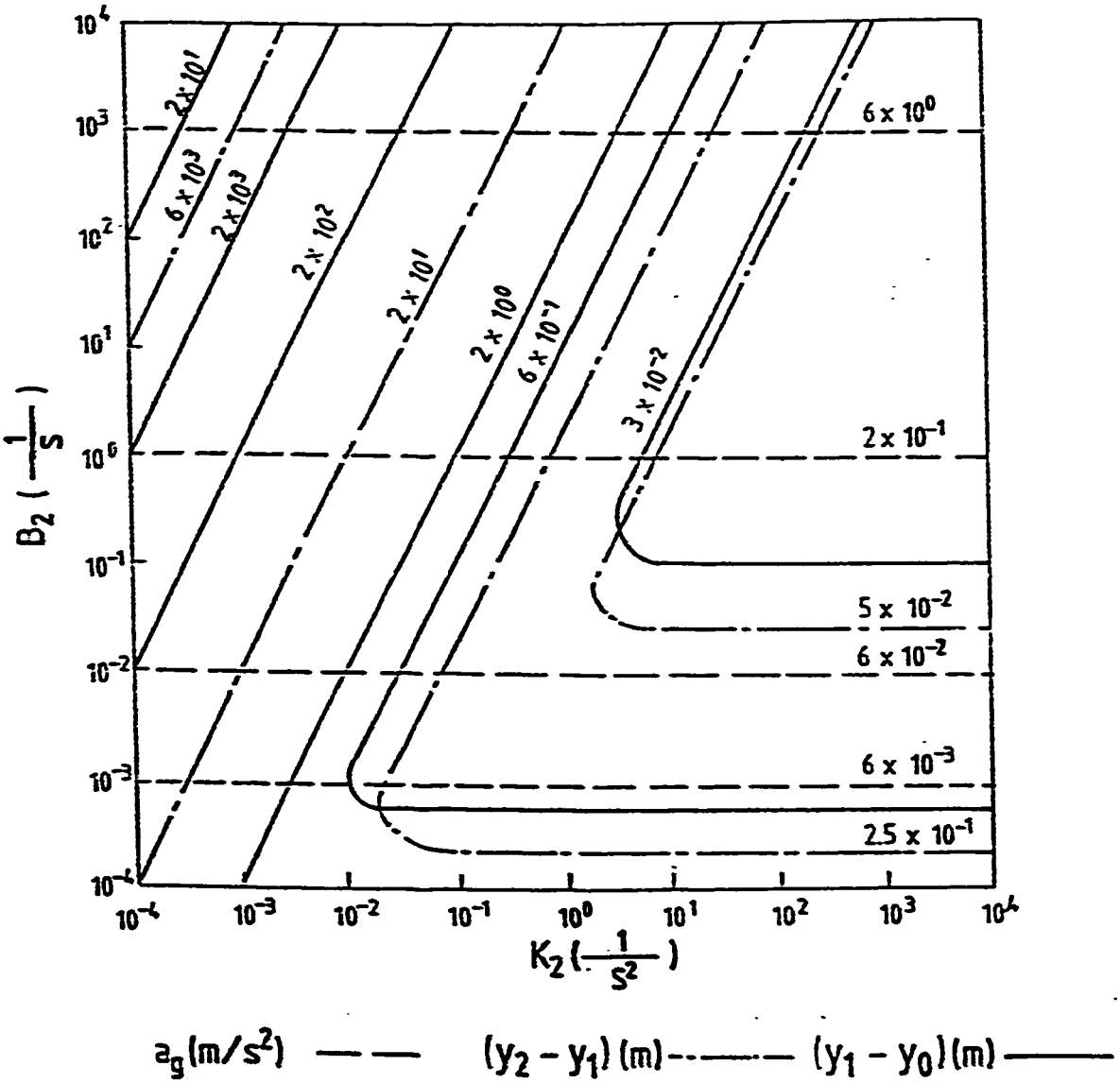

Figure 4.4 Contours of constant acceleration, secondary and primary relative displacements.

acceleration of the sprung mass is always constant for constant B_2 value and it is not a function of K_2. It can also be noted that it is possible to obtained the same primary relative displacement for the same K_2 value at two different B_2 values. The same result also applies to the secondary relative displacement.

In this section a value of M equal to 0.1 is used to study the responses of the model in this section [39].

4.2 Response of 2-DOF Model with Secondary Suspension of Maxwell Type that is in Parallel with a Spring

The 2-DOF vehicle model shown in Figure 4.5 consists of a sprung mass m_2, an unsprung mass m_1, a secondary suspension of Maxwell type that is in parallel with a spring and consists of two springs with coefficients k_2 and k_3 and a dashpot with damping coefficient b_3. The primary suspension consists of a spring with a stiffness coefficient k_1.

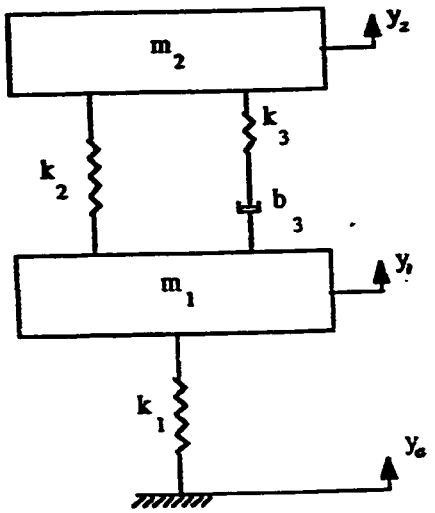

Figure 4.5. 2-DOF vehicle model with secondary suspension of Maxwell type that is in parallel with a spring.

The mean square responses of the model are derived as shown in Appendix A. The mean square relative displacement of the secondary suspension is given by,

$$\overline{(y_2 - y_1)^2} = C \cdot \frac{NUM1}{DEN} \tag{4.17}$$

where

$C = \pi . A.V,$

$$NUM1 = C_2^2 H_2 + C_1^2 H_3 \tag{4.18}$$

$$DEN = d_0 (d_1 H_4 - d_3 H_3 + d_5 H_2) \tag{4.19}$$

where

$$\begin{aligned} C_1 &= -k_1 k_3 m_2 \\ C_2 &= k_1 b_3 m_2 \\ d_0 &= k_1 k_2 k_3 \\ d_1 &= k_1 b_3 (k_2 + k_3) \\ d_2 &= m_2 k_3 (k_1 + k_2) \\ d_3 &= b_3 (k_2 + k_3)(m_1 + m_2) + m_2 k_1 b_3 \\ d_4 &= m_1 m_2 k_3 \\ d_5 &= m_1 m_2 b_3 \end{aligned} \tag{4.20}$$

$$\begin{aligned} H_2 &= -d_0 d_5 + d_1 d_4 \\ H_3 &= \frac{1}{d_0}(d_2 H_2 - d_4 H_1) \\ H_1 &= -d_0 d_3 + d_1 d_2 \end{aligned} \tag{4.21}$$

$$H_4 = \frac{1}{d_0}(d_2H_3 - d_4H_2)$$

The mean square relative displacement of the primary suspension is given by,

$$\overline{(y_1 - y_0)^2} = C.\frac{NUM2}{DEN} \qquad (4.22)$$

where

$$NUM2 = C_4^2H_0 + (C_3^2 - 2C_2C_4)H_1 + C_2^2H_2 \qquad (4.23)$$

where

$$C_4 = -m_1m_2b_3$$

$$C_3 = -m_1m_2k_3 \qquad (4.24)$$

$$C_2 = -m_2b_3(k_2+k_3) - m_1b_3(k_2+k_3)$$

and

$$H_0 = \frac{1}{d_0}(d_3H_1 - d_1H_2) \qquad (4.25)$$

H_1 to H_4 are as given by Equation (4.21). The coefficients d_0 to d_5 are as given by Equation (4.20).

The mean square acceleration of the spring mass is given by,

$$\overline{a_s^2} = C.\frac{NUM3}{DEN} \qquad (4.26)$$

where,

$$NUM3 = C_2^2H_2 + C_1^2H_3 \qquad (4.27)$$

where,

$$C_1 = k_1k_2k_3$$

$$C_2 = k_1b_3\,(k_2+k_3) \qquad (4.28)$$

H_1 to H_4 are as given by Equation (4.21) whereas the coefficient d_0 to d_5 are as given by Equation (4.20).

The analysis of the responses is simplified by writing the coefficients of Equation (4.20) is the form,

$$C_1 = -K_1K_3$$

$$C_2 = -K_1B_3$$

$$d_0 = K_1K_2K_3$$

$$d_1 = K_1B_3(K_2+K_3)$$

$$d_2 = K_3(K_1+K_2) \qquad (4.29)$$

$$d_3 = B_3(K_2+K_3)(1+M)+K_1B_3$$

$$d_4 = MK_3$$

$$d_5 = MB_3$$

and the coefficients of Equation (4.24) in the form,

$$C_4 = -MB_3$$

$$C_3 = -MK_2 \qquad (4.30)$$

$$C_2 = -B_3(K_2+K_3)$$

and the coefficients of Equation (4.28) in the form,

$$C_1 = K_1K_2K_3$$

$$C_2 = K_1 B_3 (K_2 + K_3) \tag{4.31}$$

where $K_1 = k_1/m_2$, $K_2 = k_2/m_2$, $K_3 = k_3/m_2$, $B_3 = b_3/m_2$ and $M = m_1/m_2$. This shows that the responses do not depend directly on the sprung or unsprung masses, but they depend on the stiffness and damping coefficients to the spring mass ratios and the mass ratio M.

The rms responses of the model are given by,

$$(y_2 - y_1)_{rms} = \sqrt{C. \frac{NUM1}{DEN}} \tag{4.32}$$

$$(y_1 - y_0)_{rms} = \sqrt{C. \frac{NUM2}{DEN}} \tag{4.33}$$

$$a_s = \sqrt{C. \frac{NUM3}{DEN}} \tag{4.34}$$

In order to analyze the responses of the model, contours of constant K_3 and B_3 values are plotted in Figures 4.6 - 4.10. From Figure 4.6, where a small value of K_2 is used to plot the contours, it can be noted that there are two limited regions where no values of acceleration or secondary relative displacement can be obtained. The first limited region is similar to the region of the 2-DOF model which has a secondary suspension of Maxwell type (Figure 4.2). The second limited region is observed to exist because of the linear relation between the secondary relative displacement and the acceleration of the sprung mass when very small values of B_3 are used. The contours of constant K_3 values show that a linear relation exists between the acceleration and the secondary relative displacement in specific regions and an inversely linear relation exists between them in other regions. This explains why it is possible to obtain more than one acceleration value for the same primary relative displacement value. It can be observed from Figure 4.6, that it is possible to obtain the same acceleration value by using either a very small value or a large value of B_3. It is clear that using the very small value of B_3 will result in large secondary relative

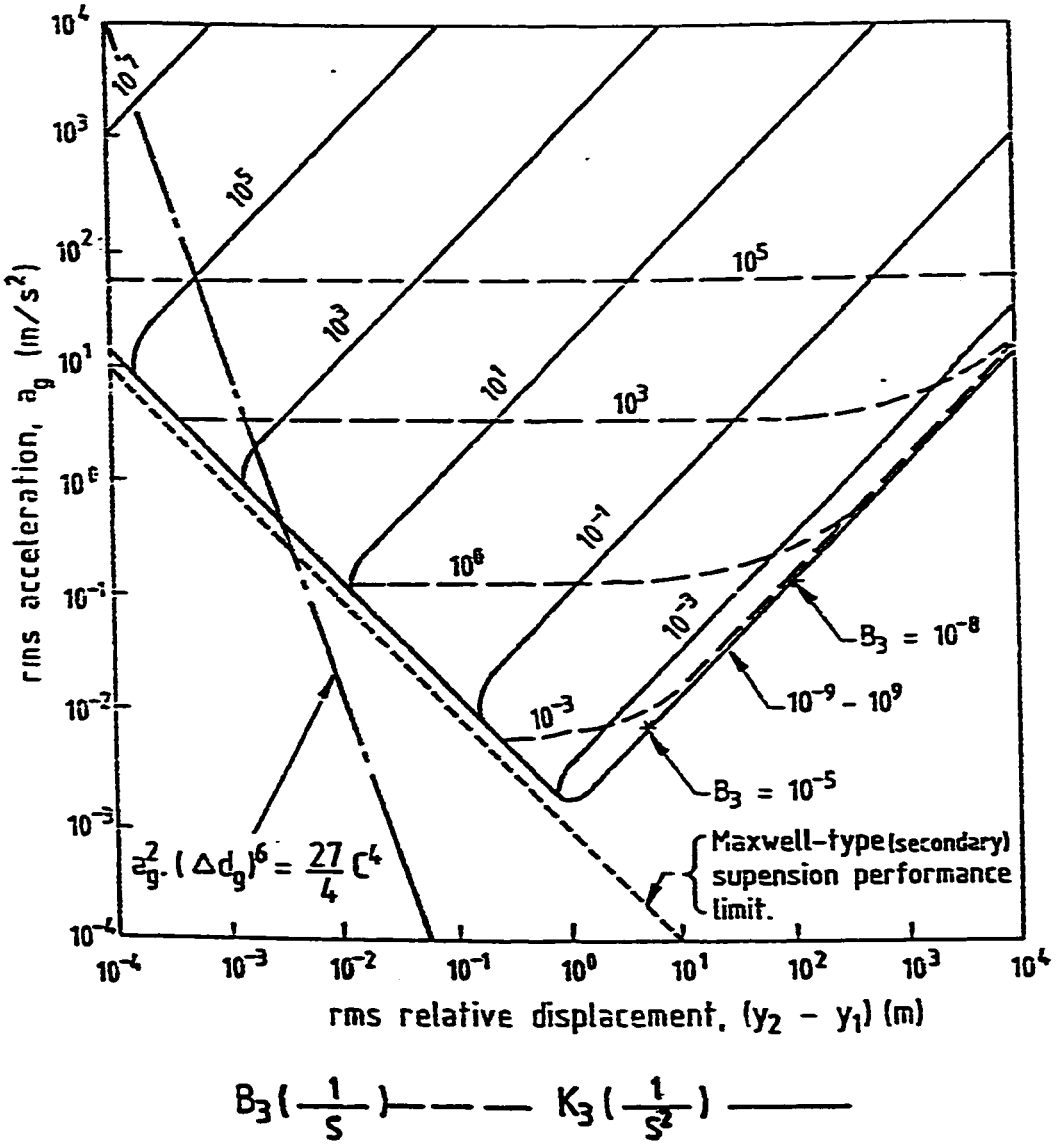

Figure 4.6 Contours of constant K_3 and B_3 values ($K_2 = 10^{-3}\ \frac{1}{s^2}$)

displacement value, while using the large value results in a constant acceleration value. Then, it becomes possible to obtain smaller secondary relative displacement values by increasing the K_3 value. The contours of constant B_3 values show that it is possible to obtain lower acceleration values for the same secondary relative displacement value by lowering the B_3 value.

Figures 4.7 and 4.8 show that increasing the K_2 value results in a similar behavior of the contours of constant K_3 and B_3 values shown in Figure 4.6, but with an increase in the values of the acceleration of the sprung mass.

From Figure 4.9, where a small value of K_2 is used to plot the contours of constant K_3 and B_3 values, it can be seen that there is a limit to the optimization of both the primary and the secondary relative displacements. The contours of constant K_3 values show that is possible to obtain two primary relative displacement values for one K_3 value. It is observed that using very small values of B_3 results in a linear relation between the secondary and the primary relative displacements regardless of how large the value of K_3 is. The existence of two primary relative displacement values for the same K_3 value is explained by the availability of the linear and the inversely linear relations between the two relative displacements for constant K_3 values. We can also observe from Figure 4.9 that it is possible to obtain one primary relative displacement value when using either a very small value or a large value of B_3. Using the very small value of B_3 clearly results in large secondary relative displacement values while using the large value of B_3 results in a constant primary relative displacement values and at the same time it becomes possible to

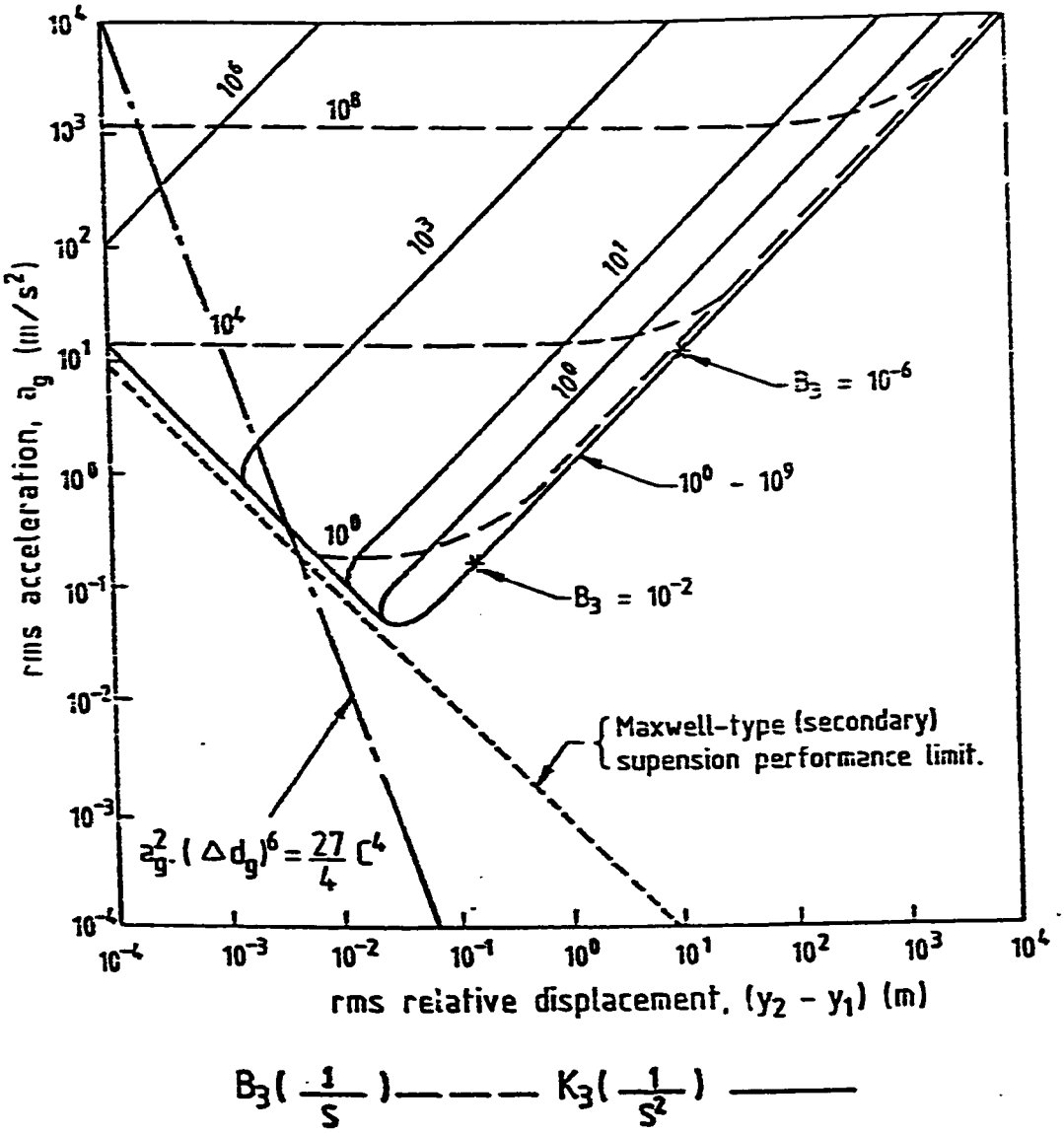

Figure 4.7 . Contours of constant K_3 and B_3 values ($K_2 = 10^0 \frac{1}{s^2}$)

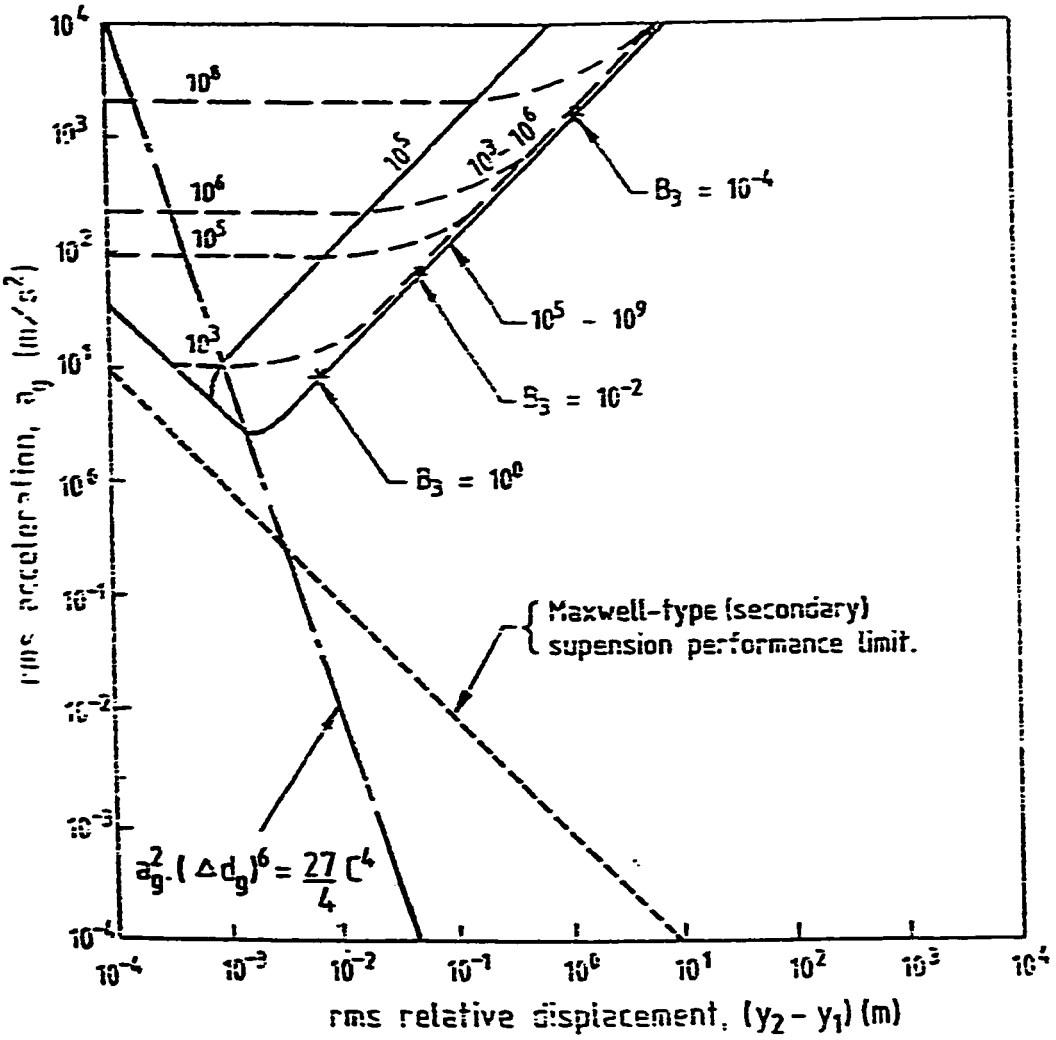

Figure 4.8 Contours of constant K_3 and B_3 values ($K_2 = 10^3 \frac{1}{S^2}$)

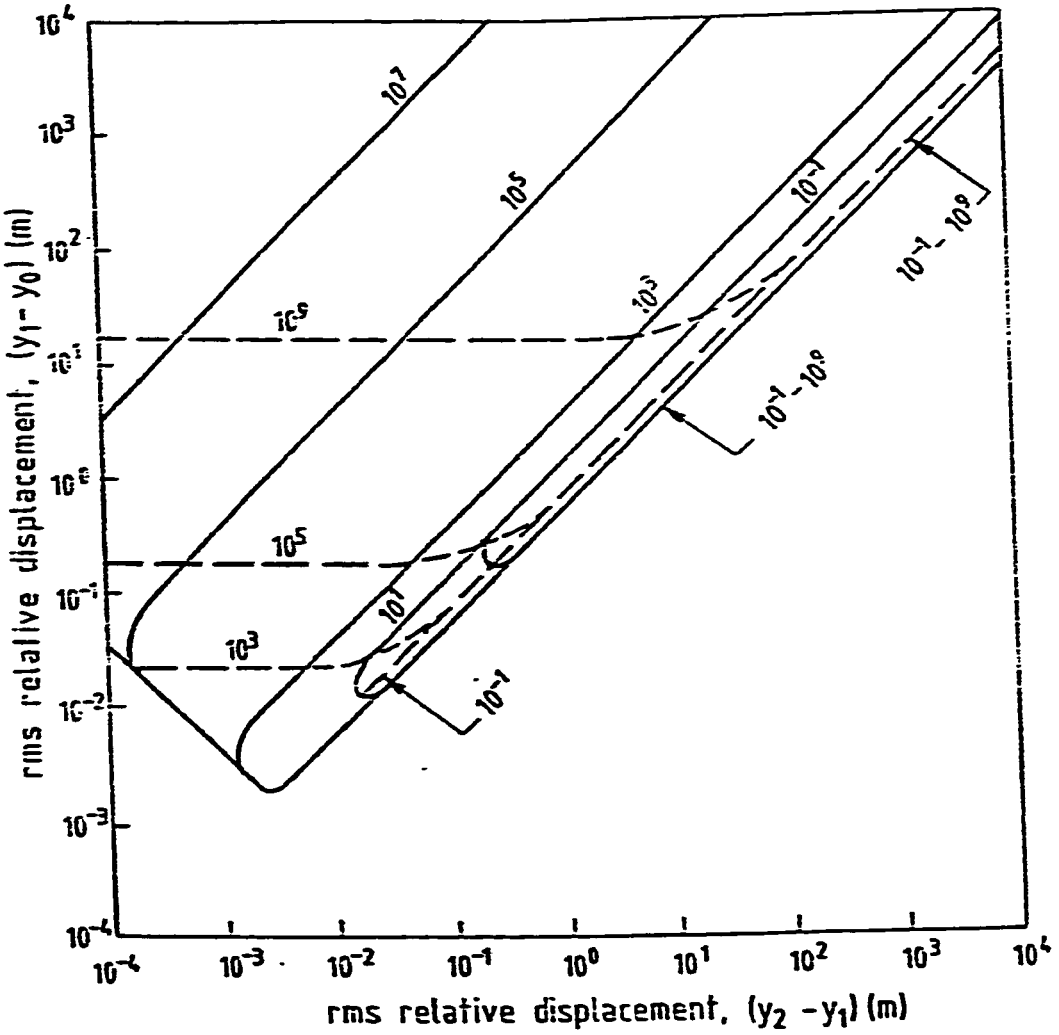

Figure 4.9 Contours of constant K_3 and B_3 values ($K_2 = 10^{-3}\frac{1}{s^2}$)

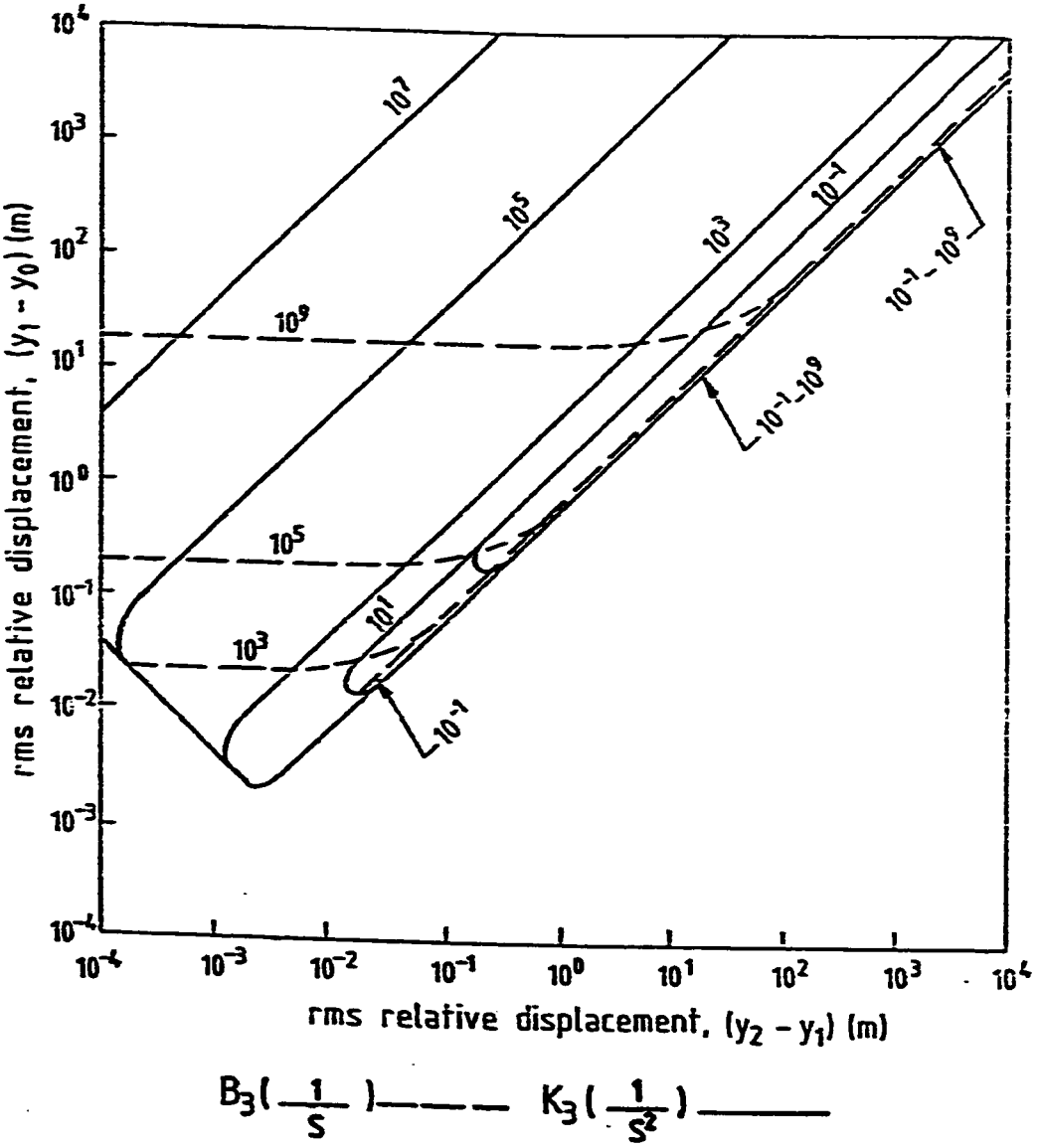

Figure 4.10 Contours of constant K_3 and B_3 values ($K_2 = 10^0 \frac{1}{s^2}$)

obtain lower primary relative displacement values by using larger K_3 values. It is also clear from the same figure that by lowering the B_3 values, it becomes possible to lower the primary relative displacement value.

From Figure 4.10, it is clear that using a larger K_2 value has no effect on the relation between the secondary and the primary relative displacement.

In this section, a value of M equal to 0.1 is used to study the responses of the model [39].

4.3 Response of 2-DOF Model with Secondary Suspension of Voigt Type that is in Series with a Spring

The 2-DOF vehicle model shown in Figure 4.11 consists of a sprung mass m_2 an unsprung mass m_1, a secondary suspension of Voigt type that is in series with a spring and consists of two springs with coefficients k_2 and k_3 and a dashpot with damping coefficient b_3. The primary suspension consists of a spring with a stiffness coefficient k_1.

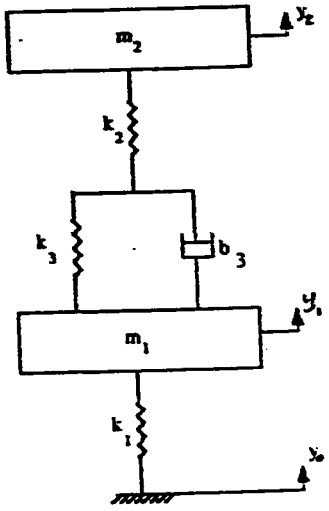

Figure 4.11. 2-DOF vehicle model with secondary suspension of Voigt type that is in series with a spring.

The mean square responses of the model are derived as shown in Appendix A. The mean square relative displacement of the secondary suspension is given by,

$$\overline{(y_2 - y_1)^2} = C \cdot \frac{NUM1}{DEN} \tag{4.35}$$

where

$C = \pi . A.V.$

$$NUMI = C_2^2 H_2 + C_1^2 H_3 \tag{4.36}$$

$$DEN = d_0(d_1 H_4 - d_3 H_3 + d_5 H_2) \tag{4.37}$$

where

$C_1 = -m_2 k_1 b_3$

$C_2 = -k_1(k_2+k_3)m_2$

$d_0 = k_1 k_2 k_3$

$d_1 = k_1 k_2 b_3$

$d_2 = k_2 k_3(m_1+m_2)+k_1 m_2(k_3+k_2)$ (4.38)

$d_3 = k_2 b_3(m_1+m_2)+k_1 m_2 b_3$

$d_4 = m_1 m_2(k_2+k_3)$

$d_5 = m_1 m_2 b_3$

and

$H_2 = -d_0 d_5 + d_1 d_4$

$$H_3 = \frac{1}{d_0}(d_2 H_2 - d_4 H_1) \tag{4.39}$$

$$H_4 = \frac{1}{d_0}(d_2H_3 - d_4H_2)$$

$$H_1 = -d_0d_3 + d_1d_2$$

The mean square relative displacement of the primary suspension is given by,

$$\overline{(y_1 - y_0)^2} = C.\ \frac{NUM2}{DEN} \tag{4.40}$$

where

$$NUM2 = C_4^2H_0 + (C_3^2 - 2C_2C_4)H_1 + (C_2^2 - 2C_1C_3)H_2 + C_1^2H_3 \tag{4.41}$$

where

$$C_4 = -m_1m_2b_3$$

$$C_3 = -m_1m_2(k_2+k_3)$$

$$C_2 = -k_2b_3(m_1+m_2) \tag{4.42}$$

$$C_1 = -k_2k_3(m_1+m_2)$$

and

$$H_0 = \frac{1}{d_5}(d_3H_1 - d_1H_2) \tag{4.43}$$

H_1 to H_4 are as given by Equation (4.39) and the coefficient d_0 to d_5 are as given by Equation (4.38).

The mean square relative displacement of the spring mass is given by,

$$\overline{a_s^2} = C.\ \frac{NUM3}{DEN} \tag{4.44}$$

where,

$$NUM3 = C_2^2H_2 + C_1^2H_3 \tag{4.45}$$

where

$$C_1 = k_1k_2k_3 \qquad (4.46)$$

$$C_2 = k_1k_2b_3$$

where H_1 to H_4 are as given by Equation (4.40). The coefficients d_o to d_5 are as given by Equation (4.38).

The analysis of the responses is simplified by writing the coefficients of Equation (4.38) in the form,

$$C_1 = -K_1B_3$$

$$C_2 = -K_1(K_2+K_3)$$

$$d_o = K_1K_2K_3$$

$$d_1 = K_1K_2B_3$$

$$d_2 = K_2K_3(1+M)+K_1(K_2+K_3) \qquad (4.47)$$

$$d_3 = K_2B_3(1+M)+K_1B_3$$

$$d_4 = M(K_2+K_3)$$

$$d_5 = MB_3$$

and the coefficients of Equation (4.42) in the form,

$$C_4 = -MB_3$$

$$C_3 = -M(K_2+K_3) \qquad (4.48)$$

$$C_2 = -K_2B_3\,(1+M)$$

$$C_1 = -K_2K_3(1+M)$$

and the coefficients of Equation (4.46) in the form,

$$C_1 = K_1K_2K_3$$

$$C_2 = K_1K_2B_3 \qquad (4.49)$$

where $K_1 = k_1/m_2$, $K_2 = k_2/m_2$, $K_3 = k_3/m_2$, $B_3 = b_3/m_2$ and $M = m_1/m_2$. This shows that the responses are dependent on the stiffness and damping coefficients to the spring mass ratios and the mass ratio M.

The rms responses of the model are given by,

$$(y_2 - y_1)_{rms} = \sqrt{C_1 \frac{NUM1}{DEN}} \qquad (4.50)$$

$$(y_1 - y_0)_{rms} = \sqrt{C_1 \frac{NUM2}{DEN}} \qquad (4.51)$$

$$a_s = \sqrt{C_2 \frac{NUM3}{DEN}} \qquad (4.52)$$

In order to analyze the responses of the model, contours of constant K_2 and B_3 values are plotted in Figure 4.12 - 4.16. From Figure 4.12, where a small value of K_3 is used to plot the contours, it can be noted that there are two limited regions where no values of acceleration or secondary relative displacement can be obtained. The first limited region is similar to the region of the 2-DOF model which has a secondary suspension of Maxwell type (Figure 4.2). The second limited region can be observed to exist because of the linear relation between the secondary relative displacement and the sprung mass acceleration when very small values of B_3 are used. The contours of constant K_2 values show that an inversely linear relation exists between the secondary relative displacement and the acceleration in certain regions and in other regions a linear relation exists between them. The linear and inversely linear relations between the acceleration and the secondary relative displacement is the reason why it is possible to obtain the same acceleration value when using a constant K_2 value. It can be observed from Figure 4.12 that using either a very

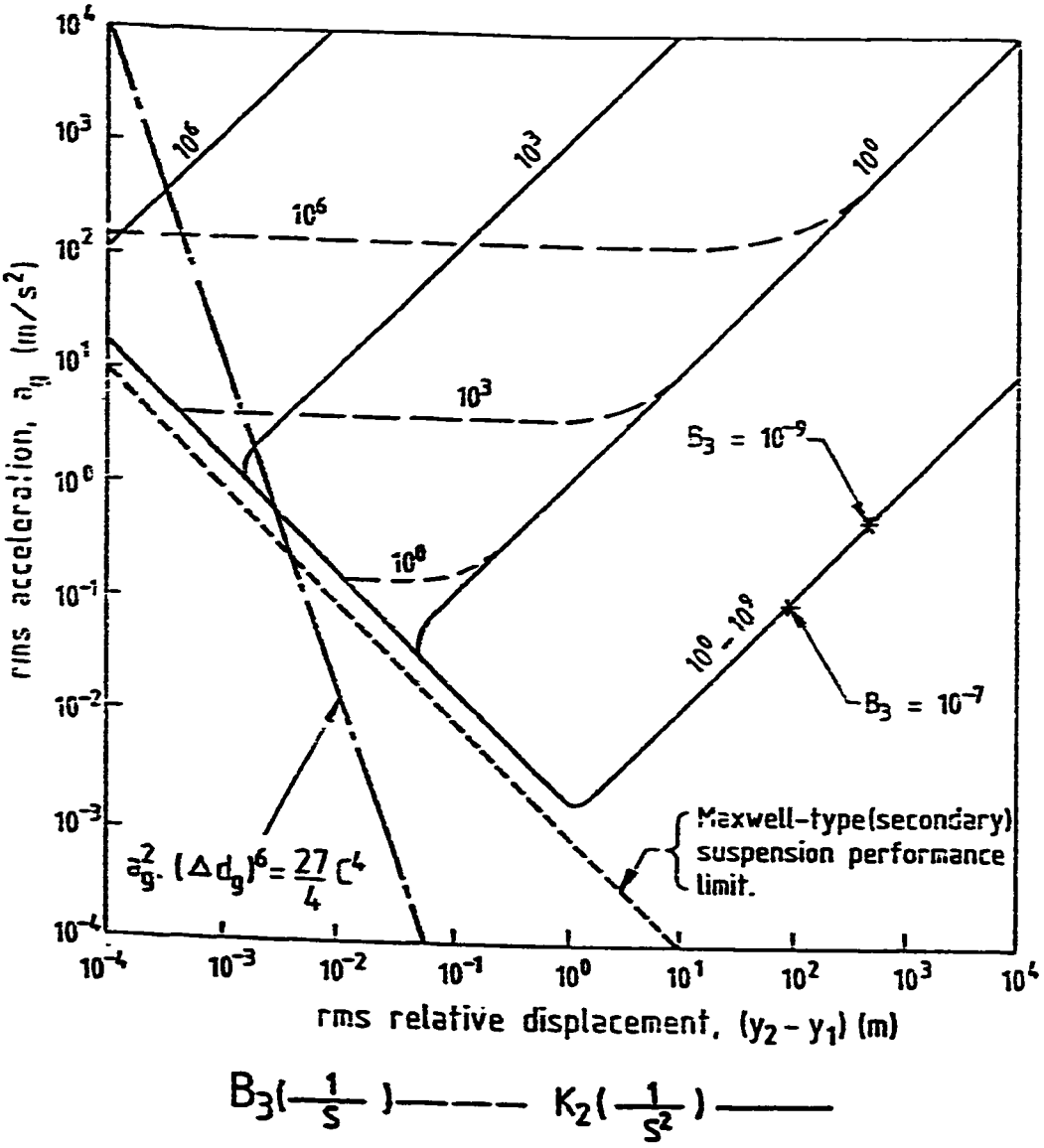

Figure 4.12 Contours of constant K_2 and B_3 values ($K_3 = 10^{-3}\frac{1}{s^2}$)

small or a large value makes it possible to obtain the same acceleration value. But, it is clear that using the very small value of B_3 results in a large relative displacement value. On the other hand, by using the large B_3 value allows us to obtain small secondary displacement values at the same constant acceleration value. Also the contours of constant B_3 values show that by lowering the B_3 values, smaller acceleration values can be obtained for the same secondary relative displacement value by lowering the B_3 value. Figures 4.13 and 4.14 display that increasing the K_3 value results in a similar behavior for the contour of constant K_2 and B_3 values shown in Figure 4.12, but with an increase in the sprung mass acceleration values.

From Figure 4.15, where a small value of K_3 is used to plot the contours of constant K_2 and B_3 values, we observe that there is a limit to the optimization of both the primary and secondary relative displacement values. The contours of constant K_2 values show that it is possible to obtain two primary relative displacement values for one K_2 value. It can be noted that using very small B_3 values results in a linear relation between the secondary and the primary relative displacements regardless of how large the K_2 value is. The existence of two primary relative displacement values for the same K_3 value is explained by the possibility of having both the linear and the inversely linear relations between the two relative displacements for constant K_2 values.

From Figure 4.15 also, we can observe that it is possible one primary relative displacement value when using either a very small or a large value of B_3. Using the very small value of B_3 clearly results in large secondary relative displacement values, while using the large B_3 value results in a constant primary relative displacement value and at the same time we can obtain lower relative displacement values by using larger K_3 values. It is

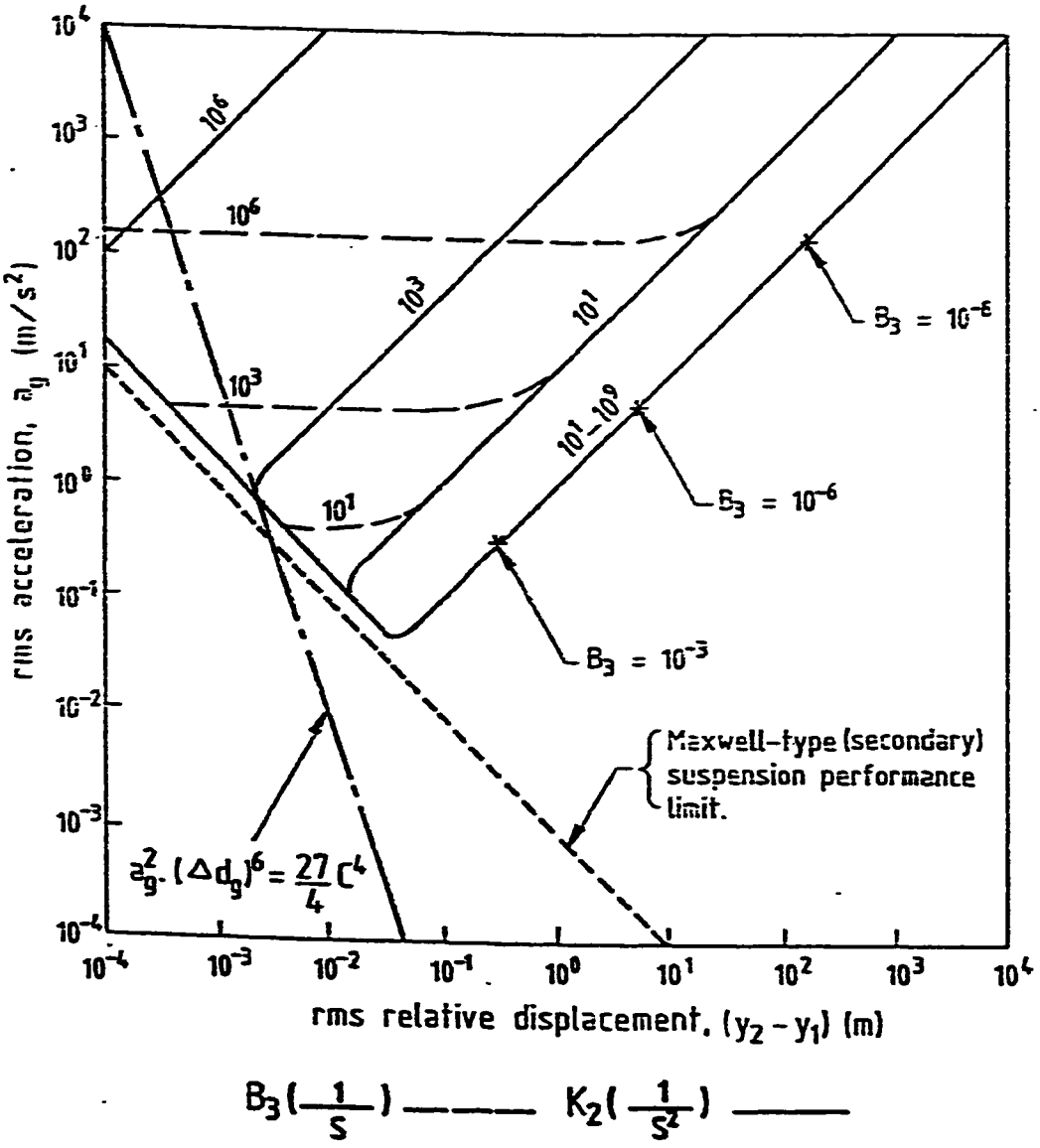

Figure 4.13 Contours of constant K_2 and B_3 values ($K_3 = 10^0 \frac{1}{s^2}$)

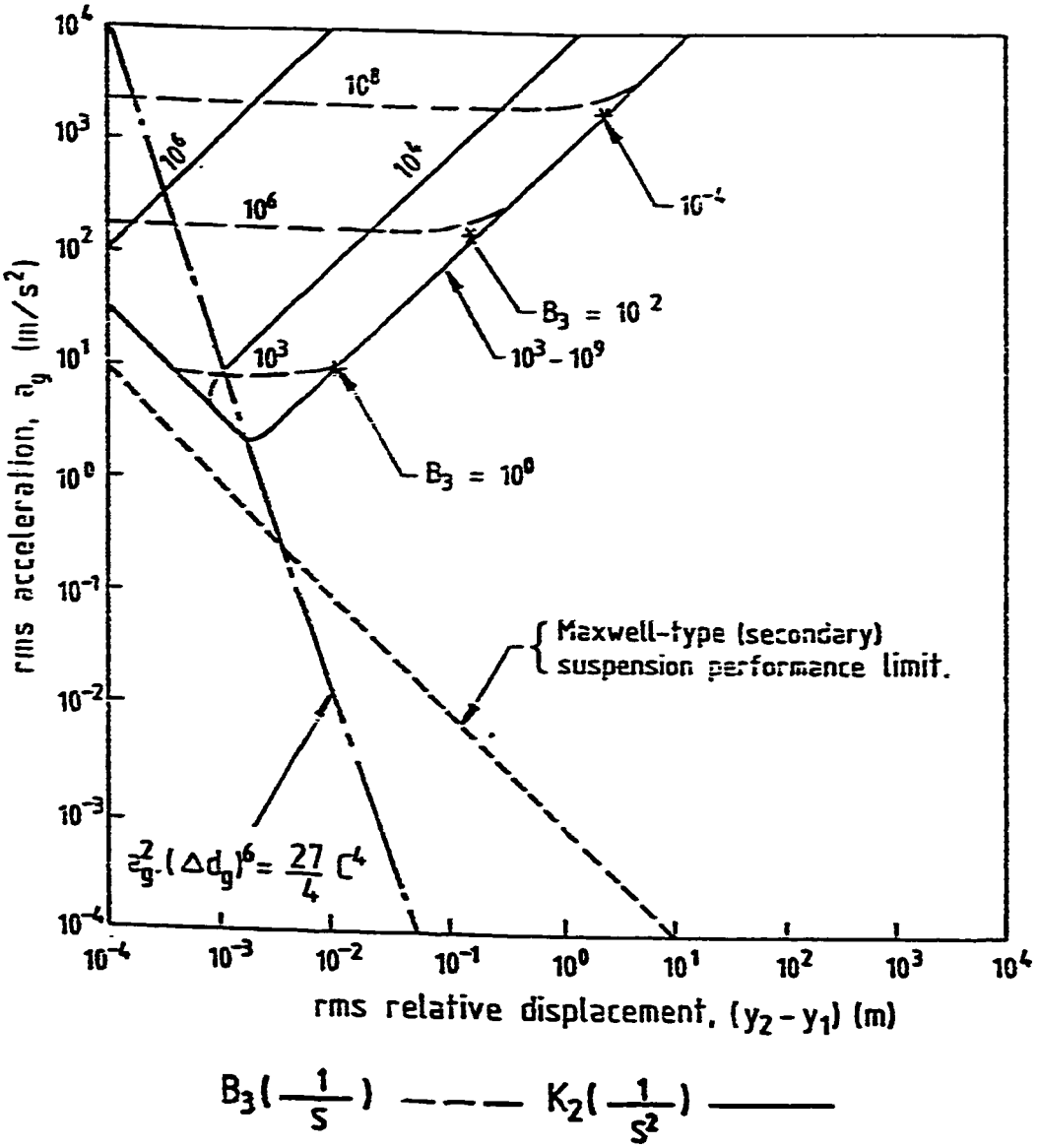

Figure 4.14 Contours of constant K_2 and B_3 values ($K_3 = 10^3 \frac{1}{s^2}$)

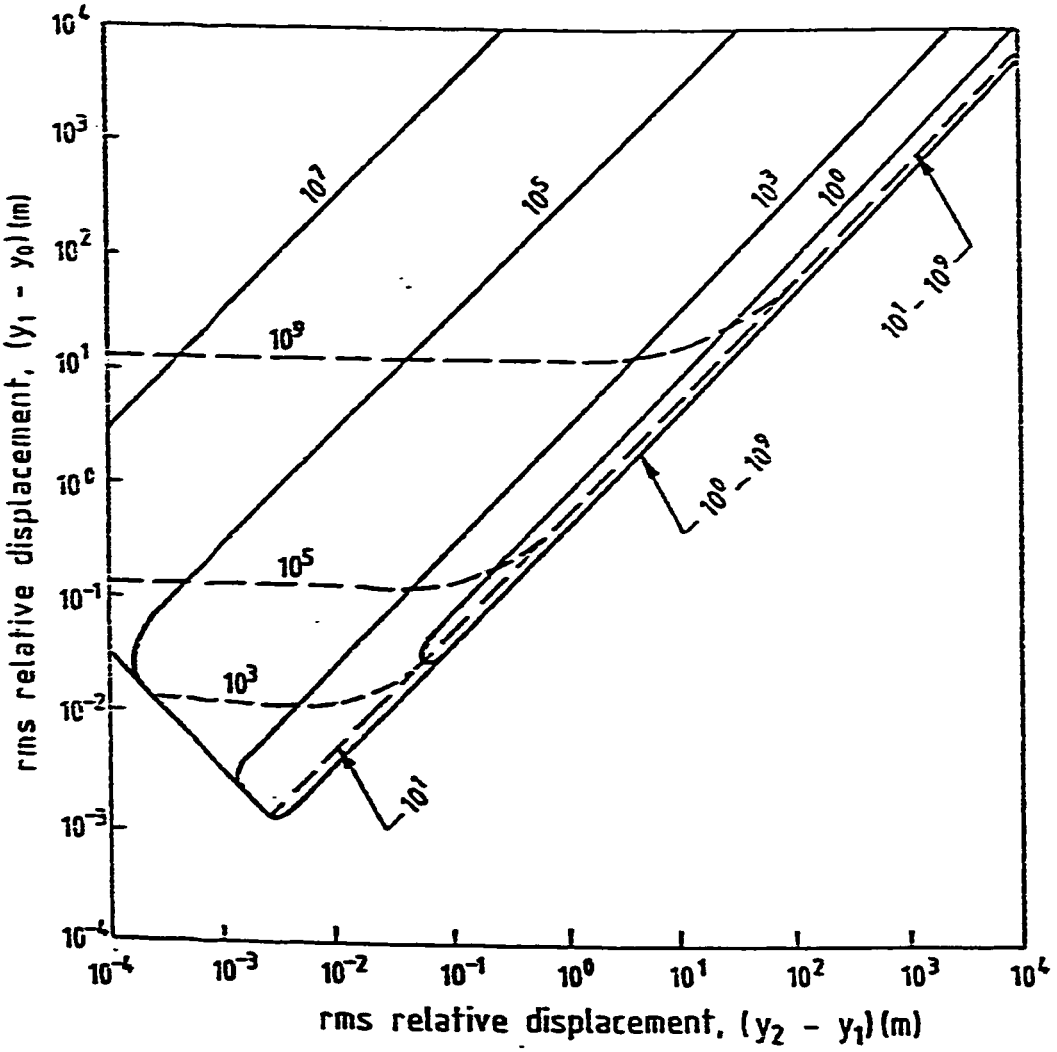

Figure 4.15 Contours of constant K_2 and B_3 values ($K_3 = 10^{-3}\ \frac{1}{s^2}$)

clear from the same figure that it is possible to obtain lower primary relative displacement values by using lower B_3 values.

From Figure 4.16, it is clear that using a larger K_3 values has no effect on the relation between the secondary and primary relative displacements.

In this section, a value of M equal to 0.1 is used to study the responses of the model [39].

4.4 Response of 2-DOF Model with Secondary Suspension of Voigt Type that is in Series with a Spring and both are in Parallel with a Spring

The 2-DOF model shown in Figure 4.17 consists of a sprung mass m_2, an unsprung mass m_1, a secondary suspension of voigt type that is in series with a spring and both are in parallel with a spring and it consists of three springs with coefficients k_2, k_3 and k_4 and a dashpot with damping coefficient b_4. The primary suspension consists of a spring with a stiffness coefficient k_1.

The mean square responses of the model are derived as shown in Appendix A. The mean square relative displacement of the secondary suspension is given by;

$$\overline{(y_2 - y_1)^2} = C \cdot \frac{NUM1}{DEN} \qquad (4.53)$$

where

$$C = \pi \cdot A.V.$$

$$NUM1 = C_2^2 H_2 + C_1^2 H_3 \qquad (4.54)$$

$$DEN = d_0(d_1 H_4 - d_3 H_3 + d_5 H_2) \qquad (4.55)$$

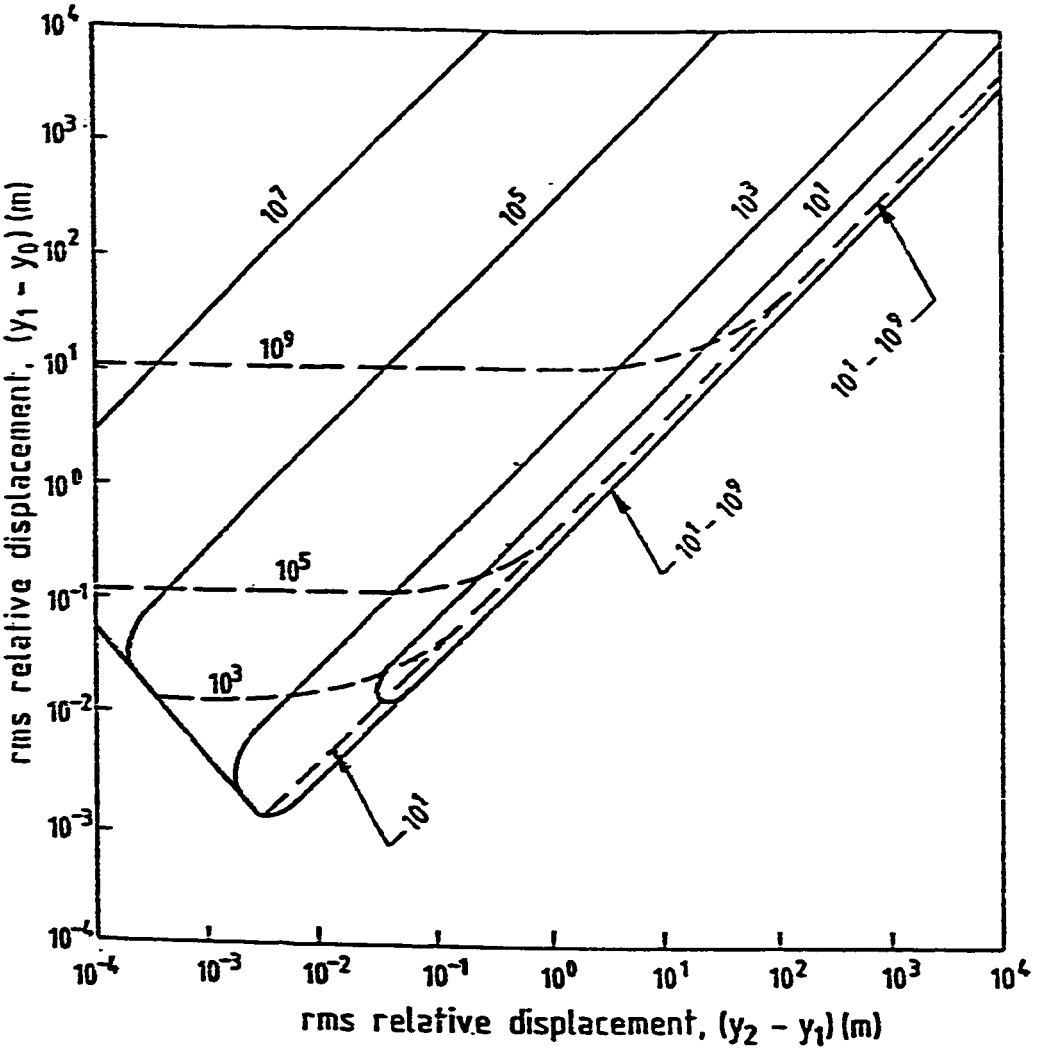

$B_3(\frac{1}{s})$ ——— $K_2(\frac{1}{s^2})$ ———

Figure 4.16 Contours of constant K_2 and B_3 values ($K_3 = 10^0 \frac{1}{s^2}$)

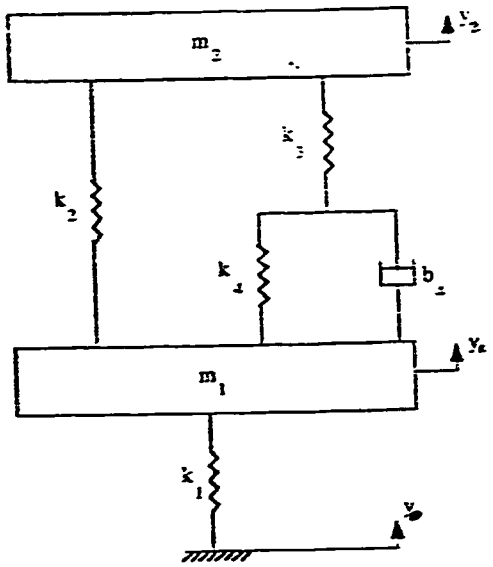

Figure 4.17. 2-DOF vehicle model with secondary suspension of Voigt type that is in series with a spring and both are in parallel with a spring.

where,

$$C_1 = -k_1 m_2 (k_3+k_4)$$

$$C_2 = -k_1 m_2 b_4$$

$$d_0 = k_1(k_2k_3+k_2k_1+k_3k_4)$$

$$d_1 = b_4 k_1 (k_2+k_3) \qquad (4.56)$$

$$d_2 = (m_1+m_2)(k_2k_3+k_2k_4+k_3k_4)$$

$$d_3 = m_2k_1+(m_1+m_2)(k_2+k_3)$$

$$d_4 = m_1m_2\,(k_3+k_4)$$

$$d_5 = m_1m_2b_4$$

and

$$H_2 = -d_0d_5+d_1d_4$$

$$H_3 = \frac{1}{d_0}(d_2H_2 - d_4H_1) \qquad (4.57)$$

$$H_4 = \frac{1}{d_0}(d_2H_3 - d_4H_2)$$

$$H_1 = -d_0d_3 + d_1d_2$$

The mean square relative displacement of the primary suspension is given by;

$$\overline{(y_1 - y_o)^2} = C \cdot \frac{NUM2}{DEN} \qquad (4.58)$$

where

$$NUM2 = C_4^2H_o + (C_3^2 - 2C_2C_4)H_1 + (C_2^2 - 2C_1C_3)H_2 + C_1^2H_3 \qquad (4.59)$$

where

$$C_4 = -m_1m_2b_4$$

$$C_3 = -m_1m_2(k_3+k_4) \qquad (4.60)$$

$$C_2 = -(m_1+m_2)(k_2+k_3)b_4$$

$$C_1 = -(m_1+m_2)(k_2k_3+k_2k_4+k_3k_4)$$

and,

$$H_o = \frac{1}{d_5}(d_3H_1 - d_1H_2) \qquad (4.61)$$

H_1 to H_4 are as given by Equation (4.57) and the coefficient d_0 to d_5 are as given by Equation (4.56).

The mean square acceleration of the sprung mass is given by,

$$\overline{a_1^2} = C \cdot \frac{NUM3}{DEN} \qquad (4.62)$$

where,

$$NUM3 = C_2^2 H_2 + C_1^2 H_3 \qquad (4.63)$$

where,

$$C_1 = k_1(k_2k_3+k_2k_4+k_3k_4)$$

$$C_2 = k_1b_4(k_2+k_3) \qquad (4.64)$$

H_1 to H_4 are as given by Equation (4.57) whereas the coefficients d_o to d_5 are as given by Equation (4.56).

The analysis of the responses is simplified by writing the coefficients of Equation (4.56) in the form,

$$C_1 = -K_1 (K_3+K_4)$$

$$C_2 = -K_1B_4$$

$$d_o = K_1(K_2K_3+K_2K_1+K_3K_4)$$

$$d_1 = B_4K_1(K_2+K_3)$$

$$d_2 = (1+M)(K_2K_3+K_2K_4+K_3K_4) \qquad (4.65)$$

$$d_3 = K_1 + (1+M)(K_2+K_3)$$

$$d_4 = M(K_2+K_4)$$

$$d_5 = MB_4$$

and the coefficients of Equation (4.60) in the form,

$$C_4 = -MB_4$$

$$C_3 = -M(K_3+K_4) \qquad (4.66)$$

$$C_2 = -(1+M)(K_2+K_3)B_4$$

$C_1 = -(1+M)(K_2K_3+K_2K_4+K_3K_4)$

and the coefficients of Equation (4.64) in the form,

$C_1 = K_1(K_2K_3+K_2K_4+K_3K_4)$

$C_2 = K_1B_4(K_2+K_3)$ (4.67)

where $K_1 = k_1/m_2$, $K_2 = k_2/m_2$, $K_3 = k_3/m_2$, $K_4 = k_4/m_2$, $B_4=b_4/m_2$ and $M = m_1/m_2$. This shows that the responses are dependent on the stiffness and damping coefficients to the sprung mass ratios and the mass ratio M.

The rms responses of the model are given by;

$$(y_2 - y_1)_{rms} = \sqrt{C_1 \frac{NUM1}{DEN}} \quad (4.68)$$

$$(y_1 - y_0)_{rms} = \sqrt{C_1 \frac{NUM2}{DEN}} \quad (4.69)$$

$$a_2 = \sqrt{C_1 \frac{NUM3}{DEN}} \quad (4.70)$$

The contours of constant K_3 and B_4 values are plotted in Figures 4.18 - 4.22 in order to analyze the responses behavior of the model. From Figure 4.18, where small values of K_3 and B_4 values are used, it can be noted that there are two limited regions where no acceleration or secondary relative displacements can be obtained. The first region is clearly similar to the region of the 2-DOF model with Maxwell type as a secondary suspension (Figure 4.2). The other limited region is observed to exist because of the linear relation between the acceleration and the secondary relative displacement when the K_3 value is very small. The existence of both linear and inversely linear relations between the acceleration and the primary relative displacements creates more than one acceleration value for a constant K_3 value and at more than one B_4 value. The contours of constant B_4 values in Figure 4.18 show that it is possible to obtain smaller acceleration values for the same

secondary relative displacement by using smaller B_4 values. It is also obvious that the acceleration is constant for constant B_4 values, but for very small K_4 values, the constant B_4 contours show that a linear relation exists between the secondary relative displacement and the acceleration.

Figures 4.19 and 4.20 show that using larger K_2 and K_4 values results in a similar behavior of the contours of constant K_3 and B_4 values, but with an increase in the sprung mass acceleration values.

From Figure 4.21, where small values of K_2 and K_4 are used to plot the contours of constant K_3 and B_4 values, we observe that there is a limit to the optimization of both the primary and the secondary relative displacement values. The contours constant K_3 values show that it is possible to obtain two primary relative displacement values for one K_3 value. The linear and inversely linear relation between the two relative displacements produce two primary relative displacements for the same K_3 value. Figure 4.22 shows that it is possible to obtain one primary relative displacement value by using either a very small or a large B_4 value. Using the larger B_4 value creates a constant primary relative displacement for different K_3 values and this shows that it is possible to obtain lower secondary relative displacement values for the same primary relative displacement value. On the other hand, using very small B_4 values produce large secondary relative displacement values. It can also be noted that using lower B_4 values will produce lower primary relative displacement value for the same primary relative displacement value.

From Figure 4.22, it is possible to see that using larger K_2 and K_4 values has no effect on the relation between both the secondary and primary relative displacements.

A value of M equal to 0.1 is used to study the model response in this section [39].

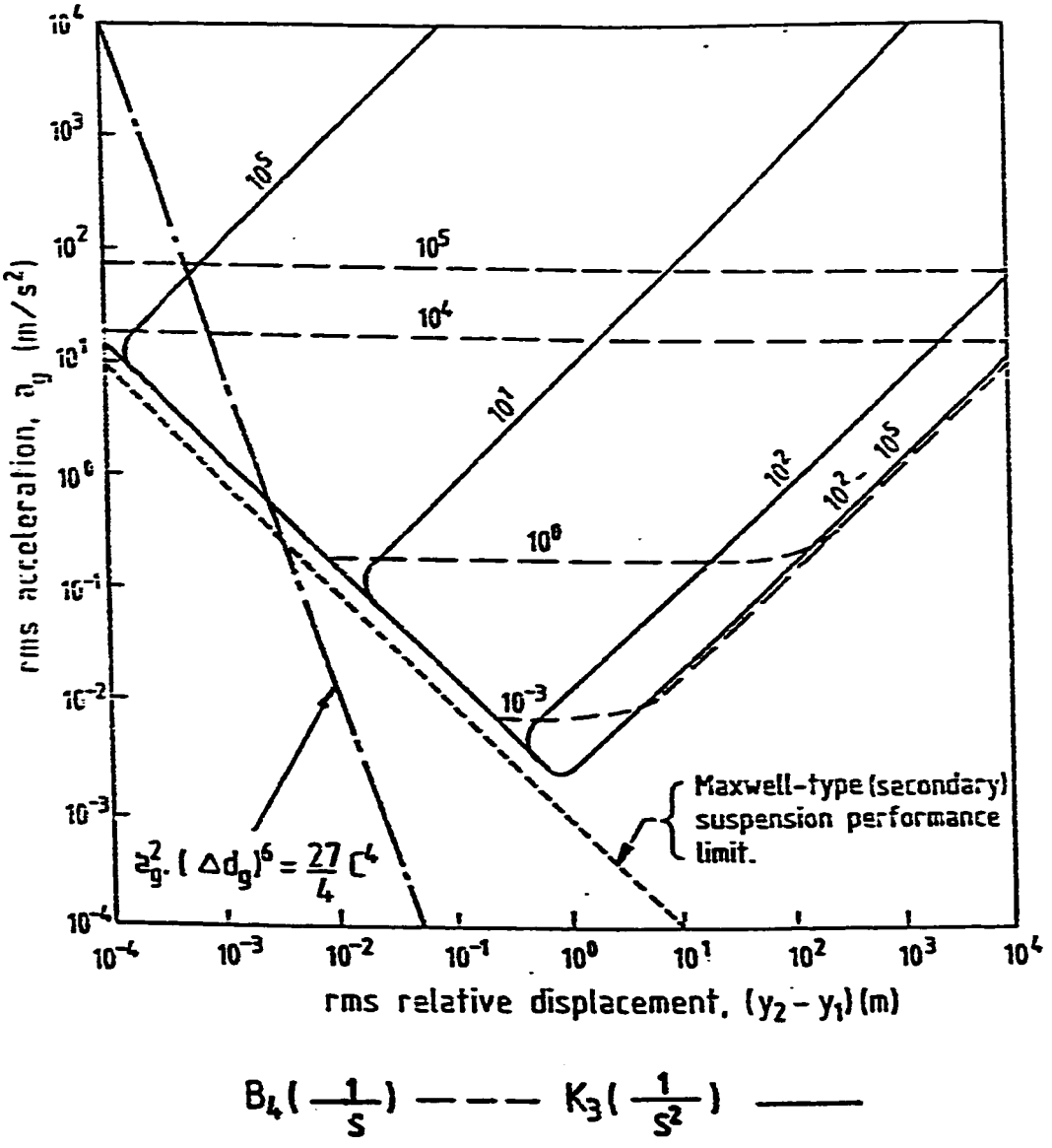

Figure 4.18 Contours of constant K_3 and B_4 values ($K_2 = K_4 = 10^{-3}\,\frac{1}{s^2}$)

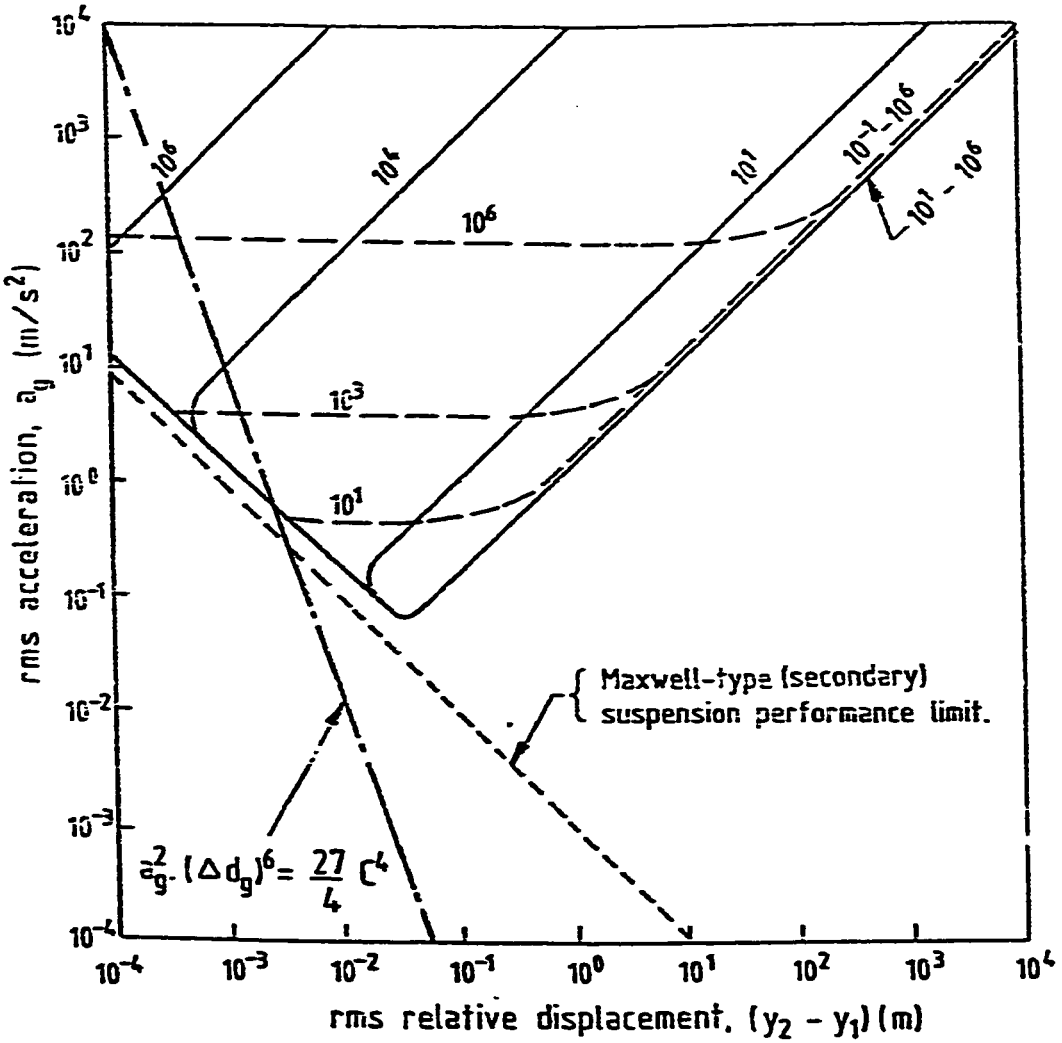

Figure 4.19 Contours of constant K_3 and B_4 values ($K_2 = K_4 = 10^0 \frac{1}{s^2}$)

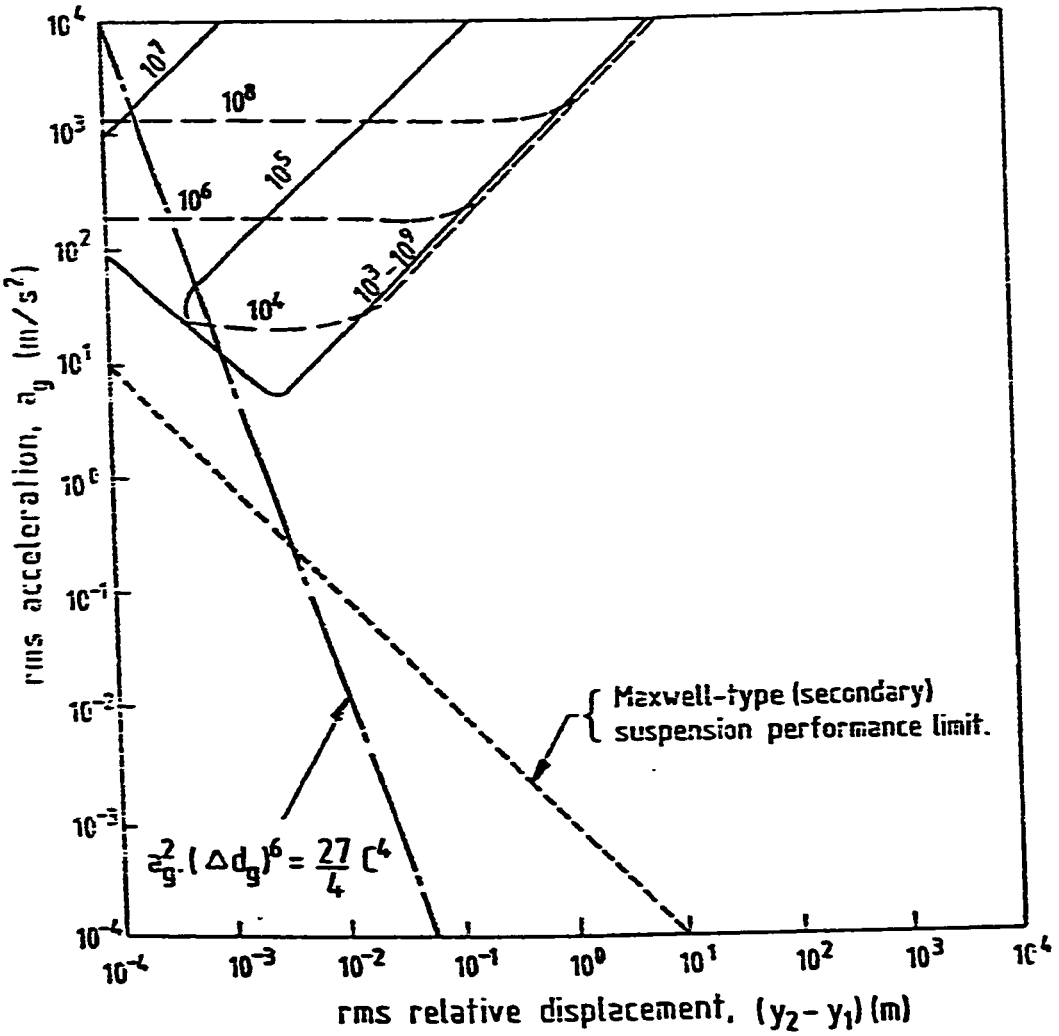

Figure 4.20 Contours of constant K_3 and B_4 values ($K_2 = K_4 = 10^3 \frac{1}{s^2}$)

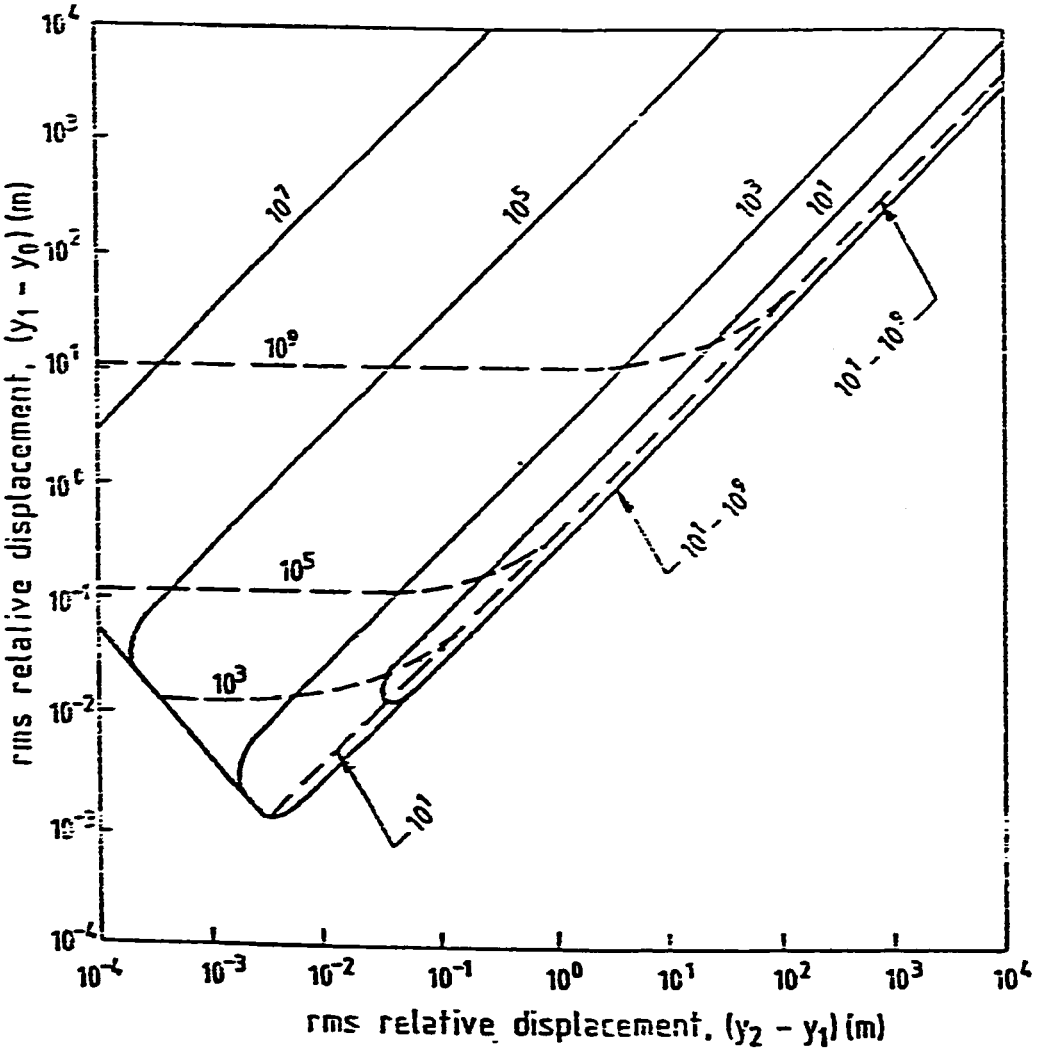

Figure 4.21 Contours of constant K_3 and B_4 values ($K_2 = K_4 = 10^{-3}\frac{1}{s^2}$)

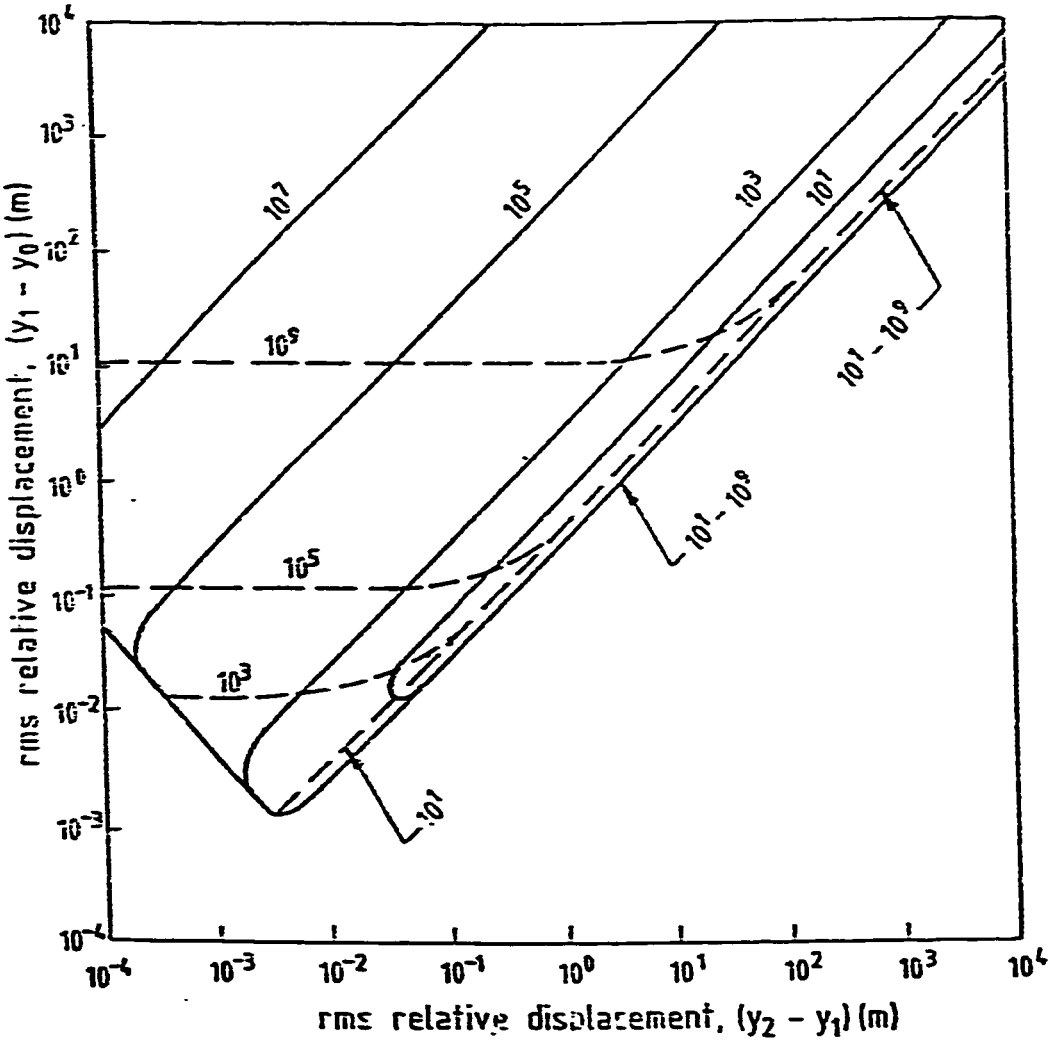

$B_4(\frac{1}{s})$ ——— $K_3(\frac{1}{s^2})$ ———

Figure 4.22 Contours of constant K_3 and B_4 values ($K_2 = K_4 = 10^0 \frac{1}{s^2}$)

4.5 Response of 2-DOF Model with Secondary Suspension of Voigt Type that is in Series with a Spring and both are in Parallel with a Maxwell Type Suspension

The 2-DOF model shown in Figure 4.23 consists of a sprung mass m_2, an unsprung mass m_1, a secondary suspension of Voigt type that is in series with a spring and both are in parallel with Maxwell type suspension and it consists of three springs with coefficients k_2, k_3 and k_4 and two dashpots with damping coefficients b_2 and b_4. The primary suspension consists of a spring with a stiffness coefficient k_1.

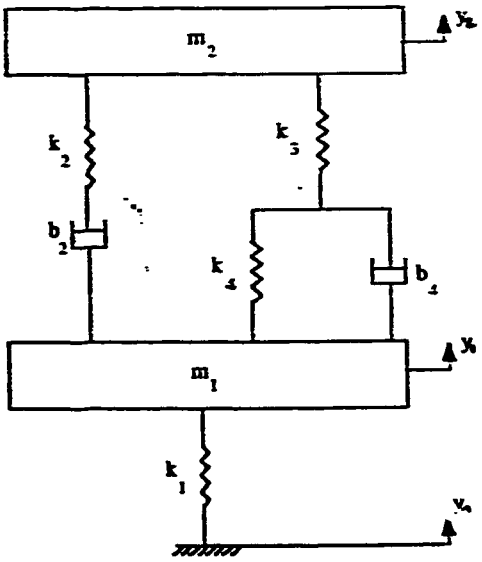

Figure 4.23. 2-DOF vehicle model with secondary suspension of Voigt type that is in series with a spring and both are in parallel with Maxwell type suspension.

The mean square responses of the model are derived as shown in Appendix A. The mean square relative displacement of the secondary suspension is given by;

$$\overline{(y_2 - y_1)^2} = C \cdot \frac{NUM1}{DEN} \qquad (4.71)$$

where

$$C = \pi . A.V.$$

$$NUM1 = C_3^2 H_2 + C_2^2 H_3 + C_1^2 H_4 \qquad (4.72)$$

$$DEN = d_0(d_1 H4 - d_3 H3 + d_5 H_2) \qquad (4.73)$$

where

$$C_1 = -m_2 k_1 k_2 (k_3 + k_4)$$

$$C_2 = -m_2 k_1 (k_2 b_4 + (k_3 + k_4) b_2)$$

$$C_3 = -m_2 k_1 b_2 b_4 \qquad (4.74)$$

$$d_0 = k_1 k_2 k_3 k_4$$

$$d_1 = k_1 b_2 (k_2 k_3 + k_2 k_4 + k_3 k_4) + k_1 k_2 k_3 b_4$$

$$d_2 = (m_1 + m_2) k_2 k_3 k_4 + k_1 k_2 m_2 (k_3 + k_4) + b_2 b_4 k_1 (k_2 + k_3)$$

$$d_3 = (m_1 + m_2)(b_2 (k_2 k_3 + k_2 k_4 + k_3 k_4) + k_2 k_3 b_4) + k_1 m_2 (k_2 b_4 + (k_3 + k_4) b_2)$$

$$d_4 = m_1 m_2 k_2 (k_3 + k_4) + (m_1 + m_2) b_2 b_4 (k_2 + k_3) + k_1 m_2 b_2 b_4$$

$$d_5 = m_1 m_2 (k_2 b_4 + (k_3 + k_4) b_2)$$

$$d_6 = m_1 m_2 b_2 b_4$$

and

$$H_2 = d_o d_3 d_5 + d_1^2 d_6 - d_1 d_2 d_5$$

$$H_3 = d_o d_5^2 + d_1 d_3 d_6 - d_1 d_4 d_5 \qquad (4.75)$$

$$H_4 = \frac{1}{d_0}(d_2 H_3 - d_4 H_2 + d_6 H_1)$$

$$H_1 = -d_0 d_1 d_5 + d_0 d_3^2 + d_1^2 d_4 - d_1 d_2 d_3$$

The mean square relative displacement of the primary suspension is given by,

$$\overline{(y_1 - y_0)^2} = C \cdot \frac{NUM2}{DEN} \qquad (4.76)$$

where

$$NUM2 = C_5^2 H_0 + (C_4^2 - 2C_3C_5)H_1 + (C_3^2 - 2C_2C_4 + 2C_1C_5) H_2 + (C_2^2 - 2C_1C_3)H_3 + C_1^2 H_4 \qquad (4.77)$$

where

$$C_1 = -(m_1+m_2)k_2k_3k_4$$

$$C_2 = -(m_1+m_2)(b_2(k_2k_3+k_2k_4+k_3k_4)+k_2k_3b_4)$$

$$C_3 = -(m_1+m_2)(k_2+k_3)b_2b_4 - m_1m_2k_2(k_3+k_4) \qquad (4.78)$$

$$C_4 = -m_1m_2 (k_2b_4+(k_3+k_4)b_2)$$

$$C_5 = -m_1m_2b_2b_4$$

and

$$H_0 = \frac{1}{d_0}(d_4H_1 - d_2H_2 + d_0H_3) \qquad (4.79)$$

H_1 to H_4 are as given by Equation (4.75) and the coefficients d_0 to d_5 are as given by Equation (4.74).

The mean square acceleration of the sprung mass is given by,

$$\overline{a^2} = C \cdot \frac{NUM2}{DEN} \qquad (4.80)$$

$$NUM3 = C_3^2 H_2 + C_2^2 H_3 + C_1^2 H_4 \qquad (4.81)$$

where

$$C_1 = k_1k_2k_3k_4$$

$$C_2 = k_1b_2(k_2k_3+k_2k_4+k_3k_4)+k_1k_2k_3b_4 \qquad (4.82)$$

$$C_3 = k_1b_2b_4(k_2+k_3)$$

H_1 to H_4 are as given by Equation (4.75) and the coefficients d_o to d_5 are as given by Equation (4.74).

The analysis of the responses is simplified by writing the coefficients of Equation (4.74) in the form,

$$C_1 = -K_1K_2(K_3+K_4)$$

$$C_2 = -K_1 (K_2B_4+(K_3+K_4)B_2$$

$$C_3 = -K^1B_2B_4$$

$$d_o = K_1K_2K_3K_4$$

$$d_1 = K_1B_2(K_2K_3+K_2K_4+K_3K_4)+K_1K_2K_3B_4 \qquad (4.83)$$

$$d_2 = (1+M)K_2K_3K_4+K_1K_2(K_3+K_4)+B_2B_4K_1(K_2+K_3)$$

$$d_3 = (1+M)(B_2(K_2K_3+K_2K_4+K_3K_4)+K_2K_3B_4)+K_1(K_2B_4+(K_3+K_4)B_2)$$

$$d_4 = MK_2(K_3+K_4)+(1+M)B_2B_4(K_2+K_3)+K_1B_2B_4$$

$$d_5 = M(K_2B_4+(K_3+K_4)B_2)$$

$$d_6 = MB_2B_4$$

and the coefficients of Equation (4.78) in the form,

$$C_1 = -(1+M)K_2K_3K_4$$

$$C_2 = -(1+M)(B2(K_2K_3+K_2K_4+K_3K_4)+K_2K_3B_4)$$

$$C_3 = -(1+M)(K_2+K_3)B_2B_4-MK_2(K_3+K_4) \qquad (4.84)$$

$$C_4 = -M(K_2B_4+(K_3+K_4)B_2)$$

$$C_5 = -MB_2B_4$$

and the coefficients of Equation (4.82) in the form,

$$C_1 = K_1K_2K_3K_4$$

$$C_2 = K_1B_2(K_2K_3+K_2K_4+K_3K_4)+K_1K_2K_3B_4 \qquad (4.85)$$

$$C_3 = K_1B_2B_4(K_2+K_3)$$

where $k_1 = k_1/m_2$, $K_2 = k_2/m_2$, $k_3 = k_2/m_2$, $K_4 = k_4/m_2$, $B_2 = b_2/m_2$, $B_4 = b_4/m_2$ and $M = m_1/m_2$. This shows that the responses are independent of the masses m_1 and m_2, but they are dependent on the stiffness and damping coefficients to the sprung mass ratio and the mass ratio M.

The rms responses of the model are given by,

$$(y_2 - y_1)_{rms} = \sqrt{C.\frac{NUM1}{DEN}} \qquad (4.86)$$

$$(y_1 - y_o)_{rms} = \sqrt{C.\frac{NUM2}{DEN}} \qquad (4.87)$$

$$a_s = \sqrt{C.\frac{NUM3}{DEN}} \qquad (4.88)$$

In order to analyze the responses behavior of the model, the contours of constant K_2 and B_2 values are plotted in Figures 4.24 - 4.28. From Figure 4.24, it can be noted that there are two limited regions where no acceleration or secondary relative displacement values can be obtained. The first region is similar to the region of the 2-DOF model with Maxwell type secondary suspension (Figure 4.2). The other limited region exists because

of the linear relation between the acceleration and the secondary relative displacement for small values of B_2. The contours of constant B_2 values show limiting behavior on the minimization of the acceleration and the secondary relative displacements. It can be observed from Figure 4.24 that the secondary relative displacement takes a constant value when the value of K_2 is much less than the value of B_2. On the other hand, if the value of K_2 is equal to or smaller than the B_2 value, then acceleration becomes constant for a constant B_2 value.

Figure 4.25 and 4.26 show that using larger K_2 and K_4 values results in a similar behavior for the contours of constant K_2 and B_2 values, but with an increase in the sprung mass acceleration values.

From Figure 4.27, it is observed that there is a limit to the minimization of both the primary and secondary relative displacement values. The contours of constant K_2 values show that it is possible to obtain two primary relative displacement values for one K_2 value. The linear relation between the two relative displacements for constant K_2 and B_2 contours as shown in Figure 4.27 creates a limited region where no values of the two relative displacement are obtained.

It is shown in Figure 4.28 that using larger K_3, K_4 and B_4 values results in no change on the relation between the secondary and primary relative displacements.

A value of M equal to 0.1 is used to study the responses of model in this section [39].

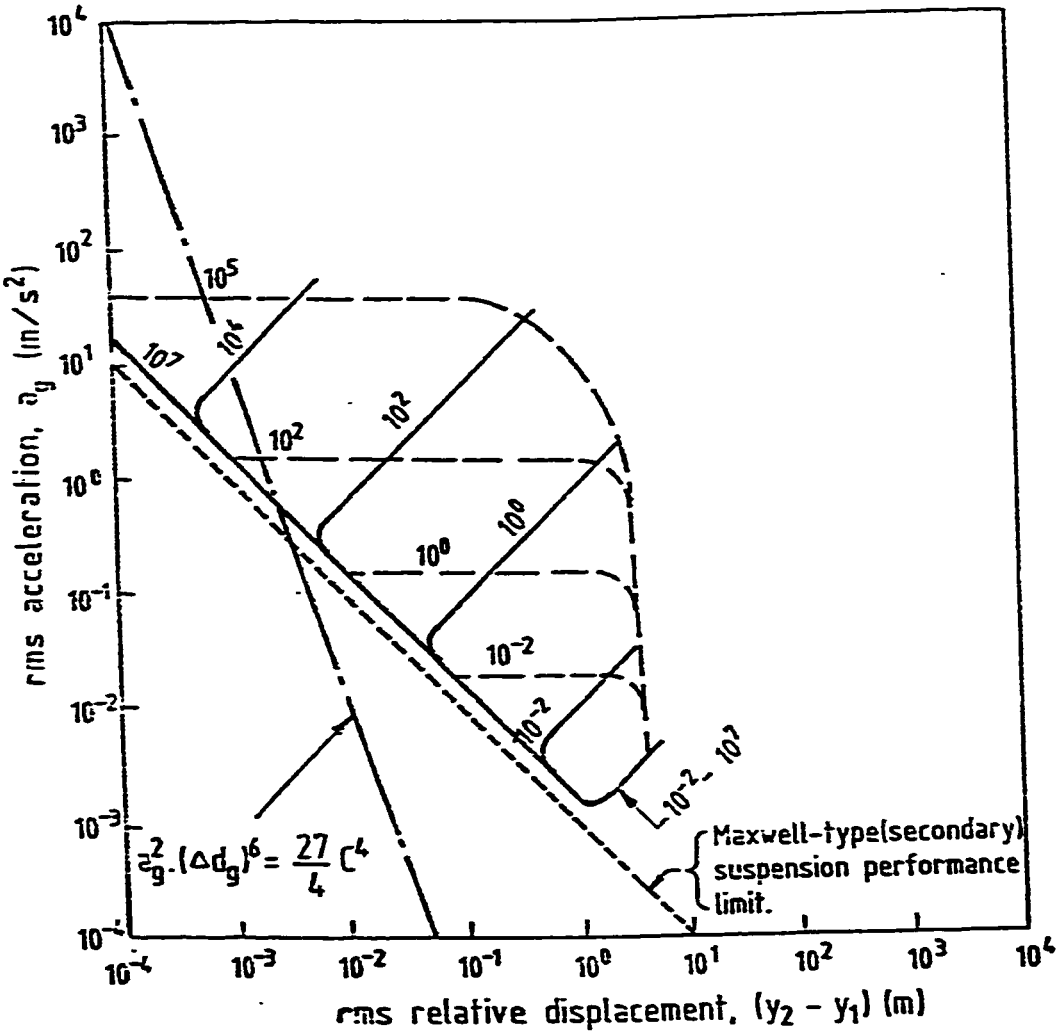

$B_2(\frac{1}{s})$ ——— $K_2(\frac{1}{s^2})$ ———

Figure 4.24 Contours of constant K_2 and B_2 values ($K_3 = K_4 = 10^{-3}\frac{1}{s^2}$ and $B_4 = 10^{-3}\frac{1}{s}$)

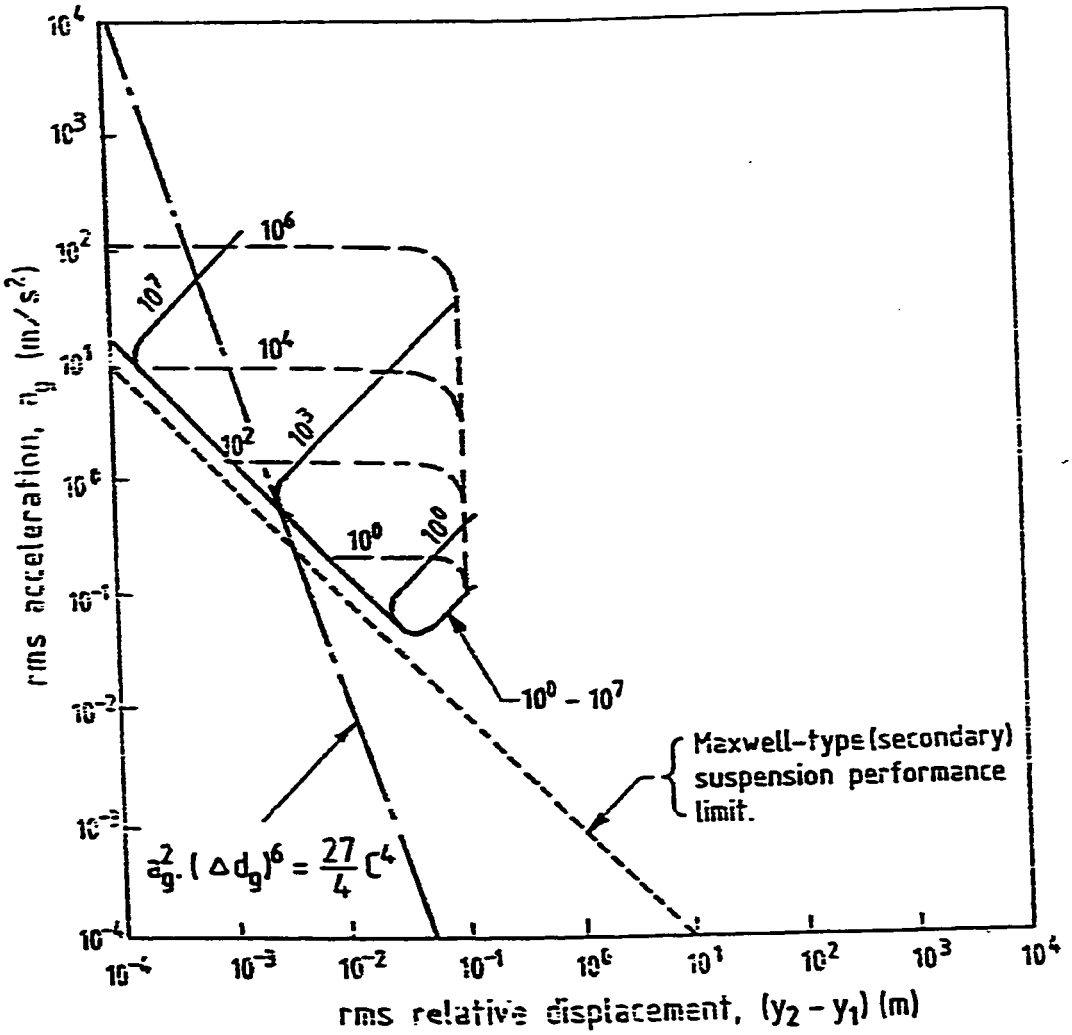

Figure 4.25 Contours of constant K_2 and B_2 values ($K_3 = K_4 = 10^0 \frac{1}{S^2}$ and $B_4 = 10^0 \frac{1}{S}$)

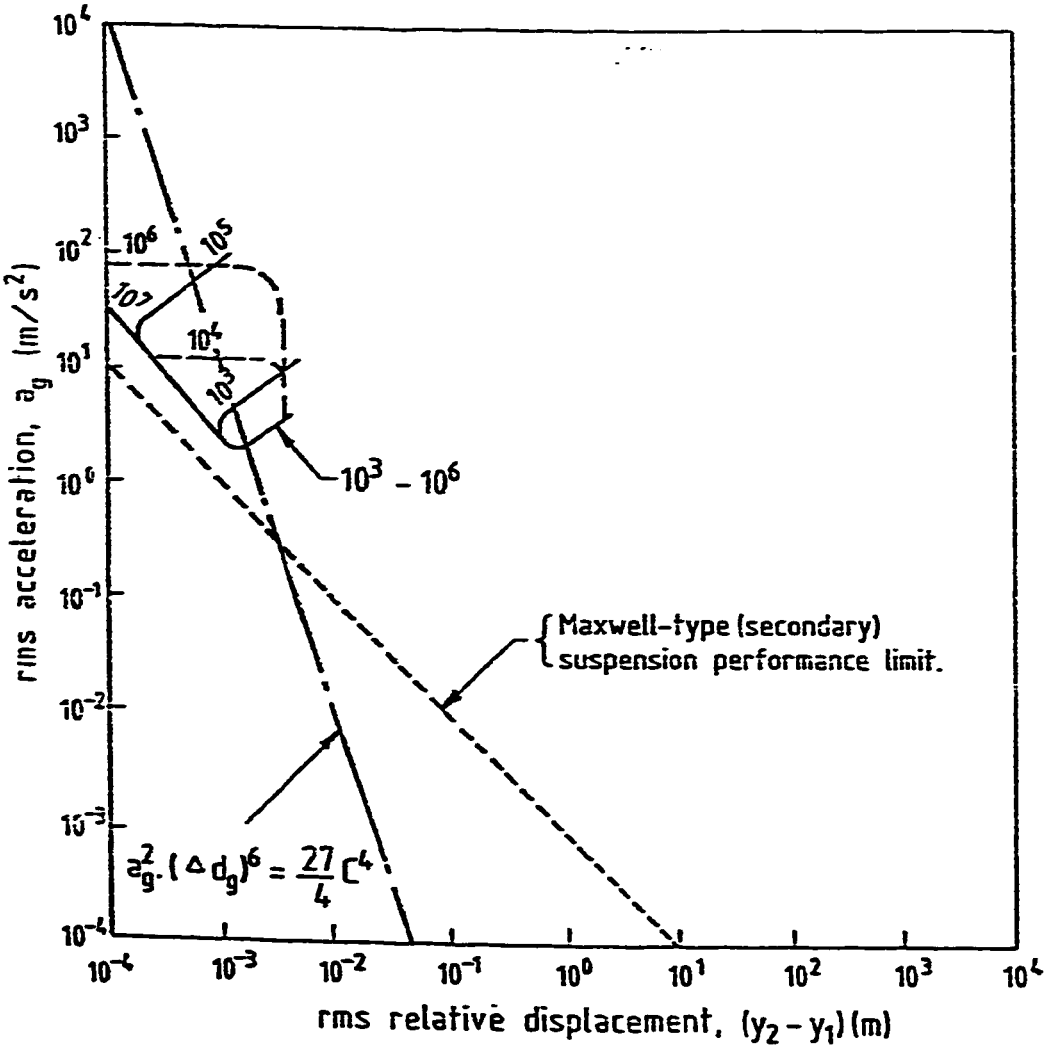

$B_2(\frac{1}{S})$ ——— $K_2(\frac{1}{S^2})$ ———

Figure 4.26 Contours of constant K_2 and B_2 values ($K_3 = K_4 = 10^3 \frac{1}{S^2}$ and $B_4 = 10^3 \frac{1}{S}$)

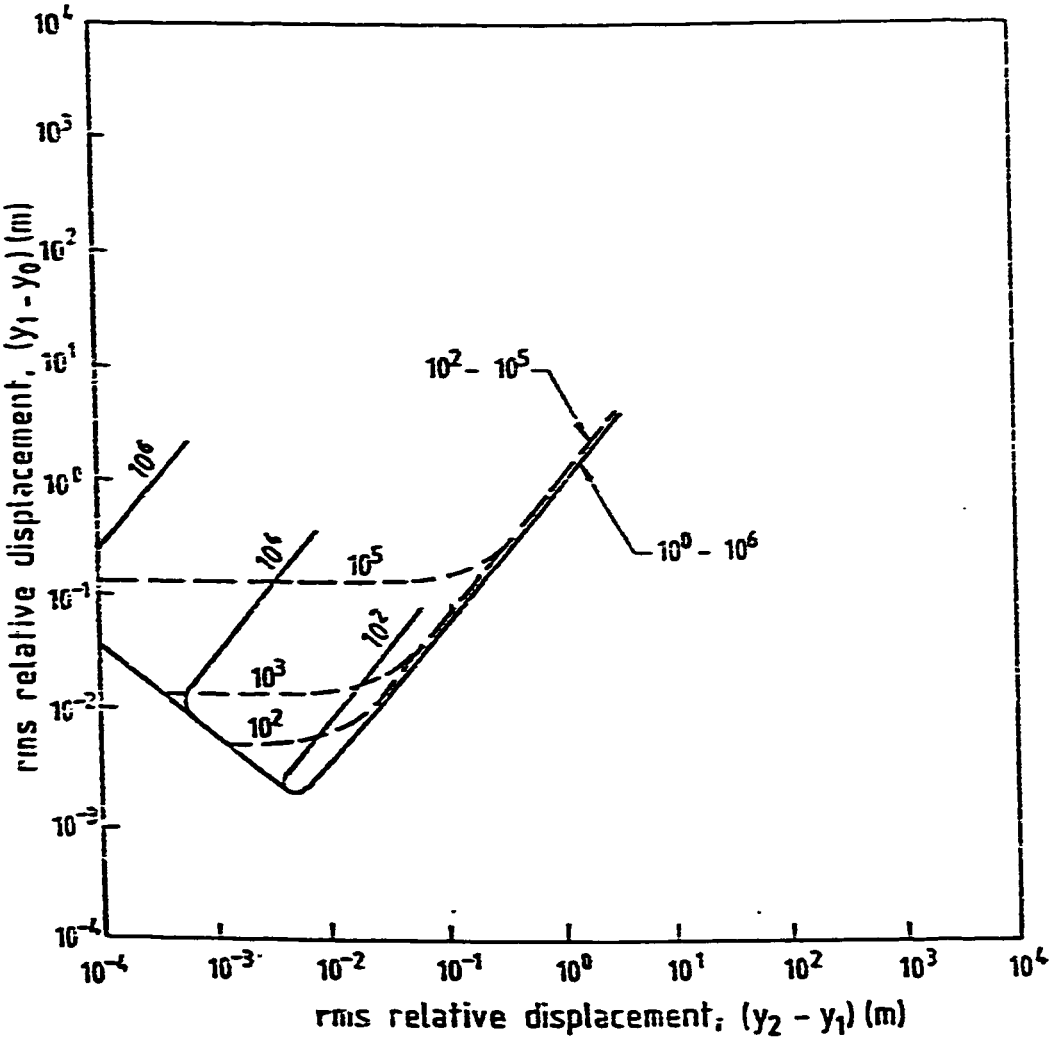

Figure 4.27 Contours of constant K_2 and B_2 values ($K_3 = K_4 = 10^{-3}\frac{1}{s^2}$ and $B_4 = 10^{-3}\frac{1}{s}$)

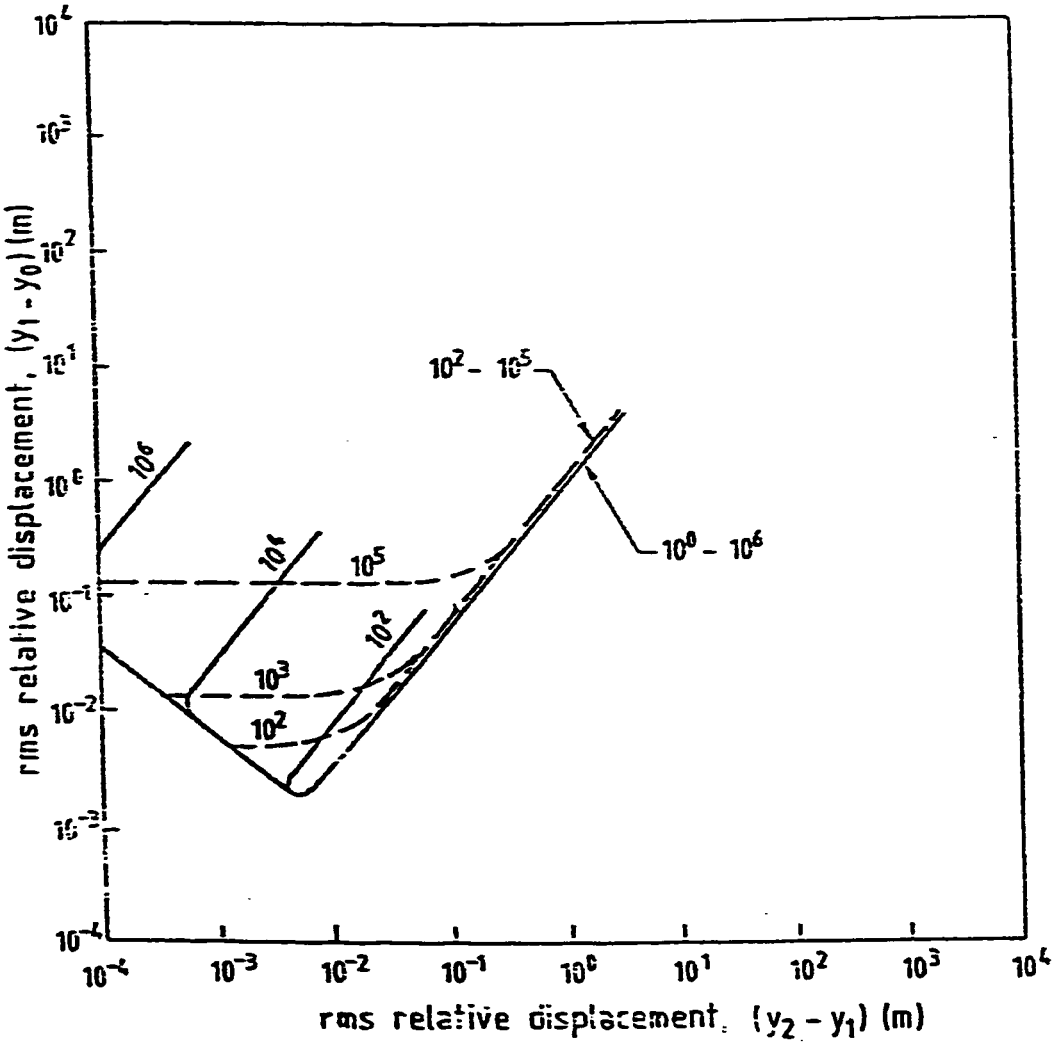

Figure 4.28 Contours of constant K_2 and B_2 values ($K_3 = K_4 = 10^0 \frac{1}{S^2}$ and $B_4 = 10^0 \frac{1}{S}$)

4.6 Comparison of the Responses of the 2-DOF Models

In the previous sections of this chapter, the responses of five different 2-DOF suspension models were analyzed separately when subjected to the road input described in Chapter 2. In this section, the different responses of the models are compared to select the optimum 2-DOF model.

It was shown in Section 4.1 that there is a limit to the optimization of both the acceleration and the secondary relative displacement for the 2-DOF model with secondary type Maxwell suspension, because of the inversely linear relation between the two responses. The line representing this limited region where no acceleration or secondary relative displacement values appear is shown in the figures where the two responses of the other models have been analyzed for different suspension parameters.

In Section 4.2, the 2-DOF model with a secondary suspension of Maxwell type that is in parallel with a spring is analyzed. From Figure 4.6, it is possible to observe a similar limited region to the one of the 2-DOF model with Maxwell type secondary suspension and it can be noted that it is possible in some regions to obtain values of acceleration or secondary relative displacement that are very close to the values that can be obtained by the 2-DOF model with Maxwell type secondary suspension only. But it is not possible in some regions to obtain acceleration values that can be obtained by the 2-DOF model with Maxwell type secondary suspension because of the linear relation that exists between the acceleration and the secondary relative displacement. From Figures 4.7 and 4.8, it can be seen that increasing the K_2 value reduces the possibility of obtaining small acceleration values similar to those can be obtained by the 2-DOF model with Maxwell type secondary suspension.

It can be seen from Figures 4.12 - 4.14 in Section 4.3 that exactly similar conclusions can be made for the 2-DOF model with secondary suspension of Voigt type that is in series with a spring when the acceleration and secondary relative responses according to different K_3 values are compared to the responses of the 2-DOF model with secondary suspension of Maxwell type suspension.

In Section 4.4, it is shown that by adding a spring in parallel with the Voigt type suspension that is in series with a spring, it is possible to obtain acceleration and relative displacement values that are similar to those that can be obtained by the Maxwell type suspension only when small K_2 and K_4 values are used.

In Section 4.5, the response of the 2-DOF model with secondary suspension of Voigt type that is in series with a spring and both are in parallel with Maxwell type suspension are analyzed in Figures 4.24 - 4.26 at different levels of equal K_3, K_4 and B_4 values. It can be observed in Figure 4.24 that by using small K_3, K_4 and B_4 values, it is possible to obtain acceleration and relative displacement values that are close to those that can be obtained by the 2-DOF model with Maxwell type suspension, but it is also noted that it is not possible to obtain small acceleration values similar to those that can be obtained by the 2-DOF model with Maxwell type secondary suspension because of the linear relation that exists between the two responses. It is clear from Figures 4.25 and 4.26 that using larger K_3, K_4 and B_4 values increases the acceleration and it becomes less possible to obtain small acceleration values as those that could be obtained by the 2-DOF model with Maxwell type suspension only.

From the above comparisons of the limits of response of the 2-DOF model with secondary suspension of Maxwell type and the limits of response of the other two models it is possible to say that the other four suspension models can be used to obtain acceleration

and secondary relative displacement values that can be very close to the values that can be obtained by the 2-DOF model with secondary suspension of Maxwell type, but in some regions it is not possible to obtain small acceleration values as those that can be obtained by the 2-DOF model with Maxwell type suspension. It can be concluded that the 2-DOF model with secondary suspension of Maxwell type can produce small acceleration values that cannot be obtained by any other 2-DOF model.

CHAPTER 5

APPLICATION OF MULTI-OBJECTIVE OPTIMIZATION METHODS TO OBTAIN REQUIRED SUSPENSION RESPONSES

In this chapter, the min-max optimization method is applied to a 2-DOF vehicle suspension model in order to determine the suspension parameters required to obtain a given response.

5.1 The Min-Max Optimization Method

The min-max optimum is a method that compares relative deviations from the separately attainable minima of the objective functions. To describe the method mathematically consider the ith objective function $F_i(x)$ where x is a vector of design variables. The relative deviation $F_i(x)$ from a desired function value F_i can be evaluated from

$$Z_i^{\cdot}(x) = \frac{|F_i(x) - F_i|}{|F_i|} \tag{5.1}$$

or from

$$Z_i^{\cdot\cdot}(x) = \frac{|F_i(x) - F_i|}{|F_i(x)|} \tag{5.2}$$

Now, defining the vector of maximum relative deviations as;

$$Z(x) = \left[Z_1(x), - - - , Z_i(x), - - - , Z_k(x)\right]^T \tag{5.3}$$

where

$$Z_i(x) = \max\left[Z_i^{\cdot}(x), Z_i^{\cdot\cdot}(x)\right] \tag{5.4}$$

the optimum can be described as follows: Knowing the extremes of the objective functions which can be obtained by solving the optimization problem for each ceriterion separately,

the optimum solution is the one which gives the smallest values of the relative increments of all the objective functions[28].

In this study, a set of desirable function values in terms of rms acceleration and relative displacement of a 2-DOF vehicle suspension model is assumed. A set of optimum suspension of parameter values are calculated by minimizing the relative deviations of actual function values from the desirable function values.

5.2 Application of the Min-Max Method to a 2-DOF Vehicle Suspension Model

It is required to determine the suspension stiffness coefficient values k_2, k_3, k_4, and the dumping coefficient values b_2 and b_4 of the 2-DOF suspension model shown in Figure 5.1 that will produce the desirable response of the model.

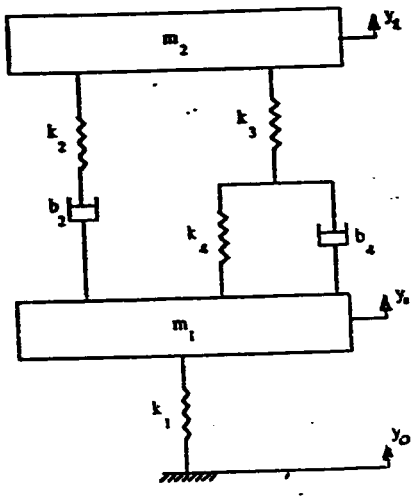

Figure 5.1. 2-DOF vehicle suspension model.

The objective functions of the model are defined as the rms primary relative displacement, rms secondary relative displacement and rms acceleration response of the model.

$$F_1(x) = (y_2 - y_1)_{rms} \tag{5.5}$$

$$F_2(x) = (y_1 - y_o)_{rms} \tag{5.6}$$

$$F_3(x) = a_g \tag{5.7}$$

where the responses are defined by Equations (4.86) - (4.88) and the design vector x consists of the parameters k_2, k_3, k_4, b_2 and b_4. The corresponding desirable function values are selected with reference to Figures 4.24 and 4.27 as

$$F_1 = 10^{-2} \quad (m) \tag{5.8}$$

$$F_2 = 10^{-2} \quad (m) \tag{5.9}$$

$$F_3 = 3 * 10^{-1} \quad (m/s^2) \tag{5.10}$$

The suspension parameter values are discretized in step within the range (10^{-6} to 10^{6}) and the optimum regions are determined. After these, parameter values are again discretized with smaller steps within these ranges drawn to 0.001 change at each step. The optimum objective function values are found as:

$$F_1(x) = 1.1 * 10^{-2} \quad (m) \tag{5.11}$$

$$F_2(x) = 8.9 * 10^{-3} \quad (m) \tag{5.12}$$

$$F_3(x) = 3.3 * 10^{-1} \quad (m/s^2) \tag{5.13}$$

where the components of the design vector x are found to be

$$k_2 = 9075 \text{ N/m}$$

$$k_3 = 0.25 \text{ N/m}$$

$$k_4 = 0.25 \text{ N/m} \qquad (5.14)$$

$$b_2 = 675 \text{ N.s/m}$$

$$b_4 = 0.25 \text{ N.s/m}$$

The results are based on the following parameters[39].

$$m_1 = 25 \text{ kg}$$

$$m_2 = 250 \text{ kg} \qquad (5.15)$$

$$k_1 = 10^5 \text{ N/m}$$

The optimum objective functions values are found to be very close but not equal to the desirable functions values. This is because it is not always possible to obtain the ideal solution through an optimization process which provides the best compromise among the competing objective functions.

It has been possible to determine the design vector that provides the optimum objective function values because the desirable function values were selected from a feasible region of solutions as shown in Figures 4.24 and 4.27. If the desirable function, values are selected outside the feasible region, it will not be possible to obtain close objective function values because the relative deviations of the calculated objective functions from the desired values will be very large and this may indicate that the desired values cannot be obtained. Of course, this point should be carefully investigated in future.

CHAPTER 6

CONCLUSIONS

The responses of five different one-degree of freedom models are analyzed in the study when subjected to random road inputs and random aerodynamic disturbances. Also, the responses of five different two-degree of freedom suspension models are analyzed when subjected to random road inputs. These investigations are made to improve the understanding of the performance of passive vehicle suspension systems and their performance limits. Different regions where the models responses cannot be obtained are identified. The inversely linear relation between the model responses is the reason in some cases for the existence of these limited regions. In other cases the linear relation between the model responses is the reason for the existence of the limited regions. When the inversely linear relation exists between the responses it is not possible to obtain a certain small value of one response without increasing the value of the other response. Whereas if the linear relation exists between the responses, then it becomes possible to obtain both the desired model responses. Also, the existence of more than one response value for specific parameter values is explained. Comparisons between the one-degree of freedom models lead to the conclusion that the one-degree of freedom model with Maxwell type suspension provides the best performance among all the one-degree of freedom models. On the other hand, by the use of certain suspension parameters in the other one-degree of freedom models, their performances can approach the performance of the one-degree of freedom model with Maxwell type suspension. Similarly, the comparisons between the responses of the two-degree of freedom models show that the two degree of freedom model with Maxwell type secondary suspension achieves the best performance when it is subjected to road input only. However, it is possible to obtain a close performance to the performance

of the Maxwell type two degree of freedom model by using other two-degree of freedom suspension models.

Additional specific conclusions drawn from the present investigation are:

1. The responses of the different 1-DOF models to the road input are dependent on the stiffness and damping coefficient ratios to the vehicle mass.

2. The responses of the different 2-DOF models to the road input unsprung are dependent on the unsprung to sprung mass ratio and on the stiffness and damping coefficients ratios to the vehicle mass.

3. Smaller suspension stiffness values help in reducing the acceleration levels when the model is subjected to the road input only.

4. Larger stiffness values help in reducing the effects of the aerodynamic forces by reducing the suspension travel.

A multiobjective optimization method is used in the study to show how it is possible to obtain a set of suspension parameters for a specific response of the vehicle.

It is hoped that the plotted contours for different suspension changes serve as test data for future development of similar numerical schemes. It also furnishes a large set of data to be used in the dynamic analysis of suspension models with similar configurations.

REFERENCES

1. Hedrick, J. K., Billington, G. F., Dreesbagh, D. A. (June 1974). "Analysis, Design, and Optimization of High Speed Vehicle Suspensions Using State Variable Techniques", *JDSMC*, 193-203

2. Hedrick, J. K (1972). "Some Optimal Control Techniques Applicable to Suspension System Design", *TRANS. ASME*, Paper No. 73-ICT-55

3. Sevin, E. (May 1972). "Automated Design Parameter Identification; A New Approach", *Journal of Engineering for Industry*, 388-394

4. Young, J. W., Wormley, D. N. (June 1973). "Optimization of Linear Vehicle Suspensions Subjected to Simultaneous Guideway and External Force Disturbances", *JDSMC*, 213-219

5. Thompson, A. G. (1976). "An Active Suspension with Optimal Linear State Feedback", Vehicle System Dynamics, Vol. 5, 187-203

6. Hedrick, J. K., Butsyen, T. (1988): "Invariant Properties of Automative Suspensions", *I Mech E*, 35-42

7. Margolis, D. L. (April 1983). "A procedure for Comparing Passive, Active, and Semi-Active Approaches to Vibration Isolation", *Journal of the Franklin Institute*, Vol. 315, No. 4, 225-238

8. Yue, C., Butsuen, T., Hedrick, J. K, (June 1989). "Alternative Control Laws for Automotive Active Suspensions", *JDSMC* , Vol.111, 286-291

9. Margolis, D. L. (1982). "Semi-Active Heave and Pitch Control for Ground Vehicles", *Vehicle System Dynamics*, Vol. 11, 31-42

10. ElMadany, M. M., Abduljabbar, Z. (1991). "Alternative Control Laws for Active and Semi-Active Automotive Suspensions- A Comparative Study", *Computers & Structures*, Vol. 39, No. 6, 623-629

11. Parak, P. and Harvot, D. (1988): "Application of the LQG Approach to Design of an Automotive Suspension for Three-Dimensional Vehicle Models", *IMECH* , 11-26

12. ElMadany, M. M. (1990). "The Performance of Passive Cab Suspension Systems in Tractor - Semitrailer Vehicles", *J. King Saud Univ.*, Vol. 2, Eng. Sci (1), 131-152

13. Garivaltis, D. S., Garg, V., D'souza, A. F. (1980). "Dynamic Response of a Six - Axle Locomotive to Random Track Inputs", *Vehicle System Dynamics*, Vol. 9 117-147

14. Sevin, E., Pilkey, W. D., Kalinowski, A. J. (1969). "Optimum Performance Bounds and Synthesis of Dynamic Systems", In "Computational Approaches in App. Mechanics", Ed: E. Sevin, *ASME Monograph*, 107-132

15. Dahlberg, Tore (1980). "Comparison of Ride Comfort Criteria for Computer Optimization of Vehicles Travelling on Randomly Profiled Roads", *Vehicle System Dynamics*, Vol. 9, 291-307

16. Dahlberg, Tore (1979). "Optimization Criteria for Vehicles Travelling on a Randomly Profiled Road - a Survey", *Vehicle System Dynamics*, Vol. 8, 291-307

17. ElMadany, M. M. (1988). "Design and Optimization of Truck Suspensions Using Covariance Method", *Computers & Structures*, Vol.28, No. 2, 241-249

18. Harvot, D., Hubbard, M. (September 1981). "Optimum Vehicle Suspensions Minimizing RMS Rattlespace, Sprung-Mass Acceleration and Jerk", *JDSMC*, Vol. 103, 228-236

19. Karnopp, D. C. (1978). "Vehicle Response to Stochastic Roadways", *Vehicle System Dynamics*, Vol. 7, 97-109

20. Harvot, D. (1982). "A Class of Active LQG Optimal Actuators", *Automatica*, Vol. 18, No. 1, 117-119

21. Harvot, D. (1990). " Optimal Active Suspension Structures for Quarters - Car Vehicle Models", *Automatica*, Vol. 26, No. 5, 845-860.

22. Tabak, D., Schy, A. A., Giesy, D. P., Johnson, K. G., (1979). "Application of Multiobjective Optimization in Aircraft Control System Design", *Automatica*, Vol. 15, 595

23. Kuhn, H. N., Tucker, A. W. (1951). "Nonlinear Programming", *In Proceedings of the second berkeley symposium on mathematical statistics and probability, (Ed: J. Neyman)*, University of California, Berkeley, CA, 481-491

24. Evans, G. W. (November 1984). "An Overview of Techniques for Solving Multiobjective Programs", *Management Science*, Vol. 30, No. 11, 1268-1282

25. Hwang, C. L., Masud, A. S. M, (1978): *Multiple Objective Decision Making - Methods and Applications*, Springer - Verlag - Berlin.

26. Stadler, W. (1979): "A Survey of Multicriteria Optimization of the Vector Maximum Problem", *J. Optimization Theory and Appl.*, Part I:1776-1960, Vol. 29, No.1, 1.

27. Freiheit, T. T., Rao, S. S. (1988): "A modified Game Theory Approach to Multiobjective Optimization", *ASME Advances in Design Automation*, Vol. 14.

28. Osyczka, A. (1984): *Multicriterion Optimization in Engineering with Fortran Programs*, John Wiley, New York.

29. Rao, S. S. "Design of Vibration Isolation Systems Using Multiobjective Optimization Techniques", *ASME*, Paper No.84-DET-60.

30. Eschenauer, H., Koski, J., Osyczaka, A., (1990): *Multicriteria Design Optimization*, Springer - Verlag - Berlin.

31. Lee, S. J., Kapoor, S. G., (1986): "A Shape and Size Optimization Algorithm for Machine Tool Element Design", *Eng. Optimization*.

32. Dlesk, D. C. and Liebman, J. S. (1983): "Multiple Objective Engineering Design", *Eng. Optimization*, Vol. 6, 161.

33. Osyczka, A. (1978): "An Approach to Multicriterion Optimization Problems for Engineering Design", *Computer Methods in Applied Mechanics and Engineering*, Vol. 15, 309.

34. Diaz, Alegandro (1987): "Interactive Solution to Multiobjective Optimization Problems", *International Journal for Numerical Methods in Engineering*, Vol. 24, 1865-1877.

35. Haug, E., Aurora, J. (1979): *Applied Optimal Design*, Wiley, New York.

36. Hati, S. K., Rao, S. S., (January 1983), "Cooperative Solution in the Synthesis of Multidegree - of - Freedom Shock Isolation Systems", *JVASRD*, Vol. 105, 101-103.

37. Newton, C. Gould, A. Kaiser, F. (1967). "Analytical Design of Linear Feedback Controls", John Wiley, New York.

38. SCHAUM's OUTLINE SERIES. Mathematical Handbook for Formulas and Tables.

39. Sharp, R. Corolla, D. (1987). "Road Vehicle Suspension System Design - a Review", Vehicle System Dynamics, Vol. 16, 167-192.

APPENDIX A

MODELS OF THE SUSPENSION SYSTEMS AND DERIVATIONS OF MODEL RESPONSES

In this Appendix, the equivalent transfer function of the different suspension models used in the study are presented. Then, the model responses are derived using the equivalent transfer functions. In deriving the model-response equations it is assumed that the corresponding mechanical system is in equilibrium position initially although the Maxwell type suspension and others similar to it are not in equilibrium at any time.

A-1 Models of the Suspensions and their Equivalent Transfer Functions

The force produced by a suspension system with an equivalent transfer function G(s), as shown in Figure A-1, is given by

$$F(s) = G(s).(y_2(s) - y_1(s)) \qquad \text{(A-1)}$$

where s is the Laplace operator.

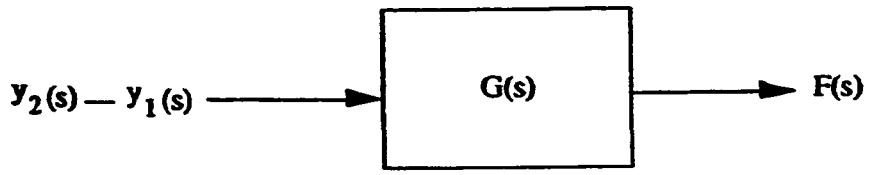

Figure A-1. Suspension system with an equivalent transfer function.

Suspension models and their transfer functions are given in Table A-1.

Table A-1. Suspension models and their transfer functions.

(a) Maxwell-type suspension

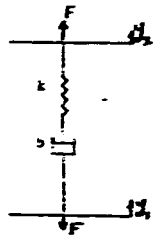

$$G_1(s) = \frac{kbs}{k + bs} \qquad \text{(A-2)}$$

(b) Maxwell type suspension that is in parallel with a spring

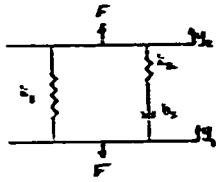

$$G_2(s) = k_1 + \frac{k_2 b_2 s}{k_2 + b_2 s} \qquad \text{(A-3)}$$

(c) Voigt type suspension that is in series with a spring

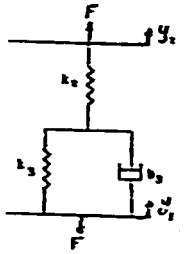

$$G_3(s) = \frac{k_2(k_3 + b_3 s)}{k_2 + k_3 + b_3 s} \qquad \text{(A-4)}$$

(d) Voigt type suspension that is in series with a spring and both are in parallel with a spring

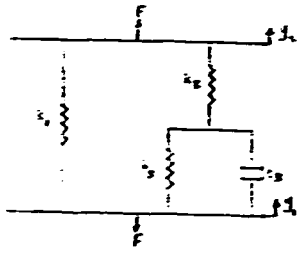

$$G_4(s) = k_1 + \frac{k_2(k_3 + b_3 s)}{k_2 + k_3 + b_3 s} \qquad \text{(A-5)}$$

(e) Voigt type suspension that is in series with a spring and both are in parallel with Maxwell type suspension

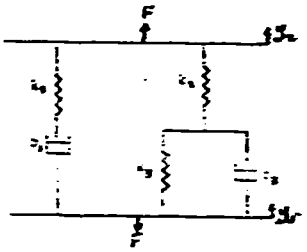

$$G_5(s) = \frac{k_1 b_1 s}{k_1 + b_1 s} + \frac{k_2(k_3 + b_3 s)}{k_2 + k_3 + b_3 s} \qquad \text{(A-6)}$$

A-2 Derivation of the 1-DOF Model Responses

The mean square acceleration and relative displacement responses of the 1-DOF models are derived in this section. Individual response to road input and external force input are derived separately assuming that the inputs are independent.

The 1-DOF suspension model shown in Figure A-2 consists of a vehicle mass m, an equivalent suspension transfer function g(t) in the time domain.

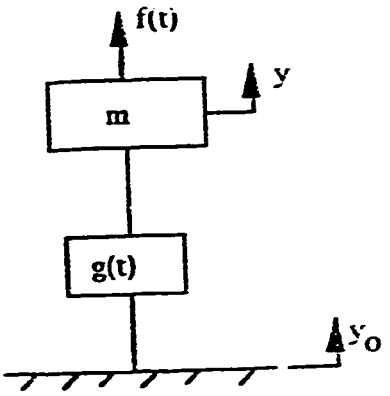

Figure A-2. 1-DOF suspension model.

When the model is subjected to the road input only (f(t) = o), Newton's second law can be written as

$$m\ddot{y}(t) = -g(t)(y(t)-y_o(t)) \qquad \text{(A-7)}$$

By taking the Laplace transform of Equation (A-7), we obtain:

$$ms^2(t) = -G(s)(y(s)-y_o(s)) \qquad \text{(A-8)}$$

where G(s) is the equivalent transfer function of the suspension system in the Laplace domain. From Equation (A-8), the relative displacement of the suspension system due to the ground input only can be written as,

$$\Delta y_g = h_1(s).y_o \qquad \text{(A-9)}$$

where

$$h_1(s) = \frac{-ms^2}{ms^2 + G(s)} \qquad \text{(A-10)}$$

The acceleration of the mass due to the road input only is s^2y in Laplace domain and it is given by,

$$a_g = h_2(s) . y_e \qquad \text{(A-11)}$$

where

$$h_2(s) = \frac{s^2 G(s)}{ms^2 + G(s)} \qquad \text{(A-12)}$$

The spectral density of the relative displacement due to the road input only is given by

$$S_{\Delta y_g}(s) = h_1(s) . h_1(-s) . S_{y_e}(s) \qquad \text{(A-13)}$$

where $S_{y_e}(s)$ is as given by Equation (2.1). In order to find the mean square relative displacement, Equation (A-13) can be factored as [37].

$$S_{\Delta y_g}(s) = AV . \frac{C_1(s) . C_1(-s)}{d_1(s) . d_1(-s)} \qquad \text{(A-14)}$$

Then, to get the mean square relative displacement due to the ground input, we use the relation

$$\overline{\Delta y_g^2} = 2\pi AV . I \qquad \text{(A-15)}$$

where I is given in Appendix E.2 of reference [37].

The mean square value of acceleration of the mass due to the road input can be calculated in the same way. Using Equation (A-11), we can write the spectral density of the acceleration.

$$S_{a_g}(s) = h_2(s) . h_2(-s) . S_{y_e}(s) \qquad \text{(A-16)}$$

In order to find the mean square acceleration, Equation (A-16) can be factored as [37].

$$S_{a_g}(s) = AV . \frac{C_2(s) . C_2(-s)}{d_2(s) . d_2(-s)} \qquad \text{(A-17)}$$

Then, to get the mean square acceleration due to the ground input we use the relation,

$$\overline{a_g^2} = 2\pi AV.I \qquad \text{(A-18)}$$

where I is given in Appendix E.2 of reference[37].

When the model is subjected to the external force input only ($y_o = o$), Newton's second law can be written as

$$m\ddot{y}(t) = f(t) - g(t).y(t) \qquad \text{(A-18)}$$

By taking the Laplace transform of Equation (A-18), we can obtain;

$$ms^2y = F(s)-G(s).y \qquad \text{(A-19)}$$

From Equation (A-19), the relative displacement of the suspension system due to the external force input only can be written as

$$\Delta y_F = h_3(s).y_o \qquad \text{(A-10)}$$

where

$$h_3(s) = \frac{1}{ms^2 + G(s)} \qquad \text{(A-21)}$$

The acceleration of the mass due to the external force input only is s^2y in the Laplace domain and it is given by;

$$a_F = h_4(s).F \qquad \text{(A-22)}$$

where

$$h_4(s) = \frac{s^2}{ms^2 + G(s)} \qquad \text{(A-23)}$$

The spectral density of the relative displacement due to the external force input only is given by

$$S_{\Delta y_F}(s) = h_3(s).h_3(-s).S_F(s) \qquad \text{(A-24)}$$

where $S_F(s)$ is given by Equation (2.2). In order to find the mean square relative displacement, Equation (A-24) is factored as [37].

$$S_{\Delta y_F}(s) = \beta\upsilon.\frac{C_3(s).C_3(-s)}{d_3(s).d_3(-s)} \qquad \text{(A-25)}$$

Then, to get the mean square relative displacement due to the external force input we use the relation

$$\overline{\Delta y_F^2} = 2\pi\beta\upsilon.I \qquad \text{(A-26)}$$

where I is given in Appendix E.2 of reference [37].

The spectral density of the acceleration due to the external force input is given by;

$$S_{a_F}(s) = h_4(s).h_4(-s).S_F(s) \qquad \text{(A-27)}$$

where $S_F(s)$ is given by Equation (2.2). In order to find the mean square relative displacement due, Equation (A-27) is factored as [37].

$$S_{\Delta y_F}(s) = \beta\upsilon.\frac{C_4(s).C_4(-s)}{d_4(s).d_4(-s)} \qquad \text{(A-28)}$$

To get the mean square acceleration due to the external force input we use the relation

$$\overline{a_F^2} = 2\pi\beta\upsilon.I \qquad \text{(A-29)}$$

where I is given in Appendix E.2 of reference [37].

Now, the responses of any of the 1-DOF models used in this study can be obtained by substituting the equivalent transfer function of its suspension, as given in Table A-1, into Equations (A-10), (A-12) and (A-23) to obtain the function $h_1(s)$ - $h_4(s)$ and hence using these functions to obtain the spectral densities of the responses given by Equations (A-13), (A-16), (A-24) and (A-27). The spectral densities are than integrated after factorization to obtain the mean square responses given by Equations (A-15), (A-18), (A-26) and (A-29).

A-3 Derivations of the 2-DOF Model Responses

The mean square acceleration and relative displacement responses of the 2-DOF models due to the road input only are derived in this section.

The 2-DOF suspension model shown in Figure A-3 consists of a sprung mass m_2, an unsprung mass m_1, a secondary suspension with stiffness coefficient k_1 and an equivalent suspension transfer function g(t) in the time domain.

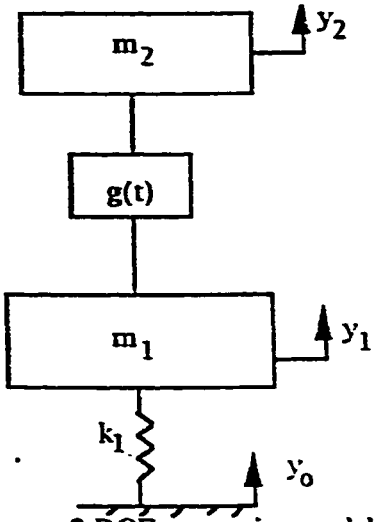

Figure A-3. 2-DOF suspension model.

Newton's second law for the sprung mass can be written as

$$m_2\ddot{y}_2 = -g(t)\,(y_2(t)-y_1(t)) \qquad \text{(A-122)}$$

and for the unsprung mass as

$$m_1\ddot{y}_1 = g(t)(y_2(t)-y_1(t)) - k_1(y_1(t) - y_o(t)) \qquad \text{(A-123)}$$

By taking the Laplace transform of Equations (A-122) and (A-123), we obtain;

$$m_2S^2y_2 = -G(s)(y_2(s)-y_1(s)) \qquad \text{(A-124)}$$

and

$$m_1S^2y_1 = G(s)(y_2(s) - y_1(s)) - k_1 (y_1(s) - y_o(s)) \qquad \text{(A-125)}$$

where G(s) is the equivalent transfer function of the primary suspension system in the Laplace domain. By solving Equations (A-124) and (A-125) simultaneously, the secondary relative displacement, the primary relative displacement and the acceleration of the sprung mass are solved as;

$$y_2 - y_1 = h_1(s).\ y_o \qquad \text{(A-126)}$$

$$y_1 - y_o = h_1(s).\ y_o \qquad \text{(A-127)}$$

$$a_g = h_3(s)\ .\ y_o \qquad \text{(A-128)}$$

where

$$h_1(s) = \frac{N1(s)}{D(s)} \qquad \text{(A-129)}$$

$$h_2(s) = \frac{N2(s)}{D(s)} \qquad \text{(A-130)}$$

$$h_3(s) = \frac{N3(s)}{D(s)} \qquad \text{(A-131)}$$

where

$$N1(s) = -k_1 m_2 s^2 \tag{A-132}$$

$$N2(s) = -m_1 m_2 s^4 - (m_1+m_2)G(s)s^2 \tag{A-133}$$

$$N_3(s) = k_1 s^2 G(s)$$
$$D(s) = (m_1 s^2 + G(s) + k_1)(m_2 s^2 + G(s)) - G^2(s) \tag{A-134}$$

$$S_{y_2 - y_1}(s) = h_1(s).h_1(-s).S_{y_0}(s) \tag{A-135}$$

$$S_{y_1 - y_0}(s) = h_2(s).h_2(-s).S_{y_0}(s) \tag{A-136}$$

$$S_{z_g}(s) = h_3(s).h_3(-s).S_{y_0}(s) \tag{A-137}$$

where $S_{y_0}(s)$ is given by Equation (2.1). In order to find the mean square responses, Equations (A-135), (A-136) and (A-137) are factored as[37].

$$S_{y_2 - y_1}(s) = AV.\frac{C_1(s).C_1(-s)}{d_1(s).d_2(-s)} \tag{A-138}$$

$$S_{y_1 - y_0}(s) = AV.\frac{C_2(s).C_2(-s)}{d_2(s).d_2(-s)} \tag{A-139}$$

$$S_{z_g}(s) = AV.\frac{C_3(s).C_3(-s)}{d_3(s).d_3(-s)} \tag{A-140}$$

Then, to get the mean square responses due to the road input, we use the relations:

$$\overline{(y_2 - y_1)^2} = 2\pi AV.I \tag{A-141}$$

$$\overline{(y_1 - y_0)^2} = 2\pi AV.I \tag{A-142}$$

$$\overline{z_g^2} = 2\pi AV.I \tag{A-143}$$

where I is as given in Appendix E-2 of reference[37].

Now, the responses of any of the 2-DOF models used in this study can be obtained by substituting the equivalent transfer function of its secondary suspension, as given in Table A-2, into Equations (A-129), (A-130) and (A-131) to obtain the function $h_1(s)$ - $h_3(s)$ and hence using them to obtain the spectral densities of the responses given by Equations (A-135), (A-136) and (A-137). The spectral densities are then integrated after factorization to obtain the mean square responses given by Equations (A-141), (A-142) and (A-143).

Table A-2. Suspension systems used in primary suspensions and their transfer functions.

(a) Maxwell type suspension	
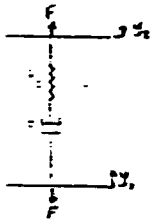	$G_1(s) = \frac{k_1 b_1 s}{k_1 + b_1 s}$ (A-144)
(b) Maxwell type suspension that is in parallel with a spring	
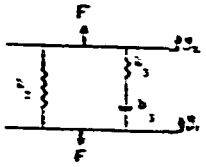	$G_2(s) = k_2 + \frac{k_3 b_3 s}{k_3 + b_3 s}$ (A-145)
(c) Voigt type suspension that is in series with a spring	
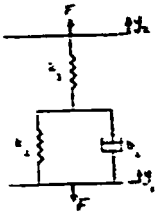	$G_3(s) = \frac{k_2(k_3 + b_3 s)}{k_2 + k_3 + b_3 s}$ (A-146)

(d) Voigt type suspension that is in series with a spring and both are in parallel with a spring

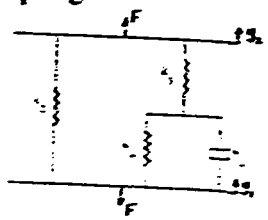

$$G_4(s) = k_2 + \frac{k_3(k_4 + b_4 s)}{k_3 + k_4 + b_4 s} \qquad \text{(A-147)}$$

(e) Voigt type suspension that is in series with a spring and both are in parallel with Maxwell type suspension

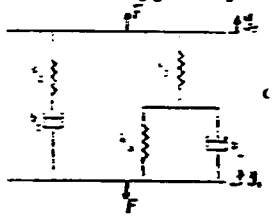

$$G_5(s) = \frac{k_2 b_2 s}{k_2 + b_2 s} + \frac{k_3(k_4 + b_4 s)}{k_3 + k_4 + b_4 s} \qquad \text{(A-148)}$$

APPENDIX B

A MATHEMATICAL INVESTIGATION OF THE LIMITING VALUES OF SUSPENSION RESPONSES

In this Appendix, the limiting values of the mean square responses are investigated mathematically.

B-1 1-DOF MODEL WITH MAXWELL TYPE SUSPENSION

Let us indicate by d and a for the mean square relative displacement (Equation (3.3)) and the mean square acceleration (Equation (3.4)) respectively. Then, we can write;

$$d = C\left(\frac{1}{B} + \frac{B}{K}\right) \qquad \text{(B-1)}$$

$$a = C.K.B. \qquad \text{(B-2)}$$

where $C = \pi A.V.$

a) Solving Equation (B-1) in terms of K, we get

$$K = \frac{CB^2}{Bd - C} \qquad \text{(B-3)}$$

which means that for a positive K, we have

$$d > C/B \qquad \text{(B-4)}$$

b) Solving Equation (B-2) for K, we have

$$K = \frac{a}{CB} \qquad \text{(B-5)}$$

Substituting for K in Equation (B-1), we get

$$d = \frac{C}{B} + \frac{(BC)^2}{a} \qquad \text{(B-6)}$$

Equation (B-6) can be written in the form of the following characteristic equation:

$$B^3 - \left(\frac{ad}{C^2}\right)B + \frac{a}{c} = 0 \qquad \text{(B-7)}$$

Solving Equation (B-7) for B, for given a, d and C we obtain the roots [38].

$$B_1 = S + T \qquad \text{(B-8)}$$

$$B_2 = -\frac{S+T}{2} + \frac{S-T}{2}\sqrt{-3}$$

$$B_3 = -\frac{S+T}{2} + \frac{S-T}{2}\sqrt{-3}$$

where

$$S = \left(\frac{-a}{2C} + \sqrt{D}\right)^{1/3} \qquad \text{(B-9)}$$

and

$$T = \left(\frac{-a}{2C} - \sqrt{D}\right)^{1/3} \qquad \text{(B-10)}$$

where

$$D = \frac{a^2}{4C^2} - \frac{a^3d^3}{27C^6} \qquad \text{(B-11)}$$

The following three cases can be distinguished with regard to D:

1. One root is real and negative and two complex conjugate if D>o, from which we can detect that

$$ad^3 > \frac{27}{4}C^4 \qquad \text{(B-12)}$$

2. All roots are real and at least two are equal if D = o or if

$$ad^3 = \frac{27}{4}C^4 \qquad \text{(B-13)}$$

In this case, the first root will be

$$B_1 = -2\left(\frac{a}{c}\right)^{1/3} \qquad \text{(B-14)}$$

which is not an acceptable one (negative).

The other two equal roots will be

$$B_2 = B_3 = \left(\frac{a}{2c}\right)^{1/3} \qquad \text{(B-15)}$$

Substituting for B from Equation (B-15) into Equation (B-2), then

$$K = \left(\frac{2a^2}{c^2}\right)^{1/3} \qquad \text{(B-16)}$$

From Equation (B-15) and (B-16), then

$$B = \left(\frac{K}{2}\right)^{1/2} \qquad \text{(B-17)}$$

3. All roots are real, positive and unequal if D<o or if that

$$ad^3 > \frac{27}{4}C^4 \qquad \text{(B-18)}$$

From the above analysis of the cubic characteristic equation, it is clear that the relation:

$$ad^3 \geq \frac{27}{4}C^4 \qquad \text{(B-19)}$$

provides a feasible region for the acceleration and the displacement functions of this suspension model.

B-2 1-DOF Model with Maxwell Type Suspension that is in Parallel with a Spring

Let us indicate by d and a for the mean square relative displacement (Equation (3.31)) and for the mean square acceleration (Equation (3.32)), then we can write.

$$d = C\left(\frac{B_2}{K_2^2}.N + \frac{1}{B_2}\right) \tag{B-20}$$

$$a = C\left(\frac{B_2}{K_2^2}.N^3 + \frac{K_1^2}{B_2}\right) \tag{B-21}$$

where $C = \pi.A.V.$ and

$$N = K_1 + K_2 \tag{B-22}$$

Solving Equation (B-20) for B_2, we have

$$B_2 = \frac{1}{2}\left[\frac{K_2^2 d}{CN} \pm L^{1/2}\right] \tag{B-23}$$

where

$$L = \left(\frac{K_2^2 d}{CN}\right)^2 - \frac{4K_2^2}{N} \tag{B-24}$$

If $L = 0$, then we can solve Equation (B-24) for

$$d_{min} = \left(\frac{4C^2 N}{K_2^2}\right)^{1/2} \tag{B-25}$$

Now, substituting for d when $L = o$ in Equation (B-23), we obtain;

$$B_2 = \frac{K_2}{(K_1 + K_2)^{1/2}} \tag{B-26}$$

By minimizing d (Equation (B-20)) with respect to B_2, we get

$$\frac{\partial d}{\partial B_2} = C\left(\frac{N}{K_2^2} - \frac{1}{B_2^2}\right) = 0 \qquad \text{(B-27)}$$

Solving Equation (B-27) for B_2, we obtain:

$$B_2 = \frac{K_2}{(K_1 + K_2)^{1/2}} \qquad \text{(B-28)}$$

which is the same as Equation (B-26). Since the second derivative is positive, this is the minimum.

Solving Equation (B-21) for B_2, we have

$$B_2 = \frac{1}{2}\left[\frac{K_2^2 a}{CN^3} \pm H^{1/2}\right] \qquad \text{(B-29)}$$

where

$$H = \left(\frac{K_2^2 a}{CN^3}\right)^2 - \frac{4K_1^2 K_2^2}{N^3} \qquad \text{(B-30)}$$

If H = 0, then we can solve Equation (B-30) for

$$a_{min} = \frac{2cK_1}{K_2} . N^{3/2} \qquad \text{(B-31)}$$

Now, substituting for a when H = 0 in Equation (B-29), we obtain

$$B_2 = \frac{K_1 K_2}{(K_1 + K_2)^{3/2}} \qquad \text{(B-32)}$$

By minimizing a (Equation (B-21)) with respect to B_2, we get

$$\frac{\partial a}{\partial B_2} = C\left(\frac{N^3}{K_2^2} - \frac{K_1^2}{B_2^2}\right) = 0 \qquad \text{(B-33)}$$

Solving Equation (B-33) for B_2, we obtain

$$B_2 = \frac{K_1 K_2}{(K_1 + K_2)^{3/2}} \qquad \text{(B-34)}$$

which is the same as Equation (B-32). Since the second derivative is positive, this is the minimum.

B-3 1-DOF Model with Voigt Type Suspension that is in Series with a Spring

Let us indicate by d and a for the mean square relative displacement Equation (3.86) and the mean square acceleration Equation (3.87). then, we can write:

$$d = C\left(\frac{B_3}{K_2} + \frac{N^2}{B_3 K_2^2}\right) \qquad \text{(B-35)}$$

$$a = C\left(K_2 B_3 + \frac{K_2^2}{B_3}\right) \qquad \text{(B-36)}$$

where $C = \pi$. A.V. and

$$N = K_2 + K_3 \qquad \text{(B-37)}$$

Solving Equation (B-35) for B_3, we have

$$B_3 = \frac{1}{2}\left[\frac{K_2 d}{C} \pm L^{1/2}\right] \qquad \text{(B-38)}$$

where

$$L = \left(\frac{dK_2}{C}\right)^2 - \frac{4N^2}{K^2} \qquad \text{(B-39)}$$

If L = 0, then we can solve Equation (B-39) for

$$d_{min} = \frac{2CN}{K_2^{3/2}} \qquad \text{(B-40)}$$

Now, substituting for d when L = 0 in Equation (B-38), we obtain

$$B_3 = \frac{K_2 + K_3}{\sqrt{K_2}} \qquad \text{(B-41)}$$

By minimizing d (Equation (B-35)) with respect to B_3, we get

$$\frac{\partial d}{\partial B_3} = C\left(\frac{1}{K_2} - \frac{N^2}{B_3^2 K_2^2}\right) = 0 \qquad \text{(B-42)}$$

Solving Equation (B-42) for B_3, we obtain

$$B_3 = \frac{K_2 + K_3}{\sqrt{K_2}} \qquad \text{(B-43)}$$

which is the same as Equation (B-41). Since the second derivative is positive, this is the minimum.

Solving Equation (B-36) for B_3, we have

$$B_3 = \frac{1}{2}\left[\frac{a}{CK_2} \pm H^{1/2}\right] \qquad \text{(B-44)}$$

where

$$H = \left(\frac{a}{CK}\right)^2 - \frac{4K_3^2}{K^2} \qquad \text{(B-45)}$$

If H = 0, then we can solve Equation (B-45) for

$$a_{min} = (2CK_2^{1/2}K_3)^{1/2} \qquad \text{(B-46)}$$

Now, substituting for a when $H = 0$ in Equation (B-44), we obtain

$$B_3 = \frac{K_3}{\sqrt{K_2}} \tag{B-47}$$

By minimizing a (Equation (B-36)) with respect to B_3, we get

$$\frac{\partial a}{\partial B_3} = C\left(K_2 - \frac{K_3^2}{B_3^2}\right) = 0 \tag{B-48}$$

Solving Equation (B-48) for B_3, we obtain

$$B_3 = \frac{K_3}{\sqrt{K_2}} \tag{B-49}$$

which is the same as Equation (B-47). Since the second derivative is positive, this is the minimum.

B-4 1-DOF Model with Voigt Type Suspension that is in Series with a Spring and Both are in Parallel with a Spring

Let us indicate by d and a for the mean square relative displacement (Equation (3.136)) and the mean square acceleration (Equation (3.137)). Then, we can write

$$d = C\left[\frac{N_1 B_3}{K_2^2} + \frac{N_2^2}{B_3 K_2^2}\right] \tag{B-50}$$

$$a = C\left[\frac{N_1^2 B_3}{K_2^2} + \frac{(K_1 N_2 + K_2 K_3)^2}{B_3 K_2^2}\right] \tag{B-51}$$

where $C = \pi$. A.V. and

$$N_1 = K_1 + K_2 \tag{B-52}$$

$$N_2 = K_2 + K_3 \tag{B-53}$$

Solving Equation (B-50) for B_3, we have

$$B_3 = \frac{1}{2}\left[\frac{\alpha K_2^2}{CN_1} \pm L^{1/2}\right] \qquad \text{(B-54)}$$

where

$$L = \left(\frac{\alpha K_2^2}{CN_1}\right)^2 - 4\frac{N_2^2}{N_1} \qquad \text{(B-55)}$$

If $L = 0$, then we can solve Equation (B-55) for

$$d_{min} = \frac{2\alpha N_2 N_1^{1/2}}{K_2^2} \qquad \text{(B-56)}$$

Now, substituting for d when $L = 0$ in Equation (B-54), we get

$$B_3 = \frac{K_2 + K_3}{(K_1 + K_2)^{1/2}} \qquad \text{(B-57)}$$

By minimizing d (Equation (B-50)) with respect for B_3 we get

$$\frac{\partial d}{\partial B_3} = C\left[\frac{N_1}{K_2^2} - \frac{N_2^2}{B_3^2 K_2^2}\right] \qquad \text{(B-58)}$$

Solving Equation (B-58) for B_3, we obtain

$$B_3 = \frac{K_2 + K_3}{(K_1 + K_2)^{1/2}} \qquad \text{(B-59)}$$

which is the same as Equation (B-57). Since the second derivative is positive, this is the minimum.

Solving Equation (B-51) for B_3, we have

$$B_3 = \frac{1}{2}\left[\frac{aK_2^2}{2cN_1^3} \pm H^{1/2}\right] \qquad \text{(B-60)}$$

where

$$H = \left(\frac{aK_2^2}{cN_1^3}\right)^2 - 4\frac{(K_1N_2 + K_2K_3)^2}{N_1^3} \qquad \text{(B-61)}$$

If $H = 0$, then we can solve Equation (B-61) for

$$a_{min} = \frac{2c(K_1N_2 + K_2K_3)N_1^{3/2}}{K_2^2} \qquad \text{(B-62)}$$

Now, substituting for a when $H = 0$ in Equation (B-60), we obtain

$$B_3 = \frac{(K_1K_2 + K_1K_3 + K_2K_3)}{(K_1 + K_2)^{3/2}} \qquad \text{(B-63)}$$

By minimizing a (Equation (B-51)) with respect to B_3, we get

$$\frac{\partial a}{\partial B_3} = C\left(\frac{N_1^3}{K_2^2} - \frac{(K_1N_2 + K_2K_3)^2}{B_2^3K_2^2}\right) \qquad \text{(B-64)}$$

Solving Equation (B-64) for B_3, we obtain

$$B_3 = \frac{(K_1K_2 + K_1K_3 + K_2K_3)}{(K_1 + K_2)^{3/2}} \qquad \text{(B-65)}$$

which is the same as Equation (B-63). Since the second derivative is positive, this is the minimum.